Calcium/Phosphate Regulation: A Control Engineering Approach

Christopher Robert Christie

Dissertation submitted to the faculty of the Virginia Polytechnic Institute and State University in partial fulfillment of the requirements for the degree of

Doctor of Philosophy

In

Chemical Engineering

Luke E.K. Achenie, Chair

Babatunde A Ogunnaike

Aaron S. Goldstein

Alexander Leonessa

November 13, 2013

Blacksburg, VA

Keywords: calcium regulation; mathematical model; parathyroid hormone (PTH); engineering control system, calcium-related pathologies

Calcium/Phosphate Regulation: A Control Engineering Approach

Christopher R. Christie

Abstract

Calcium (Ca) homeostasis is the maintenance of a stable plasma Ca concentration in the human body in the presence of Ca variability in the physiological environment (e.g. by ingestion and/or excretion). For normal physiological function, the total plasma Ca concentration must be maintained within a very narrow range (2.2-2.4mM). Meeting such stringent requirements is the task of a regulatory system that employs parathyroid hormone (PTH) and calcitriol (CTL) to regulate Ca flux between the plasma and the kidneys, intestines and bones. On the other hand, plasma phosphate control is less tightly, but simultaneously, regulated via the same hormonal actions. Chronic imbalances in plasma Ca levels are associated with disorders of the regulatory organs, which cause abnormal hormonal secretion and activity. These changes in hormonal activity may lead to long-term problems, such as, osteoporosis (increased loss of bone mineral density), which arises from primary hyperparathyroidism (PHPT) – hyper secretion of PTH.

Existing *in silico* models of Ca homeostasis in humans are often cast in the form of a single monolithic system of differential equations and are not easily amenable to the sort of tractable quantitative analysis from which one can acquire useful fundamental insight. In this research, the regulatory systems of plasma Ca and plasma phosphate are represented as an engineering control system where the physiological sub-processes are mapped onto corresponding block components (sensor, controller, actuator and process) and underlying mechanisms are represented by differential equations. Following validation of the overall model, Ca-related pathologies are successfully simulated through induced defects in the control system components.

A systematic approach is used to differentiate PHPT from other diseases with similar pathophysiologies based on the unique hormone/ion responses to short-term Ca disturbance in each pathology model. Additionally, based on the changes in intrinsic parameters associated with PTG behavior, the extent of PHPT progression can be predicted and the enlarged gland size estimated *a priori.*

Finally, process systems engineering methods are used to explore therapeutic intervention in two Ca-related pathologies: Primary (PHPT) and Secondary (SHPT) Hyperparathyroidism. Through

parametric sensitivity analysis and parameter space exploration, the calcium-sensing receptor (sensor) is identified as a target site in both diseases and the extent of potential improvement is determined across the spectrum of severity of PHPT. The findings are validated against existing drug therapy, leading to a method of predicting drug dosage for a given stage of PHPT. Model

Predictive Control is used in drug therapy in SHPT to customize the drug dosage for individual patients given the desired PTH outcome, and drug administration constraints.

To Delfa Salmon, for your unwavering love and support.

May I inherit half your strength.

Contents

1. Background & Literature Review 1
1.1. Mathematical modeling in physiological control systems 1
1.2. Calcium in the body, its role and regulation – A synopsis 2
1.3. Calcium and Phosphate Control – Organs & Processes 5
1.4. Pathologies associated with Ca metabolism in adults 9
1.5. Approaches to Ca homeostasis modeling 16
1.6. Controller Design in Biological Systems 18
1.7. Opportunities for improvement in modeling Ca regulation 20
1.8. References 22
2. A control engineering model of calcium regulation 33
2.1. Introduction 33
2.2. Materials and Methods 35
2.3. Results 43
2.4. Discussion and Conclusions 49
2.5. References 52
3. Modeling Phosphate Control and Chronic Kidney Disease 56
3.1. Phosphate Control 56
3.2. Chronic Kidney Disease 60
3.3. Model Validation 61
3.4. References 71
4. A Model-Based Approach to Diagnosing Primary Hyperparathyroidism 74
4.1. Introduction 74
4.2. Materials and Methods 75
4.3. Results 77
4.4. Discussion 85
4.5. References 89
5. Potentiation of the calcium-sensing receptor across the spectrum of primary hyperparathyroidism 92
5.1. Introduction 92
5.2. Materials and Methods 93
5.3. Results 95

5.4. Discussion 101
5.5. References 104
6. Identifying potential therapeutic targets in hyperparathyroidism 107
6.1. Introduction 107
6.2. Modeling & Computational Strategy 108
6.3. Results & Discussion 111
6.4. Conclusions 123
6.5. Reference 125
7. Conclusions and Future work 135
7.1. Conclusion 135
7.2. Future work 139

List of Figures

Figure. 1.1. A physiological representation of the calcium regulatory system. 3

Figure 1.2. A schematic representation of osteoblastic and osteoclastic proliferation..... 8

Figure 2.1. Diagrams of Ca regulation. 34

Figure 2.2. Model of the Ca-sensing receptor (CaR). 39

Figure 2.3 The Ca-PTH curve. 40

Figure 2.4. Response of healthy subjects to induced hypo- and hypercalcemia: 44

Figure 2.5. Simulations of pathologies as ECS component defects: 46

Figure 2.6. Simulations of pathologies as component defects in the ECS Ca model 48

Figure 3.1. Engineering control system block diagram of plasma phosphate regulation..... 56

Figure 3.2. The engineering control system block diagram representation of combined plasma calcium and phosphate regulation. 59

Figure 3.3. Calciotropic response, for both models, to induced hypocalcemia (2-hr infusion of sodium EDTA (33)) in healthy subjects:..... 62

Figure 3.4. Ca and PTH response during 2-hr infusion of: 63

Figure 3.5. Model prediction and clinical observation of Calciotropic response to 2-hr clinical infusion of calcium gluconate in PHPT subjects. 64

Figure 3.6. Comparison of Simulated results and clinical observations of plasma biochemistry changes among patients with varied severity of kidney disease (as determined by a decline in renal function/GFR) (36). 66

Figure 3.7. Simulated results of calciotropic response to progressive decline in renal function: . 68

Figure 4.1. PTH suppression from Ca loading 78

Figure 4.2. Model groups and individuals intra- and post- infusion profiles. 80

Figure 4.3. Simulation Results. 84

Figure 4.4. Analysis of parathyroid function..... 85

Figure 5.1. Simulated calciotropic response (ionized Ca, PTH, CTL, urinary Ca (Cau) and CB ratio) to changes in sensor gain in: 96

Figure 5.2. Simulation results of sensor gain changes in healthy model (ACa =1) and various stages of PHPT (ACa >1): 97

Figure 5.3. Simulation results of : 98

Figure 5.4. Simulation results of CNC therapy: 99

Figure 5.5. 12-hr moving average of calciotropic response to twice daily dose of cinacalcet over 20 days. 100

Figure 6.1. Model parameter sensitivities for selected parameters with the greatest influence on: 111

Figure 6.2. Simulated calciotropic response (ionized Ca, PTH, CTL, urinary Ca (Cau) and CB ratio) to changes in sensor gain in PHPT..... 113

Figure 6.3.Simulation results of response to CNC administration. 115

Figure 6.4. Comparison of Simulated results and clinical observations of plasma biochemistry changes among patients with varied severity of kidney disease (as determined by a decline in renal function/GFR) (32). 118

Figure 6.5. Simulation results of sensor gain changes in SHPT:..... 119

Figure 6.6. Simulation results of CNC therapy in SHPT. 120

Figure 6.7. Simulation results of MPC use in CNC therapy in SHPT subjects..... 122

List of Tables

Table 1.1. Stages of Chronic Kidney Disease 12

Table 2.2. Model Equations..... 37

Table 2.3. Parameter Estimates 38

Table 4.4. Parameter estimates and correlation with parathyroid function and mass 81

Table 6.5. Maximum Normalized Sensitivity Coefficient at steady-state for Select Parameters 111

Table 6.6. Comparison of reductions in calciotropic responses between Days 1 and Day 15 116

Table 6A.7. Model Equations – Ca/Phosphate Control (Healthy) 129

Table 6A.8. Model Equations – Pathologies as Component defects..... 130

Table 6A.9. Parameter Estimates 132

Table 6A.10. Parameter estimates for pathologies..... 133

1. Background & Literature Review

1.1. Mathematical modeling in physiological control systems

Since the development of control theory and, more so, the advent of digital computers, physiologists, mathematicians and engineers have sought to provide a better understanding of different physiological control systems through the applying a mathematical approach based on control theory (1). A significant amount of research has been carried out on some of these systems leading to the development of medical devices for patient treatment. In the clinical setting, some of these devices are being used to assist in processes such as: blood pressure control, body-temperature control, and tremor control for patients with epilepsy and Parkinson's disease (2).

The control engineering framework provides an efficient means of organizing the sub-processes constituting Ca regulation. This organization may seem counterintuitive to how physiological control systems are often viewed; however, this approach facilitates a fundamental understanding of the complex process of Ca regulation. To date, relatively little has been published on the application of mathematical modeling to calcium (Ca) control; and, none of the published research has explored Ca regulation using a control engineering framework.

The increasing availability of detailed information and clinical data regarding the physiology involved in Ca regulation, and the existence of previous models allow for applying control engineering framework to the development of a representative model of plasma Ca regulation. Such a model can provide insight into the mechanisms involved in Ca regulation in both the healthy and diseased states. Ultimately, these insights may allow for the development and integration of external controllers in improving quality of care in patients with Ca-related pathologies.

The literature review presented herein focuses on: i) the role of calcium in the body and how it is regulated; ii) the pathologies associated with defects in the Ca regulatory system; iii) approaches to modeling Ca regulation; iv) external controllers used in biomedical applications. Finally, from the review of the body of research on modeling Ca regulatory, the opportunities for improvement are identified, thus setting the path for this research.

1.2. Calcium in the body, its role and regulation – A synopsis

Calcium (Ca) is distributed in three major areas in the human body. The skeleton/bone is the major storage site of Ca, which accounts for approximately 99% of the total body calcium. Here, most of the calcium exists in the form of bone mineral (hydroxyapatite) with the remainder making up the bone fluid. The remaining 1% of calcium is distributed between both the intracellular fluid and extracellular fluid (ECF)—or plasma (3). Plasma Ca concentration is approximately three orders of magnitude greater than in the intracellular environment. (4).

The role of calcium varies depending on its location. Within the skeletal system, Ca is one of the chief components of bone mineral, which provides the strength and rigidity necessary for the bone to support the body and protect vital organs (5). Within the cell, Ca is important for intracellular processes, including: cellular volume and enzyme regulation, muscular excitation and hormonal secretion (4, 6, 7); while, plasma Ca is necessary for blood coagulation and membrane function (4).

Notwithstanding the disparity of Ca levels among the different locations, Ca-dependent biochemical processes require that plasma Ca concentration—the nexus between the skeletal and intracellular environments – be kept within a narrow range, 2.45 ± 0.25mM for normal bodily functions (4, 5). This narrow range of homeostasis is maintained under varying conditions in the physiological environment (e.g., lactation, excess or inadequate Ca intake or excretion), through the varied processes of the body's Ca regulatory system. Temporal or chronic disturbances in plasma Ca levels may result in impaired cellular activities leading to various pathological conditions.

Intracellular calcium homeostasis is just as important as, and is impacted greatly by, plasma Ca regulation. Likewise, bone remodeling—although largely dependent on the biomechanical needs of bone cells— is impacted by and depends on plasma Ca levels (5). However, intracellular Ca control is beyond the scope of this research and bone Ca will be dealt with inasmuch as it impacts on plasma Ca homeostasis.

1.2.1. Plasma Calcium Regulation

Although all calcium in the plasma exists in the ionized form, in medical literature, the term ionized Ca refers to the portion of Ca that is free (unbounded) and accounts for approximately 50% of the total plasma Ca. Approximately 12% of plasma Ca forms soluble complexes with organic and inorganic anions, the remainder is protein-bound (5). However, only ionized Ca is

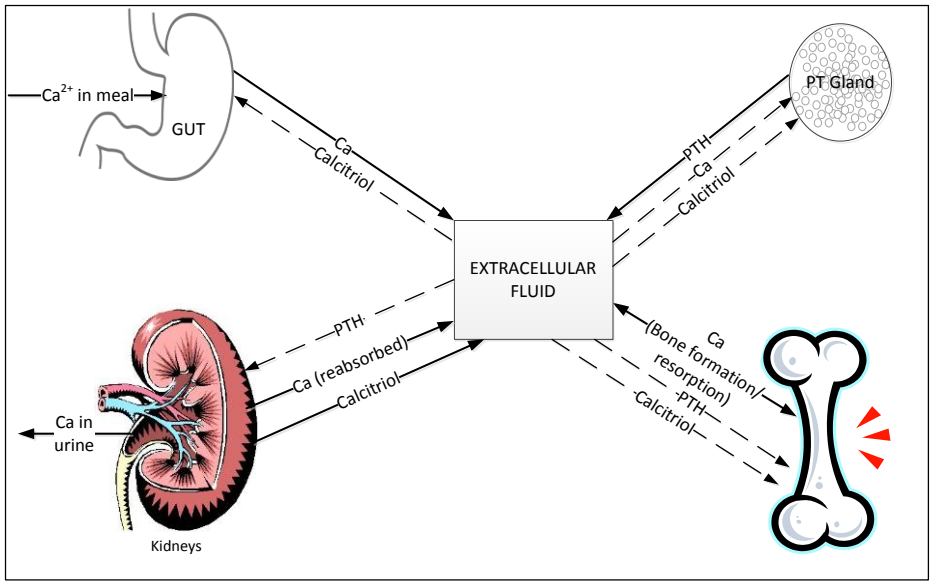

Figure. 1.1. A physiological representation of the calcium regulatory system.

Dashed arrows represent the stimuli and solid arose, the transfer of ions and/or hormones between the extracellular fluid (ECF) and the PTG, bone, intestines and kidneys.

affected during regulatory control (4, 5). As such, and unless expressly stated, the term plasma Ca will be used to refer to ECF Ca and ionized Ca.

In the human body, Ca homeostasis is achieved through the actions of four organs: the parathyroid glands (PTG) — a group of four glands located on the surface of the thyroid gland— kidneys, bone and intestines. Calcium transfer between the plasma, and the kidneys, intestines and bone is regulated by the secretion of three hormones, namely, parathyroid hormone (PTH), calcitonin (CTN) and calcitriol (CTL). CTN plays a minor role in calcium metabolism in humans, as neither CTN insufficiency or excess has an impact on plasma calcium or bone mineral density (3, 4, 8). As such, the impact of CTN on Ca regulation is not addressed in this research.

A schematic representation of Ca regulation is shown in Fig. 1.1; Ca-sensing receptors (CaR) located on the surface of parathyroid (PT) cells detect plasma Ca levels and respond to even small changes (±2%). When Ca is low, the CaRs cause the chief cells of the parathyroid gland to secrete more PTH, which in turn acts on the kidneys and bone. In the kidneys, PTH has a two-fold effect: firstly, it stimulates the production and secretion of CTL; secondly, it promotes increased Ca and reduced phosphate (PO_4) reabsorption in the renal tubules. In the bone, increased PTH levels ultimately lead to net bone resorption (3-5).

CTL, secreted from the kidneys, acts on the PTG, intestines and bone. In the PTG, it inhibits PTG cellular proliferation thereby reducing the capacity of the PTG to produce and secrete PTH. CTL increases intestinal calcium and phosphate absorption; and, in the bone, CTL acts in concert with PTH to stimulate osteoclastic bone resorption (3-5).

Typically, the Ca excreted by the kidneys is balanced by Ca from intestinal absorption and likewise the Ca released from bone resorption is balanced by concurrent bone formation. Any short-term deficit of plasma Ca not matched by intestinal absorption is relieved by bone resorption, while excess plasma Ca is either excreted or formed into bone (3, 5).

1.2.2. Phosphate regulation

Phosphate, like calcium, is largely stored in the bone with the remainder distributed between the intra- and extracellular fluids. Phosphate regulation is not as well researched as Ca regulation, however, they are both regulated by the same hormones and as such their control occurs in tandem. However, unlike the tight regulation of plasma calcium, phosphate control is loosely controlled. Increased phosphate levels stimulate increased secretion of fibroblast growth factor -23 (FGF-23) from the bone. Both phosphate and FGF-23 stimulate PTH secretion and counteract the stimulatory effect of PTH on CTL production. Increased PTH and FGF-23 levels inhibit phosphate reabsorption in the renal tubules; while sustained increases in PTH levels induce net bone resorption. Decreased CTL cause reduced intestinal phosphate absorption and inhibits PTH secretion. Therefore, as with calcium, serum phosphate levels are controlled by the net effect of intestinal absorption, renal excretion and bone transfer (9).

1.3. Calcium and Phosphate Control – Organs & Processes

This section focuses on the ion- and hormone-mediated processes occurring within the different regulatory organs.

1.3.1. The Parathyroid Gland (PTG) – Ca sensing & PTH secretion

Many plasma constituents have been reported to affect PTG function, both *in vitro* and *in vivo*. Some of these agents fall into the following general groups: organic and inorganic ions (e.g. Ca, Mg, La, Eu, phosphate, polyamines etc.), amines, calcitriol, steroids, lipid metabolites, and peptides (10). However, only a review of the relevant stimulants (calcium, phosphate and calcitriol) will be addressed here.

1.3.1.1. Ion-sensing and "signal" transmission

On their outer surface, calcium-sensing receptors (CaR) have a long amino-terminal domain that comprises determinants of calcium ion binding. CaR are connected to the surface of the chief (C) cells of the PTG through their coupling to G-proteins. The coupling is enabled through structures within the intracellular environment of the CaR. The detected Ca level is transmitted to the C-cells via these G-proteins thereby inducing action within the PT cells (10). There are no phosphate-sensing receptors within the PTG, however, elevated plasma phosphate levels stimulate PTH production in the gland by lowering plasma Ca (11).

1.3.1.2. PTH Production & Secretion

PTH, a non-glycosylated protein whose active form is PTH(1-84), is synthesized through a series of pathways beginning at the transcription of the PTH gene, forming messenger RNA (mRNA) within the nucleus of the parathyroid cells (10). PTH gene transcription and PTH mRNA synthesis are reported to be significantly reduced by increased levels of both calcitriol and FGF-23 (12-14). Additionally, the stability of the transcription product (PTH mRNA) is strengthened at low Ca levels and high phosphate levels (15). Conversely, PTH mRNA stability decreases at high Ca and low phosphate levels.

The PTH precursor is then synthesized in the cytoplasm following which, a series of cleavage steps occurs ending with the active PTH first appearing in the Golgi apparatus. Once formed, the PTH migrates in two general forms: 1) small vesicles that eventually fuse to the cell membrane where the contents are secreted, into the plasma, independent of a stimulus; and, 2) mature and

immature secretory granules, from which the contents are released through a stimulus-mediated pathway. Mature granules are formed from the fusion of several immature granules (10). The two general forms of PTH in the cell allow for a tonic and pulsatile release of PTH. The frequency and amounts of PTH secreted during each pulse change depending on the prevailing calcemic conditions (low, normal or high Ca); however, the pulsatile pattern remains (16).

Although the steps involved in the Ca-mediated secretion are not fully understood, research has shown that the Ca-regulated pathway comprises a number of membrane-trafficking events. These events are highlighted during hypercalcemia, where high Ca levels act to: inhibit the formation of vesicles; block the fusion of vesicles and granules to the cell membrane; and inhibit granular maturation (10).

In comparison to PTH production and secretion, less research has been carried out on PTG cellular proliferation. Parathyroid cellular proliferation is virtually non-existent under normocalcemic conditions (17); however, *in vitro* studies have shown that hypocalcemic conditions contribute to increased parathyroid cell proliferation (18) and calcitriol levels inhibit PT cellular proliferation (19, 20). Also, PT cells have been found to multiply at elevated phosphate levels *in vivo* (21, 22).

1.3.2. The Kidneys

Among their many functions, the kidneys play a dual role in maintaining Ca and phosphate homeostasis through calcitriol production and reabsorption of glomerular filtrate, both of which are differentially regulated by PTH and FGF-23.

1.3.2.1. Calcitriol Production

Vitamin D, usually ingested or synthesized in the skin by exposure to UV light, goes through a series of hydroxylation steps in the liver and kidneys before it is converted to its biologically active form, calcitriol (4). In the liver vitamin D undergoes loosely regulated hydroxylation within the hepatocytes forming 25-hydroxyvitamin D_3 (23).

In the proximal tubule cells of the kidneys, high PTH and low phosphate levels induce the production of the enzyme, 1α-hydroxylase, which converts 25-hydroxyvitamin D_3 to its biologically active form calcitriol (1α,25-dihydroxyvitamin D_3; 1α,25-$(OH)_2D_3$) (4, 23, 24). Conversely, high FGF-23, hyperphosphatemia and calcitriol inhibit calcitriol synthesis (23, 25, 26).

Calcitriol in the plasma forms a strong bond with transcalciferin (a vitamin-D binding protein); as such, a large quantity of calcitriol is required for the liberation of the free hormone; the resultant effect being a long plasma CTL residence time, 5-12 hours (27).

1.3.2.2. Renal Reabsorption

Along with inducing calcitriol production, the binding of biologically active PTH and FGF-23 to receptors in the proximal tubule cells allow for decreased phosphate reabsorption and increased calcium reabsorption in the distal nephron (4, 11).

1.3.3. The Intestines – Absorption

Calcitriol receptors within the intestinal cells join with calcitriol forming a complex, which initiates the formation of calcium-binding proteins (CaBP). Although the mechanism through which the CaBP works is unclear, it is believed that the CaBP aids in the Ca uptake through the cells (4, 28). Additionally, CTL increases intracellular intestinal phosphate absorption through upregulation of the phosphate ion transporters in the cells (29).

1.3.4. Bone

The bone is a connective tissue made up of a collagen fiber matrix which is hardened in place by the deposition of bone mineral, which is the major constituent of bone and contains calcium, phosphate, carbonate and magnesium with a molar ratio of 40:25:5:1 (30). Bone mineral is remodeled perpetually for the maintenance of structural integrity and bone health. The remodeling process is dependent on the combined activities of bone forming (osteoblasts – OB) and bone resorbing (osteoclasts – OC) cells (31). A layer of bone fluid lies across the outer surface of the bone mineral. The bone fluid is separated from the ECF by a bone membrane made up of bone lining cells. Bone fluid is rich in Ca and phosphate as it is in equilibrium with the mineral phase, therefore transfer of Ca and phosphate ions between the bone fluid and the ECF is hormone-independent (3).

PTH and CTL promote OB and OC cellular proliferation (4, 5); however, PTH is the more important of the two hormones (31, 32). Under normal conditions, PTH secretion has both a pulsatile profile (16) which maintains a balance between OB and OC activity. However, during hypocalcemia or hyperphosphatemia, when there is a sustained increase in PTH levels, PTH inhibits the osteoblast synthesis of synthesis of collagen and other bone matrix proteins (31) resulting in net bone resorption.

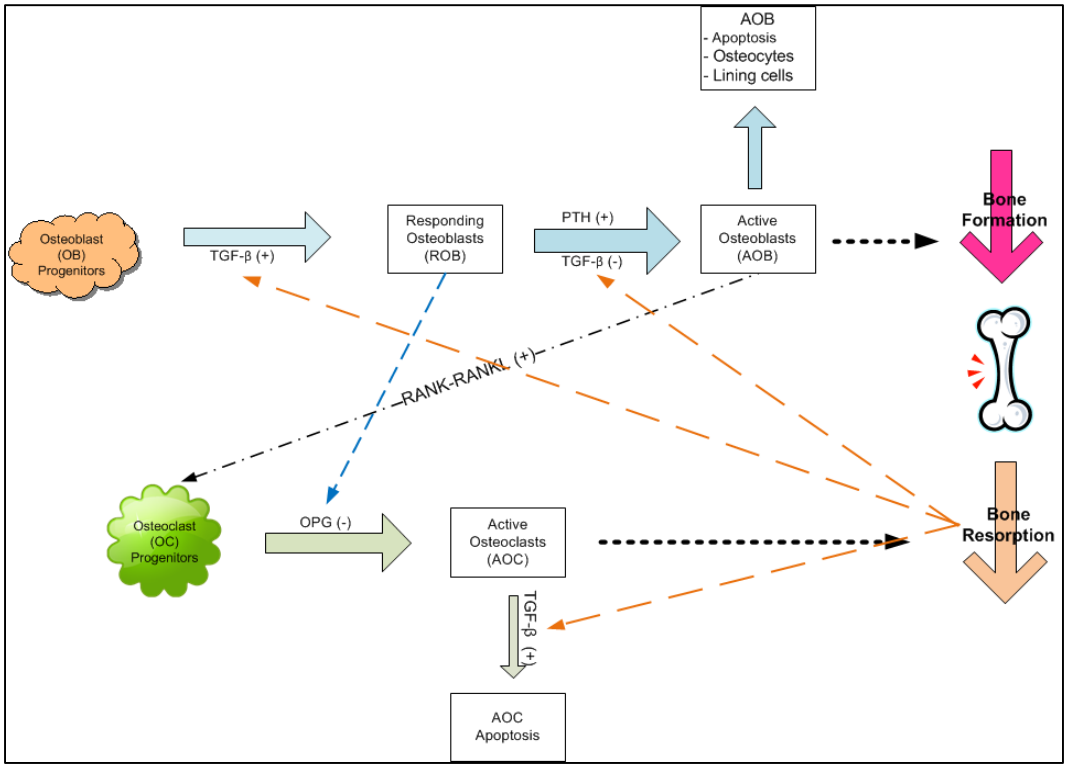

Figure 1.2. A schematic representation of osteoblastic and osteoclastic proliferation

1.3.4.1. Cellular Proliferation

Fig. 1.2 is a schematic representation of the interactions involved in cell proliferation. Although the overall action of PTH results in increased resorption (osteoclastic activity) osteoclasts do not have PTH-receptors; it is the osteoblasts and their progenitors that do (33, 34). Multi-potential stem cells go through a series of proliferation and maturation before becoming osteoblast progenitors. TGF-beta, present in the bone matrix, influence the formation of these progenitors into osteoblast precursors (preosteoblasts – ROB/OB_R) (34). At this point, PTH stimulates the maturation of ROB into osteoblasts (OB), which then carry out bone formation. Upon completion of their tasks, OBs transform into osteocytes, bone-lining cells or undergo apoptosis (34, 35).

OBs contain a receptor— Receptor Activator of Nuclear Factor κ B (RANK)—that connects to the complementary ligand, RANKL, located on the surface of osteoclast precursors (36); the bond induces OC precursor differentiation into OC (37). However, osteoprotegerin (OPG), produced by OBs (38), inhibits the RANK-RANKL binding, and hence inhibits OC formation (39). Once formed, OCs resorb bone mineral and eventually undergo apoptosis. TGF-beta, released during bone resorption (40), promotes preosteoblast formation, inhibits OB formation and induces OC

apoptosis (39, 41, 42) and are embedded in the bone matrix during osteoblastic bone formation (34).

1.3.4.2. Fibroblast growth factor (FGF-23) production

The primary site of production of FGF-23 is in osteoblasts and osteocytes in the skeleton (43). FGF-23 synthesis is stimulated by increased levels of plasma phosphate, calcitriol and PTH (44, 45). However, the magnitude of increase in FGF-23 secretion is greater for phosphate and CTL than PTH. Additionally, the phosphate–dependent and CTL–dependent FGF-23 secretion is prolonged (approximately 1 hr and 8 hrs, respectively) in comparison to PTH, approximately 0.5 hr (45-47).

1.4. Pathologies associated with Ca metabolism in adults

The primary manifestation of pathologies associated with Ca metabolism is usually a prolonged deviation in calcium levels above (hypercalcemia) or below (hypocalcemia) the normal range (normocalcemia).

Chronic hypercalcemia occurs due to a loss of control in Ca regulation resulting in an increased accumulation of Ca in the plasma whether through sustained bone resorption, intestinal absorption, and/or inadequate renal excretion. On the other hand, chronic hypocalcemia occurs as a result of an ineffective response to the regulatory hormones (PTH and calcitriol) or excess phosphate in circulation (4).

1.4.1. Genetic conditions:

1.4.1.1. Familial benign hypocalciuric hypercalcemia (FBH) and Autosomal Dominant Hypoparathyroidism (ADH)

Familial benign hypocalciuric hypercalcemia (FBH) is an inherited genetic alteration of the calcium-sensing receptor (CaR). The alterations are usually missense mutations causing varied levels of inactivation of the CaR. Consequently, there is a normal-to-slightly elevated PTH level, asymptomatic hypercalcemia, incongruously low renal Ca excretion and an absence of parathyroid adenoma (48, 49).

On the other hand, Autosomal Dominant Hypoparathyroidism (ADH) is a hereditary condition caused by an activating mutation of the CaR gene resulting in a gain-of-function in the receptor.

The physiological effects of the condition are hypocalcemia, marginally low PTH levels and hypercalciuria (48, 50).

1.4.2. Acquired conditions

1.4.2.1. Hyperparathyroidism (HPT)

HPT results from an abnormal change from within the PTG or the Ca regulatory system both of which lead to an increase in PTG activity. The disease may present itself in one of three variants: primary (PHPT), secondary (SHPT) or tertiary (THPT) hyperparathyroidism (51). In general, all forms of HPT are characterized by excessive PTH secretion resulting in increased bone resorption, hypercalcemia and hypocalciuria or depending on the severity of the disorder, hypercalciuria (4). Other medical conditions may arise as a result of the increased hormone and ion concentrations. For example, osteoporosis and osteopenia are complications of PHPT due to increased bone resorption, leading to lower bone mineral density; or kidney stones develop as a result of hypercalcemia and/or hyperphosphatemia in SHPT.

PHPT is the third most common endocrine disorder in humans, and disproportionately affects postmenopausal women. It is characterized by an increase in PTH secretion due to PTG adenoma (benign tumorous growth) or hyperplasia (increased production of normal cells) in one, or a combination, of the four PTGs (51). The specific cause of the growth is unknown, but it is believed to be associated with radiation exposure, as clinical observations have shown that individuals exposed to some forms of radiation show increased incidence in developing the disorder (52-54). At present, the only cure for PHPT is surgical removal of the affected gland; however, those who do not undergo surgery may be treated for related symptoms – low sex hormone levels and increased bone resorption. It is important to note that none of these therapies result in reduced PTH levels (55-57). Calcimimetics are being increasingly used in PHPT to lower PTH levels (51).

SHPT occurs due to a deficiency in the Ca regulatory system as a result of varied diseases/conditions including: inadequate dietary Ca intake; intestinal Ca malabsorption; vitamin-D deficiency and kidney disease. The two major areas of clinical research are vitamin D deficiency and chronic kidney disease (51). In Vitamin D deficiency, PTH levels increase due to the reduced production and secretion of calcitriol thus removing one of the controls necessary for inhibition of PTH secretion. On the other hand, PTH levels increase in chronic kidney disease due to a combination of effects – a decrease in renal mass causes a fall in calcitriol production

and a reduction in glomerular filtration rate (GFR). These result in reduced PTH clearance and reduced renal reabsorption, leading to hypocalcemia, hypophosphatemia; all three effects cause an increase in circulating PTH (58).

Treatment for SHPT depends on its causes, for Vitamin D deficiency, Ca and Vitamin D (or its analogues) to restore PTH levels. For patients with chronic kidney disease, along with hemodialysis, administration of calcitriol and its analogues and calcimimetic drugs have been used to regain normal PTH levels (51).

THPT occurs in individuals with long-established SHPT, of which the main characteristic is the non-suppressibility of PTH even by increasing Ca or calcitriol levels. This is usually the result of the underexpression of CaR on PT cells (59) or hyperplasia in any or all of the four PTGs (60, 61). Treatment includes phosphate and/or vitamin D administration for calcitriol inhibition and increasing ionized Ca (51) .

1.4.2.2. Hypoparathyroidism (HoPT)

HoPT is an uncommon disease with symptoms of hypocalcemia, low or non-existent PTH levels and high phosphate concentration. The most common cause of the condition is inadvertent or unavoidable removal or damage to the PTG during surgery (of the thyroid, PTG or neck). The other causes are autoimmune and some genetic disorders (62). Treatment for hypoparathyroidism includes: thiazide diuretics (for reducing urinary Ca excretion), Ca supplements, Vitamin D metabolites and PTH (62).

1.4.2.3. Chronic Kidney Disease (CKD)

Chronic kidney disease (CKD) is considered as a systemic damage of the kidneys or reduction in kidney function— as measured by the glomerular filtration rate (GFR)— lasting in excess of three (3) months (63). Diabetes mellitus, hypertension and cardiovascular disease are the major initiating factors of CKD accounting for more than 65% of cases between 2005 – 2010 according to data from the National Health and Nutrition Examination Survey (NHANES) . Other initiating factors include: autoimmune disease, systemic infections, urinary tract infections, urinary stones, lower urinary tract obstruction and drug toxicity. Of the complications that develop during the progression of CKD, those pertinent to Ca and phosphate regulation include GFR decline, hyperphosphatemia, altered CTL metabolism and secondary hyperparathyroidism; these are discussed below.

1.4.2.3.1. GFR Decline

The decline in GFR occurs due to the loss of an ample amount of nephrons. The nephron is the functional unit of the kidney of which there are approximately one million in each kidney and produces urine independently of each other. Each nephron is made up of two sections: (i) the glomerulus, a cluster of blood vessels (capillaries) where filtration occurs; and, (ii) the tubule, where the filtered fluid is converted to urine. The glomerulus comprises four main layers which make up the filtration barrier in the kidneys: glycocalyx, glomerular endothelium, glomerular basement membrane (GBM), and podocytes. The glycocalyx prevents the passage of large negatively charged macromolecules. The glomerular endothelium restricts the passing of cellular elements but allows the passage of water and small molecules (such as water, glucose, amino acids, salts, urea and some proteins). The glomerular basement membrane (GBM) restricts the passage of medium to large solutes (i.e. molecular weight > 1 kDa) while preventing the passage of negatively charged solutes. Finally, podocytes on surface of the GBM restrict the filtration of large anions (65, 66).

The glomerular filtration rate (GFR) is the amount of amount of glomerular filtrate formed each minute (mL/min) in all the nephrons from both kidneys. For comparison between differently sized individuals a correction factor is introduced for body surface area (BSA), hence GFR is expressed as mL/min per 1.73m^2, where the BSA for the average adult is approximately 1.73 m^2 (66).

The standard measure of overall kidney function is GFR. Within the normal population, GFR varies with age, sex and body size. In young adults the GFR is about between 120—130 mL/min per 1.73m^2 varying 15-20% among individuals. After about age 20 – 30 years the GFR declines with age reaching 70 mL/ min per 1.73m^2 by age 70 (67-69). Decreased GFR is defined as < 90 mL/min/1.73 m^2 and the interpretation of this decreased value depends on the presence of markers of kidney damage. The level of kidney function indicates the degree of CKD and is

Table 1.1. Stages of Chronic Kidney Disease

Stage	Description	GFR (mL/min per 1.73m^2)
1	Kidney damage with normal or increased GFR	≥ 90
2	Kidney damage with mild decreased GFR	60 – 89
3	Moderately decreased GFR	30 – 59
4	Severely decreased GFR	15 – 29
5	Kidney failure	< 15 (or dialysis)

shown in the Table 1.1.

The decline in GFR occurs due to the loss of an ample amount of nephrons. In an attempt to maintain the GFR, compensatory changes to the blood flow (hemodynamic response) occur in the remaining nephrons (glomerular hyperfiltration). Hyperfiltration leads to glomerular injury—in the form of glomerulosclerosis (hardening of the glomerulus) and glomerular hypertrophy (enlargement of the glomerulus)—thus, a further decline in GFR (71-74).

Increased glomerular pressure (intraglomerular hypertension)—whether due to hyperfiltration or other initiating factors—causes further damage of the glomerulus thereby reducing GFR. In intraglomerular hypertension the epithelial cells separate from the capillary wall due to additional stress on the wall and increasing glomerular diameter (caused by hypertrophy). There is now additional passage for water, solutes and some macromolecules. However, these macromolecules are unable to flow through the intact GBM and accumulate in the endothelium. Over time, the accumulation of macromolecules reduces the space in the capillary walls, ultimately leading to a decrease in glomerular filtration (i.e. GFR) (75).

Concomitant with the damage of the filtration membrane is the passage of excess proteins into the renal tubules, resulting in proteinuria which is the primary marker of kidney damage (76). Some of the filtered protein is absorbed in the tubular cells, triggering an inflammatory response which eventually leads to glomerulosclerosis and interstitial fibrosis (formation of excess fibrous connective tissue between tubular cells) (77, 78). This undoubtedly contributes to the decline in the GFR.

Another factor in the progression of GFR decline and CKD is phosphate retention. Renal phosphate clearance decreases with the onset of deteriorating GFR (71, 79). The excess circulating phosphate precipitates with calcium in the interstitial fluid of the renal tubules thus triggering an inflammatory response which leads to the formation of excess fibrous tissue (interstitial fibrosis) and eventually renal tubular atrophy (80, 81).

Of the many complications of CKD, the two directly associated with plasma calcium regulation are hyperphosphatemia—excess of phosphate levels in the plasma—and secondary hyperparathyroidism (SHPT). SHPT is a prolonged excessive secretion of PTH from the PTGs due to failure of one or more of the non-parathyroid calcium homeostatic mechanisms (51). Hyperphosphatemia (increased retention of plasma phosphate) is often a contributory factor in the development of SHPT.

At the onset of CKD, the phosphate regulatory system mitigates the increasing phosphate levels, keeping plasma phosphate within the normal range (82). However, the key hormones involved in phosphate control are abnormally adjusted: CTL is kept sub-basal and, PTH and FGF-23 remain high (83-85). With further decline in kidney function, resistance to the effect of FGF-23 occurs in both the PTG and kidneys (86, 87); resulting in increased phosphate retention leading to hyperphosphatemia, and as a result, even higher PTH and FGF-23 levels (82). Hyperphosphatemia is apparent in the more advanced stages of CKD (end-stage renal failure—Stage 5) at which point the disease is often irreversible (88).

1.4.2.3.2. Altered Calcitriol Metabolism

The metabolism of calcitriol is altered during the progression of CKD due to a combination of hyperphosphatemia, metabolic acidosis and reduced metabolic clearance.

Renal hydroxylation of 25-(OH)-D3, producing calcitriol, occurs in the proximal convoluted tubules cells (23, 89); the reduction in renal mass in CKD results in reduced sites for CTL production (90). The enzyme, renal 1α-hydroxylase is responsible for the hydroxylation step; however, its activity is suppressed by inorganic phosphate and increased by PTH (23). Therefore, increasing phosphate levels in CKD has an inhibitory effect on CTL production.

Metabolic acidosis (MA) (accumulation of acid in the plasma) is frequently encountered in CKD. MA disturbs calcium metabolism through reduced bone mineral content resulting in increased plasma Ca and phosphate (91). The increased plasma Ca indirectly suppresses CTL production via the Ca-PTH axis while, the increased phosphate levels directly inhibit CTL through reduced renal hydroxylation of CTL precursors (90).

With the reduced blood filtration in CKD, uremic toxins (nitrogenous waste compounds) and purine compounds (often the end product of digestion of certain proteins) are retained in the blood. Both sets of compounds have been shown to inhibit calcitriol production through the suppression of renal 1α-hydroxylase activity (92-94).

Although CTL production is reduced in CKD, some of the attendant effects of CKD limit the metabolic clearance of CTL thus offsetting a decrease in plasma CTL levels (95). Along with the bone, liver, intestine, CTL is also broken down in the kidneys where is it initially converted to $1,24,25(OH)_3D_3$ by the enzyme 24-hydroxylase (96). Synthesis of the enzyme is regulated, in part, by CTL (97-99), therefore, lower CTL levels result in lower 24-hydroxylase activity. Likewise, with the number of Vitamin D receptors (VDR) decreasing in CKD (58), a reduction in

physiological response to CTL follows, leading to decreased production of 24-hydroxylase (98). Additionally, uremic toxins have been found to inhibit both the synthesis of 24-hydroylase (100), as well as the enzymatic degradation of CTL (99). Therefore, the inhibitory effect of CKD plasma biochemistry on 24-hydroxylase activity results in diminished metabolic clearance of CTL.

1.4.2.3.3. Secondary Hyperparathyroidism

During the progression of CKD, increasing PTH levels occur owing to a combination of factors: reduced Vitamin D metabolites (including, CTL), increased phosphate levels and low Ca (101).

The final step in the activation of Vitamin D to form calcitriol occurs in the kidneys and is tightly regulated by PTH, Ca and phosphate (23). In the progression of CKD, production of CTL is inhibited owing to the effect of several conditions that also accompany CKD. These include: declining renal mass—reduced sites for CTL production (51); phosphate retention which inhibits renal hydroxylation of CTL-precursors (23); hyperuricaemia (high plasma urea) and metabolic acidosis (102).

PTH production and secretion is partly controlled by Vitamin D metabolites, in particular CTL. At the genetic level, PTH gene transcription is partly controlled by CTL and mediated by vitamin D receptors (VDR) in the PTG (58). The number of VDR has been found to be drastically reduced in patients with CKD (103) and rats and dogs that underwent nephrectomy (104, 105). The reduction of Vitamin D receptors (VDR) occurs due to the fact that CTL binding to VDR stabilizes the receptor and increases its half-life (106). Additionally, CTL up regulates VDR mRNA in both the kidneys and PTG thus regulating the number of VDR (58). Therefore, declining CTL, and as a result PTG-VDR reduction in CKD, causes PTG-resistance to the inhibitory effects of CTL (i.e. higher PTH levels).

Phosphate retention in CKD initiates a series of responses in the phosphate homeostatic control system which over time contribute to excess PTH secretion. Increased plasma phosphate levels stimulate FGF-23 and PTH secretion which act to reduce renal phosphate reabsorption (107). FGF-23 inhibits the production of CTL which leads to decreased intestinal phosphate absorption. However, the low CTL leads to increased PTH secretion (82). FGF-23 also directly inhibits PTH production and secretion (14, 108).

In the PTG, the specific receptor for FGF-23 is formed by the two cofactors, the enzyme Type I membrane-bound α-Klotho (Klotho) and fibroblast growth factor-receptor 1 (FGFR1)—Klotho/FGFR1 (109, 110). The detection of FGF23 by Klotho/FGFR1 initiates the inhibition of

PTH production in the PTG. Different studies have shown that there is an overall decrease in Klotho and FGFR1 in PTGs of patients with CKD (86, 111-113) which may be due to an intrinsic glandular defect, or, is a result of the dynamic biochemical changes brought on by CKD (86). This decline in Klotho and FGFR1 levels cause diminished response of PTG to FGF23, thereby indicating FGF23-resistance in the PTG of CKD patients (13, 14). As such, as CKD progresses increased phosphate retention and decreased Klotho/FGFR1 leads to increasing PTH levels even in the presence of increased FGF23 (114).

1.5. Approaches to Ca homeostasis modeling

1.5.1. General Models

From a review of the relevant literature, mathematical modeling of Ca homeostasis seems to be an understudied area. Since 1979, only a few papers have focused on describing mathematical models for calcium regulation (115-118). All the models reviewed have used the technique of compartmental modeling to isolate the different processes involved in Ca regulation and present a mathematical relationship for each.

One of the first papers published on this topic was by Jaros et al., (115) who provided a computer model of the system in the face of unreliable data and unknown mathematical relationships. They divided the regulatory system into four groups, the: 1) distribution (extracellular fluid); 2) intermediary (bone – fluid and solid); 3) terminal (intestine and kidneys); and, 4) coordinating (Parathyroid gland, thyroid gland and vitamin D metabolism) subsystems. However, graphical interpolations were used to derive many of the relationships. With these limitations, the model could only simulate short-term scenarios, and were time consuming as, based on the computing environment, each simulation required continual operator intervention for its completion.

Subsequent papers to this research framed calcium regulation in the form of a “designed” control system. Hurwitz et al., (117) improved upon the previous approach by describing the mechanism, as a feedback-control system in birds. Here the bone, kidneys and intestines were considered the “control subsystems” and the PTH and calcitriol, regulating hormones. They also provided explicit differential equations for plasma Ca, PTH and calcitriol; and expressions for the flows of bone, renal and intestinal calcium. However several of the relationships were simplified by assuming linear and polynomial dependencies on Ca, while PTH and calcitriol secretory rates were determined through tabular interpolations. In a later paper (119), they combined their Ca

regulatory model with one representing the growth dynamics in chicks to simulate the impact of growth on Ca metabolism.

A more detailed model for the human body was published by Raposo et al., (118) who improved upon the avian Ca regulatory model (117). Here they had more reliable clinical data and 'newly' established hormonal secretory expressions for PTH and calcitriol. Therefore, they could provide better mathematical representations for the ions and hormones. However, their representation of bone Ca transfer was limited and thus simplified due to insufficient data. For their model, calcium, PTH and calcitriol were the "controlling factors" and the "effector organs" were the parathyroids, bone, kidneys and intestines. They also used a hyperbolic tangent relationship to describe many of the secretory functions and defined an 'affinity' term that would be hard to determine in actual clinical conditions.

To date, the most complete model of calcium homeostasis has been that described by Peterson & Riggs (120), who adapted the model by Raposo et al., (118) and integrated aspects of bone modeling from two other papers (37, 121). For bone cell (OB and OC) proliferation, they included the work by Lemaire et al., (37), while they added a putative model for the PTH induced osteoblast intracellular activity that was qualitatively described by Bellido et al., (121). The paper largely focused on the therapeutic and diseased states effect on the bone biology.

Unfortunately, trying to replicate these last two models (118, 120) proved futile as many of the parameter estimates in both papers were missing. However, they function as a primary reference in developing the model discussed herein.

1.5.2. Models based on a control system framework

In devising a regulatory model to look at hypocalcemic pregnant cows, Ramberg et al. (116) framed the system in terms of signals: controlled (bone calcium mass and plasma calcium); disturbing (calcium intake and clearance – fecal, bone, placenta and milk); and controlling (intestinal calcium absorptive efficiency, fractional bone removal rate, and renal calcium fractional absorption). They ignored the role of hormones in the Ca regulatory system; instead, evaluating the system using material balance where only the cow's Ca inputs and outputs (diet, urine, feces, milk, bone and fetus) were taken into account.

A designed control system approach more in line with control theory was purported by Saunders et al., (122) and improved upon by El-Samad et al (123). Saunders et al., (122) postulated that Ca homeostasis, in humans, is achieved through a control scheme they defined as Integral Rein

Control (IRC). In IRC the system is under integral control and steady-state can be obtained through a few co-dependent state-variables that are independent of the external variables. A key feature of their work is that the set-points of the co-dependent variables are dynamically set rather than fixed. In the paper, calcium was the controlled variable and PTH and calcitonin the two co-dependent variables whose set points are dynamically adjusted by a third variable, CgA (a chromogranin-derived peptide co-secreted with both hormones). The only rate considered in the model is that of intestinal calcium absorption. Although the physiological premise of their paper was not completely consistent with available medical literature, it explicitly showed that integral control is involved in calcium homeostasis.

El-Samad et al., (123) then improved on this model providing a more physiologically representative model for the cow which incorporated the activity of PTH and calcitriol. They identified a proportional-integral (PI) feedback controller for regulating calcium homeostasis. Here, the renal calcium clearance is considered the disturbance; the process is ECF plasma Ca; and, the controller incorporates both PTH (proportional) and calcitriol (integral). However, their model did not address many of the intervening processes involved in Ca homeostasis and as such can only simulate an overall behavior of the Ca regulatory system.

1.6. Controller Design in Biological Systems

To date, there is no implementation of an external controller to a defective Ca regulatory model. However, such controllers have been developed for other biomedical systems, including glucose regulation (124), blood pressure control (125, 126) and delivery of anesthesia (127). Common among these works is the use of variants of model predictive control (MPC) for controller design. The success of MPC in these applications makes it attractive for use in developing an external Ca regulatory controller.

The basis of MPC design, and its superiority to classical control, is the use of a process model to predict future plant behavior and implement the necessary corrective actions such that the predicted output is as close as possible to the set point. There are four important elements to the structure of all MPC designs: 1) a desired reference trajectory for the process output (controlled variable – CV); 2) an appropriate model to predict the process output over a given time; 3) calculating the optimization objective based on specified constraints and results from the process model; and, 4) the plant measurement and predicted values are compared and the error used to update future predictions (128).

The advantages to using model predictive controllers in physiological systems include:

1. MPC takes action for any predicted excursions before they occur whereas classical controllers respond only after the disturbance has occurred. This is due to the fact that MPC estimates future controlled variable (CV) behavior based on: i) previous manipulated variable (MV) inputs; and ii) measurement of the actual CV values which is used as a feedback signal to correct the CV predictions (124).
2. MPCs can be tailored to a subject's diurnal routine such that the controller MV inputs compensate for irregular behavior before they occur. PIDs only react to CV changes once they've occurred (129).
3. CV and MV constraints are inherent in any biomedical problem which MPC easily handles. On the other hand, classical controllers require special formulations in compensating for such constraints which may result in erosion of controller performance (124, 130).
4. Additionally, MPC is able to handle time delays, nonlinear processes and multivariable problems (131).

Notwithstanding these advantages, there are a few drawbacks to MPC. Although MPC is easy to implement, the derivation of the model is more complex than the classical PID controller. Likewise, the computation time for the model can be very high and is even higher when constraints are considered. Finally, the benefits obtained from MPC is dependent on the disparity between the real process and the model used (132).

In devising a model for glucose control in diabetic patients, Parker et al., (124) used compartmental modeling techniques to construct a basic model of the diabetic patient. Once complete, they developed a linear- model predictive controller using the identified step response model. Kwok et al., used a long-range predictive control algorithm for the computerized drug delivery for blood pressure control in dogs (125) and later patients undergoing coronary artery bypass (126). Wada and Ward created a single-input multiple output controller using optimal control principles along with a pharmo-kinetic model for intravenous drug delivery to regulate drug concentrations at target site while limiting side-effect drug concentrations (127).

1.7. Opportunities for improvement in modeling Ca regulation

1.7.1. Phosphate

Owing to the limited information available regarding phosphate regulation and based on the fact that phosphate and Ca regulation occur in tandem, a minimal mathematical model is described. However, it would be helpful to have a more detailed model of phosphate regulation as it impacts PTH and CTL secretion and therefore Ca regulation. More importantly, the phosphate-PTH-CTL-Ca interactions become more important during pathological states.

1.7.2. Parathyroid hormone (PTH)

As PTH is an integral part of Ca control, it is important to be able to model as much of its physiological behavior as possible. As such, it would be worthwhile to consider the following PTH secretory behaviors and stimuli that have been neglected:

- pulsatile secretions during normo-, hypo- and hypercalcemia;
- asymmetric response to hypo- and hypercalcemic episodes;
- differential response to the rate of change of Ca;
- response to phosphate and hormone changes.

The incorporation of these complexities, especially phosphate and hormonal impacts, would aid in the development of external controllers for improving pathological conditions.

1.7.3. Calcitriol

Very little focus has been placed on calcitriol beyond its impact on intestinal calcium and PTH secretion. However, it is known to have an impact on bone cell proliferation, and FGF23 and transcalciferin affect its secretion and circulation.

1.7.4. Overall Ca regulatory model

Neither of the two recent models (118, 120) are immediately replicable as many of the parameters are missing from their reports. However both models serve as a guide in developing a working model. Also, meal Ca and phosphate are considered continuous inputs rather than transient inputs which is more consistent with physiological behavior.

1.7.5. Pharmacodynamic Models

As mathematical modeling of Ca regulation is in its infancy, there aren't any models available describing the physiological behavior in the presence of drugs and hormones used in the treatment of Ca-related disorders. A pharmacodynamic model of any of these therapies would be an important step in the development of an external controller that could be used for improving treatment.

1.7.6. External Controllers

A significant milestone in modeling Ca regulation would be the availability of an external controller to optimize clinical therapy administration (e.g. hormones, bisphosphonates or calcimimetics) while at the same time maintaining plasma levels of PTH and Ca and thereby alleviating the compounding effects of these disorders e.g. osteoporosis as a result of hyperparathyroidism.

1.8. References

1. **Khoo MCK** 2000 Physiological control systems : analysis, simulation, and estimation. New York: IEEE Press
2. **Doyle FJI, Bequette BW, Middleton R, Ogunnaike B, Paden B, Parker RS, Vidyasagar M** 2011 Control in Biological Systems. In: Samad T, Annaswamy A eds. The Impact of Control Technology: IEEE Control Systems Society
3. **Mundy GR, Guise TA** 1999 Hormonal control of calcium homeostasis. Clinical Chemistry 45:1347-1352
4. **Griffin JE, Ojeda SR** 2000 Textbook of endocrine physiology. 4th ed. New York, N.Y.: Oxford University Press
5. **Parfitt AM** 1993 Calcium homeostasis. Heidelberg, Allemagne: Springer
6. **Wong SM, Chase HS** 1986 Role of intracellular calcium in cellular volume regulation. American Journal of Physiology - Cell Physiology 250:C841-C852
7. **Krüger B, Albrecht E, Lerch MM** 2000 The Role of Intracellular Calcium Signaling in Premature Protease Activation and the Onset of Pancreatitis. American Journal of Pathology 157:43-50
8. **Kovacs WJ, Ojeda SR** 2012 Textbook of Endocrine Physiology. 6th ed. Oxford: Oxford University Press
9. **Bergwitz C, Juppner H** 2010 Regulation of phosphate homeostasis by PTH, vitamin D, and FGF23. Annual Review of Medicine 61:91-104
10. **Diaz R, Fuleihan GE-H, Brown EM** 2010 Parathyroid Hormone and Polyhormones: Production and Export. In: Comprehensive Physiology: John Wiley & Sons, Inc.
11. **Bergwitz C, Juppner H** 2011 Phosphate Homeostasis Regulatory Mechanisms. Pediatric Bone: Biology & Diseases:141-161
12. **Naveh-Many T, Silver J** 2005 Regulation of Parathyroid Hormone Gene Expression by 1,25-Dihydroxyvitamin D. In: Molecular Biology of the Parathyroid: Springer US; 84-94
13. **Krajisnik T, Björklund P, Marsell R, Ljunggren Ö, Åkerström G, Jonsson KB, Westin G, Larsson TE** 2007 Fibroblast growth factor-23 regulates parathyroid hormone and 1α-hydroxylase expression in cultured bovine parathyroid cells. Journal of Endocrinology 195:125-131
14. **Ben-Dov IZ, Galitzer H, Lavi-Moshayoff V, Goetz R, Kuro-o M, Mohammadi M, Sirkis R, Naveh-Many T, Silver J** 2007 The parathyroid is a target organ for FGF23 in rats. Journal of Clinical Investigation 117:4003-4008

15. **Kilav R, Silver J, Naveh-Many T** 2005 Regulation of Parathyroid Hormone mRNA Stability by Calcium and Phosphate. In: Molecular Biology of the Parathyroid: Springer US; 57-67
16. **Schmitt CP, Schaefer F, Bruch A, Veldhuis JD, Schmidt-Gayk H, Stein G, Ritz E, Mehls O** 1996 Control of pulsatile and tonic parathyroid hormone secretion by ionized calcium. The Journal of clinical endocrinology and metabolism 81:4236-4243
17. **Parfitt AM** 1982 Hypercalcemic hyperparathyroidism following renal transplantation: differential diagnosis, management, and implications for cell population control in the parathyroid gland. Mineral and electrolyte metabolism 8:92-112
18. **Lee MJ, Roth SI** 1975 Effect of calcium and magnesium on deoxyribonucleic acid synthesis in rat parathyroid glands in vitro. Laboratory Investigation 33:72-79
19. **Kremer R, Bolivar I, Goltzman D, Hendy GN** 1989 Influence of calcium and 1,25-dihydroxycholecalciferol on proliferation and proto-oncogene expression in primary cultures of bovine parathyroid cells. Endocrinology 125:935-941
20. **Nygren P, Larsson R, Johansson H, Ljunghall S, Rastad J, Akerstrom G** 1988 1,25(OH)2D3 inhibits hormone secretion and proliferation but not functional dedifferentiation of cultured bovine parathyroid cells. Calcified Tissue International 43:213-218
21. **Naveh-Many T, Rahamimov R, Livni N, Silver J** 1995 Parathyroid cell proliferation in normal and chronic renal failure rats. The effects of calcium, phosphate, and vitamin D. Journal of Clinical Investigation 96:1786-1793
22. **Slatopolsky E, Finch J, Ritter C, Denda M, Morrissey J, Brown A, DeLuca H** 1995 A new analog of calcitriol, 19-nor-1,25-(OH)2D2, suppresses parathyroid hormone secretion in uremic rats in the absence of hypercalcemia. American Journal of Kidney Diseases 26:852-860
23. **Jones G, Strugnell SA, DeLuca HF** 1998 Current understanding of the molecular actions of vitamin D. Physiological Reviews 78:1193-1231
24. **Fraser DR** 1980 Regulation of the metabolism of vitamin D. Physiological Reviews 60:551-613
25. **Bai X-Y, Miao D, Goltzman D, Karaplis AC** 2003 The autosomal dominant hypophosphatemic rickets R176Q mutation in fibroblast growth factor 23 resists proteolytic cleavage and enhances in vivo biological potency. Journal of Biological Chemistry 278:9843-9849

26. **Sakaki T, Kagawa N, Yamamoto K, Inouye K** 2005 Metabolism of vitamin D3 by cytochromes P450. Frontiers in Bioscience 10:119-134
27. **Kurbel S, Radic R, Kotromanovic Z, Puseljic Z, Kratofil B** 2003 A calcium homeostasis model: orchestration of fast acting PTH and calcitonin with slow calcitriol. Medical Hypotheses 61:346-350
28. **Bronner F** 2009 Recent developments in intestinal calcium absorption. Nutrition Reviews 67:109-113
29. **Katai K, Miyamoto K-i, Kishida S, Segawa H, Nii T, Tanaka H, Tani Y, Arai H, Tatsumi S, Morita K** 1999 Regulation of intestinal Na+-dependent phosphate co-transporters by a low-phosphate diet and 1, 25-dihydroxyvitamin D3. Biochemical Journal 343:705
30. **Parfitt AM** 1980 Morphologic Basis of Bone-Mineral Measurements - Transient and Steady-State Effects of Treatment in Osteoporosis. Mineral and Electrolyte Metabolism 4:273-287
31. **Haynes DR, Findlay DM** 2006 Bone Resorption. In: Wiley Encyclopedia of Biomedical Engineering: John Wiley & Sons, Inc.
32. **Parfitt AM** 1976 The actions of parathyroid hormone on bone: relation to bone remodeling and turnover, calcium homeostasis, and metabolic bone disease. Part III of IV parts; PTH and osteoblasts, the relationship between bone turnover and bone loss, and the state of the bones in primary hyperparathyroidism. Metabolism: Clinical and Experimental 25:1033-1069
33. **Gallagher JC** 2008 Advances in bone biology and new treatments for bone loss. Maturitas 60:65-69
34. **Aubin JE** 1998 Advances in the osteoblast lineage. Biochemistry and Cell Biology 76:899-910
35. **Jilka RL, Weinstein RS, Bellido T, Parfitt AM, Manolagas SC** 1998 Osteoblast programmed cell death (apoptosis): modulation by growth factors and cytokines. Journal of Bone and Mineral Research 13:793-802
36. **Teitelbaum SL** 2000 Bone resorption by osteoclasts. Science 289:1504-1508
37. **Lemaire V, Tobin FL, Greller LD, Cho CR, Suva LJ** 2004 Modeling the interactions between osteoblast and osteoclast activities in bone remodeling. Journal of Theoretical Biology 229:293-309

38. **Hofbauer LC, Khosla S, Dunstan CR, Lacey DL, Boyle WJ, Riggs BL** 2000 The roles of osteoprotegerin and osteoprotegerin ligand in the paracrine regulation of bone resorption. Journal of Bone and Mineral Research 15:2-12
39. **Greenfield EM, Bi Y, Miyauchi A** 1999 Regulation of osteoclast activity. Life sciences 65:1087-1102
40. **Bonewald LF, Dallas SL** 1994 Role of active and latent transforming growth factor beta in bone formation. Journal of cellular biochemistry 55:350-357
41. **Alliston T, Choy L, Ducy P, Karsenty G, Derynck R** 2001 TGF-beta-induced repression of CBFA1 by Smad3 decreases cbfa1 and osteocalcin expression and inhibits osteoblast differentiation. The EMBO journal 20:2254-2272
42. **Mundy GR** 1999 Cellular and molecular regulation of bone turnover. Bone 24:35S-38S
43. **Yamashita T, Yoshioka M, Itoh N** 2000 Identification of a novel fibroblast growth factor, FGF-23, preferentially expressed in the ventrolateral thalamic nucleus of the brain. Biochemical and biophysical research communications 277:494-498
44. **Nishi H, Nii-Kono T, Nakanishi S, Yamazaki Y, Yamashita T, Fukumoto S, Ikeda K, Fujimori A, Fukagawa M** 2005 Intravenous calcitriol therapy increases serum concentrations of fibroblast growth factor-23 in dialysis patients with secondary hyperparathyroidism. Nephron Clinical Practice 101:c94-c99
45. **Gutiérrez OM, Smith KT, Barchi-Chung A, Patel NM, Isakova T, Wolf M** 2012 (1-34) Parathyroid Hormone Infusion Acutely Lowers Fibroblast Growth Factor 23 Concentrations in Adult Volunteers. Clinical Journal of the American Society of Nephrology 7:139-145
46. **Nishida Y, Taketani Y, Yamanaka-Okumura H, Imamura F, Taniguchi A, Sato T, Shuto E, Nashiki K, Arai H, Yamamoto H** 2006 Acute effect of oral phosphate loading on serum fibroblast growth factor 23 levels in healthy men. Kidney International 70:2141-2147
47. **Vervloet MG, van Ittersum FJ, Büttler RM, Heijboer AC, Blankenstein MA, ter Wee PM** 2011 Effects of dietary phosphate and calcium intake on fibroblast growth factor-23. Clinical Journal of the American Society of Nephrology 6:383-389
48. **Yano S, Brown EM** 2005 The Calcium Sensing Receptor. In: Molecular Biology of the Parathyroid: Springer US; 44-56
49. **Varghese J, Rich T, Jimenez C** 2011 Benign familial hypocalciuric hypercalcemia. Endocrine Practice 17 Suppl 1:13-17

50. **Tfelt-Hansen J, Yano S, Brown EM, Chattopadyay N** 2002 The Role of the Calcium-Sensing Receptor in Human Pathophysiology. Current Medicinal Chemistry - Immunology, Endocrine & Metabolic Agents 2:175-193
51. **Fraser WD** 2009 Hyperparathyroidism. Lancet 374:145-158
52. **Phitayakorn R, McHenry CR** 2006 Incidence and location of ectopic abnormal parathyroid glands. American Journal of Surgery 191:418-423
53. **Fujiwara S, Sposto R, Ezaki H, Akiba S, Neriishi K, Kodama K, Hosoda Y, Shimaoka K** 1992 Hyperparathyroidism among atomic bomb survivors in Hiroshima. Radiation Research 130:372-378
54. **Schneider AB, Gierlowski TC, Shore-Freedman E, Stovall M, Ron E, Lubin J** 1995 Dose-response relationships for radiation-induced hyperparathyroidism. The Journal of Clinical Endocrinology & Metabolism 80:254-257
55. **Khan AA, Bilezikian JP, Kung AWC, Ahmed MM, Dubois SJ, Ho AYY, Schussheim D, Rubin MR, Shaikh AM, Silverberg SJ, Standish TI, Syed Z, Syed ZA** 2004 Alendronate in Primary Hyperparathyroidism: A Double-Blind, Randomized, Placebo-Controlled Trial. Journal of Clinical Endocrinology & Metabolism 89:3319-3325
56. **Orr-Walker BJ, Evans MC, Clearwater JM, Horne A, Grey AB, Reid IR** 2000 Effects of Hormone Replacement Therapy on Bone Mineral Density in Postmenopausal Women With Primary Hyperparathyroidism: Four-Year Follow-up and Comparison With Healthy Postmenopausal Women. Archives of Internal Medicine 160:2161-2166
57. **Rubin MR, Lee KH, McMahon DJ, Silverberg SJ** 2003 Raloxifene Lowers Serum Calcium and Markers of Bone Turnover in Postmenopausal Women with Primary Hyperparathyroidism. Journal of Clinical Endocrinology & Metabolism 88:1174-1178
58. **Slatopolsky E, Brown A, Dusso A** 1999 Pathogenesis of secondary hyperparathyroidism. Kidney International 73:S14-19
59. **Grzela T, Chudzinski W, Lasiecka Z, Niderla J, Wilczynski G, Gornicka B, Wasiutynski A, Durlik M, Boszczyk A, Brawura-Biskupski-Samaha R, Dziunycz P, Milewski L, Lazarczyk M, Nawrot I** 2006 The calcium-sensing receptor and vitamin D receptor expression in tertiary hyperparathyroidism. International Journal of Molecular Medicine 17:779-783
60. **Lindberg JS, Culleton B, Wong G, Borah MF, Clark RV, Shapiro WB, Roger SD, Husserl FE, Klassen PS, Guo MD, Albizem MB, Coburn JW** 2005 Cinacalcet HCl, an oral calcimimetic agent for the treatment of secondary hyperparathyroidism in

hemodialysis and peritoneal dialysis: a randomized, double-blind, multicenter study. Journal of the American Society of Nephrology 16:800-807

61. **Kebebew E, Duh QY, Clark OH** 2004 Tertiary hyperparathyroidism: histologic patterns of disease and results of parathyroidectomy. Arch Surg 139:974-977
62. **Bilezikian JP, Khan A, Potts JT, Jr., Brandi ML, Clarke BL, Shoback D, Juppner H, D'Amour P, Fox J, Rejnmark L, Mosekilde L, Rubin MR, Dempster D, Gafni R, Collins MT, Sliney J, Sanders J** 2011 Hypoparathyroidism in the adult: epidemiology, diagnosis, pathophysiology, target-organ involvement, treatment, and challenges for future research. Journal of Bone and Mineral Research 26:2317-2337
63. **Levey AS, Coresh J, Balk E, Kausz AT, Levin A, Steffes MW, Hogg RJ, Perrone RD, Lau J, Eknoyan G** 2003 National Kidney Foundation Practice Guidelines for Chronic Kidney Disease: Evaluation, Classification, and Stratification. Annals of Internal Medicine 139:137-147
64. **U.S. Renal Data System** USRDS 2012 Annual Data Report: Atlas of Chronic Kidney Disease and End-Stage Renal Disease in the United States, National Institutes of Health, National Institute of Diabetes and Digestive and Kidney Diseases, Bethesda, MD, 2012.
65. **Boron WFBEL** 2009 Medical physiology : a cellular and molecular approach. Philadelphia, PA: Saunders/Elsevier
66. **Guyton ACHJE** 2006 Textbook of medical physiology. Philadelphia: Elsevier Saunders
67. **Smith HW** 1951 Comparative physiology of the kidney. In: Smith HW ed. The Kidney: Structure and Function in Health and Diseases. New York: Oxford University Press; 520-574
68. **Lindeman R, Tobin J, Shock N** 1985 Longitudinal studies on the rate of decline in renal function with age. Journal of the American Geriatrics Society 33:278
69. **Wesson LG** 1969 Physiology of the human kidney.
70. 2002 K/DOQI clinical practice guidelines for chronic kidney disease: evaluation, classification, and stratification. Kidney Disease Outcome Quality Initiative. American journal of kidney diseases 39:S1-S246
71. **Metcalfe W** 2007 How does early chronic kidney disease progress?: A Background Paper prepared for the UK Consensus Conference on Early Chronic Kidney Disease. Nephrology Dialysis Transplantation 22:ix26-ix30
72. **Novick AC, Gephardt G, Guz B, Steinmuller D, Tubbs RR** 1991 Long-term follow-up after partial removal of a solitary kidney. New England Journal of Medicine 325:1058-1062

73. **Mogensen C, Christensen C** 1984 Predicting diabetic nephropathy in insulin-dependent patients. New England Journal of Medicine 311:89-93
74. **Vora J, Dolben J, Dean J, Thomas D, Williams J, Owens D, Peters J** 1992 Renal hemodynamics in newly presenting non-insulin dependent diabetes mellitus. Kidney international 41:829
75. **Rennke HG** 1994 How does glomerular epithelial cell injury contribute to progressive glomerular damage? Kidney international Supplement 45:S58-63
76. **Keane WF** 2000 Proteinuria: Its clinical importance and role in progressive renal disease. American journal of kidney diseases 35:S97-S105
77. **Perico N, Codreanu I, Schieppati A, Remuzzi G** 2005 Pathophysiology of disease progression in proteinuric nephropathies. Kidney international 67:S79-S82
78. **Imanishi M, Yoshioka K, Konishi Y, Okumura M, Okada N, Sato T, Tanaka S, Fujii S, Kimura G** 1999 Glomerular hypertension as one cause of albuminuria in type II diabetic patients. Diabetologia 42:999-1005
79. **Román-García P, Carrillo-López N, Cannata-Andía JB** 2009 Pathogenesis of bone and mineral related disorders in chronic kidney disease: key role of hyperphosphatemia. Journal of Renal Care 35:34-38
80. **Loghman-Adham M** 1993 Role of phosphate retention in the progression of renal failure. Journal of Laboratory and Clinical Medicine 122:16-26
81. **Gimenez LF, Solez K, Walker W** 1987 Relation between renal calcium content and renal impairment in 246 human renal biopsies. Kidney international 31:93
82. **Martin KJ, González EA** 2011 Prevention and Control of Phosphate Retention/Hyperphosphatemia in CKD-MBD: What Is Normal, When to Start, and How to Treat? Clinical Journal of the American Society of Nephrology 6:440-446
83. **Levin A, Bakris G, Molitch M, Smulders M, Tian J, Williams L, Andress D** 2006 Prevalence of abnormal serum vitamin D, PTH, calcium, and phosphorus in patients with chronic kidney disease: results of the study to evaluate early kidney disease. Kidney international 71:31-38
84. **Vassalotti JA, Uribarri J, Chen S-C, Li S, Wang C, Collins AJ, Calvo MS, Whaley-Connell AT, McCullough PA, Norris KC** 2008 Trends in mineral metabolism: Kidney Early Evaluation Program (KEEP) and the National Health and Nutrition Examination Survey (NHANES) 1999-2004. American journal of kidney diseases 51:S56-S68
85. **Larsson T, Nisbeth U, LJUNGGREN Ö, Jüppner H, Jonsson KB** 2003 Circulating concentration of FGF-23 increases as renal function declines in patients with chronic

kidney disease, but does not change in response to variation in phosphate intake in healthy volunteers. Kidney international 64:2272-2279

86. **Krajisnik T, Olauson H, Mirza MA, Hellman P, Åkerström G, Westin G, Larsson TE, Björklund P** 2010 Parathyroid Klotho and FGF-receptor 1 expression decline with renal function in hyperparathyroid patients with chronic kidney disease and kidney transplant recipients. Kidney international 78:1024-1032

87. **Koh N, Fujimori T, Nishiguchi S, Tamori A, Shiomi S, Nakatani T, Sugimura K, Kishimoto T, Kinoshita S, Kuroki T** 2001 Severely reduced production of klotho in human chronic renal failure kidney. Biochemical and biophysical research communications 280:1015-1020

88. **John GB, Cheng C-Y, Kuro-o M** 2011 Role of Klotho in Aging, Phosphate Metabolism, and CKD. American journal of kidney diseases 58:127-134

89. **Kawashima H, Kurokawa K** 1983 Unique hormonal regulation of vitamin D metabolism in the mammalian kidney. Mineral and electrolyte metabolism 9:227

90. **Hsu CH** 2006 Calcitriol Metabolism and Action in Chronic Renal Disease. In: Calcium and Phosphate Metabolism Management in Chronic Renal Disease: Springer; 105-130

91. **Lemann Jr J, Litzow J, Lennon E** 1966 The effects of chronic acid loads in normal man: further evidence for the participation of bone mineral in the defense against chronic metabolic acidosis. Journal of Clinical Investigation 45:1608

92. **Hsu C, Vanholder R, Patel S, De Smet R, Sandra P, Ringoir S** 1991 Subfractions in uremic plasma ultrafiltrate inhibit calcitriol metabolism. Kidney international 40:868

93. **Hsu CH, Patel SR, Young EW, Vanholder R** 1991 Effects of purine derivatives on calcitriol metabolism in rats. American Journal of Physiology-Renal Physiology 260:F596-F601

94. **Hsu C, Patel S** 1990 The effect of polyamines, methyl guanine, and guanidinosuccinic acid on calcitriol metabolism. J Lab Clin Med 115:69-73

95. **Hsu CH, Patel S, Young EW, Simpson RU** 1988 Production and metabolic clearance of calcitriol in acute renal failure. Kidney international 33:530-535

96. **Reddy GS, Tserng KY** 1989 Calcitroic acid, end product of renal metabolism of 1, 25-dihydroxyvitamin D3 through the C-24 oxidation pathway. Biochemistry 28:1763-1769

97. **Colston K, Evans I, Spelsberg TC, MAcINTYRE I** 1977 Feedback regulation of vitamin D metabolism by 1, 25-dihydroxycholecalciferol. Biochem J 164:83-89

98. **Hirst M, Feldman D** 1983 Regulation of 1, 25 (OH) 2 vitamin D3 receptor content in cultured LLC-PK1 kidney cells limits hormonal responsiveness. Biochemical and biophysical research communications 116:121

99. **Hsu CH, Patel SR, Young EW** 1992 Mechanism of decreased calcitriol degradation in renal failure. American Journal of Physiology-Renal Physiology 262:F192-F198

100. **Patel S, Ke H, Vanholder R, Koenig R, Hsu C** 1995 Inhibition of calcitriol receptor binding to vitamin D response elements by uremic toxins. Journal of Clinical Investigation 96:50

101. **Friedman TC, Norris KC** 2002 The role of vitamin D in mild to moderate chronic kidney disease. Trends in Endocrinology & Metabolism 13:189-194

102. **Baran DT, Lee SW, Jo O, Avioli LV** 1982 Acquired alterations in vitamin D metabolism in the acidotic state. Calcified tissue international 34:165-168

103. **Korkor AB** 1987 Reduced binding of [3H] l, 25-dihydroxyvitamin D3 in the parathyroid glands of patients with renal failure. New England Journal of Medicine 316:1573-1577

104. **Merke J, Hügel U, Zlotkowski A, Szabo A, Bommer J, Mall G, Ritz E** 1987 Diminished parathyroid 1, 25 (OH) 2D3 receptors in experimental uremia. Kidney international 32:350-353

105. **Brown A, Dusso A, Lopez-Hilker S, Lewis-Finch J, Grooms P, Slatopolsky E** 1989 1, 25-(OH) 2D receptors are decreased in parathyroid glands from chronically uremic dogs. Kidney international 35:19-23

106. **Wiese RJ, Uhland-Smith A, Ross TK, Prahl JM, DeLuca H** 1992 Up-regulation of the vitamin D receptor in response to 1, 25-dihydroxyvitamin D3 results from ligand-induced stabilization. Journal of Biological Chemistry 267:20082-20086

107. **Cunningham J, Locatelli F, Rodriguez M** 2011 Secondary Hyperparathyroidism: Pathogenesis, Disease Progression, and Therapeutic Options. Clinical Journal of the American Society of Nephrology 6:913-921

108. **Cozzolino M, Brancaccio D, Gallieni M, Galassi A, Slatopolsky E, Dusso A** 2005 Pathogenesis of parathyroid hyperplasia in renal failure. Journal of nephrology 18:5

109. **Kurosu H, Ogawa Y, Miyoshi M, Yamamoto M, Nandi A, Rosenblatt KP, Baum MG, Schiavi S, Hu M-C, Moe OW** 2006 Regulation of fibroblast growth factor-23 signaling by klotho. Journal of Biological Chemistry 281:6120-6123

110. **Urakawa I, Yamazaki Y, Shimada T, Iijima K, Hasegawa H, Okawa K, Fujita T, Fukumoto S, Yamashita T** 2006 Klotho converts canonical FGF receptor into a specific receptor for FGF23. Nature 444:770-774

111. **Kumata C, Mizobuchi M, Ogata H, Koiwa F, Nakazawa A, Kondo F, Kadokura Y, Kinugasa E, Akizawa T** 2010 Involvement of alpha-klotho and fibroblast growth factor receptor in the development of secondary hyperparathyroidism. American journal of nephrology 31:230-238

112. **Komaba H, Goto S, Fujii H, Hamada Y, Kobayashi A, Shibuya K, Tominaga Y, Otsuki N, Nibu K-i, Nakagawa K** 2009 Depressed expression of Klotho and FGF receptor 1 in hyperplastic parathyroid glands from uremic patients. Kidney international 77:232-238

113. **Galitzer H, Ben-Dov I, Silver J, Naveh-Many T** 2009 Parathyroid cell resistance to fibroblast growth factor 23 in secondary hyperparathyroidism of chronic kidney disease. Kidney international 77:211-218

114. **Gutierrez O, Isakova T, Rhee E, Shah A, Holmes J, Collerone G, Jüppner H, Wolf M** 2005 Fibroblast growth factor-23 mitigates hyperphosphatemia but accentuates calcitriol deficiency in chronic kidney disease. Journal of the American Society of Nephrology 16:2205-2215

115. **Járos GG, Coleman TG, Guyton AC** 1979 Model of short-term regulation of calcium-ion concentration. SIMULATION 32:193-204

116. **Ramberg CF, Jr., Johnson EK, Fargo RD, Kronfeld DS** 1984 Calcium homeostasis in cows, with special reference to parturient hypocalcemia. The American journal of physiology 246:R698-704

117. **Hurwitz S, Fishman S, Bar A, Pines M, Riesenfeld G, Talpaz H** 1983 Simulation of calcium homeostasis: modeling and parameter estimation. The American journal of physiology 245:R664-672

118. **Raposo JF, Sobrinho LG, Ferreira HG** 2002 A minimal mathematical model of calcium homeostasis. The Journal of clinical endocrinology and metabolism 87:4330-4340

119. **Hurwitz S, Fishman S, Talpaz H** 1987 Calcium dynamics: a model system approach. The Journal of nutrition 117:791-796

120. **Peterson MC, Riggs MM** 2010 A physiologically based mathematical model of integrated calcium homeostasis and bone remodeling. Bone 46:49-63

121. **Bellido T, Ali AA, Plotkin LI, Fu Q, Gubrij I, Roberson PK, Weinstein RS, O'Brien CA, Manolagas SC, Jilka RL** 2003 Proteasomal degradation of Runx2 shortens parathyroid hormone-induced anti-apoptotic signaling in osteoblasts. A putative

explanation for why intermittent administration is needed for bone anabolism. The Journal of biological chemistry 278:50259-50272

122. **Saunders PT, Koeslag JH, Wessels JA** 2000 Integral rein control in physiology II: a general model. Journal of Theoretical Biology 206:211-220

123. **El-Samad H, Goff JP, Khammash M** 2002 Calcium homeostasis and parturient hypocalcemia: an integral feedback perspective. Journal of Theoretical Biology 214:17-29

124. **Parker RS, Doyle FJ, III, Peppas NA** 1999 A model-based algorithm for blood glucose control in Type I diabetic patients. Biomedical Engineering 46:148-157

125. **Kwok KE, Shah SL, Clanachan AS, Finegan BA** 1995 Evaluation of a long-range adaptive predictive controller for computerized drug delivery systems. IEEE transactions on bio-medical engineering 42:79-86

126. **Kwok KE, Shah SL, Finegan B, Kwong GK** 1997 An observational trial of a computerized drug delivery system on two patients. Ieee T Contr Syst T 5:385-393

127. **Wada DR, Ward DS** 1995 Open-Loop Control of Multiple-Drug Effects in Anesthesia. Ieee T Bio-Med Eng 42:666-677

128. **Ogunnaike BA, Ray WH** 1994 Process dynamics, modeling, and control. Oxford ; New York: Oxford University Press

129. **Bruttomesso D, Farret A, Costa S, Marescotti MC, Vettore M, Avogaro A, Tiengo A, Dalla Man C, Place J, Facchinetti A** 2009 Closed-loop artificial pancreas using subcutaneous glucose sensing and insulin delivery and a model predictive control algorithm: preliminary studies in Padova and Montpellier. Journal of Diabetes Science and Technology 3:1014-1021

130. **Lynch SM, Bequette B** 2001 Estimation-based model predictive control of blood glucose in type I diabetics: a simulation study. Bioengineering Conference, 2001 Proceedings of the IEEE 27th Annual Northeast, 2001, pp 79-80

131. **Bleris LG, Vouzis PD, Arnold MG, Kothare MV** 2006 A co-processor FPGA platform for the implementation of real-time model predictive control. American Control Conference, 2006, 2006, p 6 pp.

132. **Camacho EF, Bordons C** 2004 Model predictive control: Springer London

2. A control engineering model of calcium regulation

2.1. Introduction

Calcium-dependent physiological processes require that, for normal human bodily functions, total extracellular fluid (ECF) Ca concentration be maintained within a narrow range, 2.45 ± 0.25mM (1, 2). This homeostatic requirement is met through the various processes constituting the body's Ca regulatory system. Disorders in the Ca regulatory mechanisms cause abnormal hormonal secretion and contribute to chronic imbalances in plasma Ca levels, often leading to many other long-term physiological problems (2, 3). For example, enlarged parathyroid glands (PTG) lead to over-secretion of parathyroid hormone (PTH) causing hypercalcemia and excessive bone loss.

Human Ca homeostasis is achieved through the coordinated actions of four organs: the PTG, kidneys, bone, and intestines. Ca transfer between the plasma and the kidneys, intestines and bone is regulated by the secretion of three hormones: calcitriol (CTL), calcitonin (CTN) and PTH (1, 2).

Figure 2.1A shows a schematic of hormonal Ca and phosphate (PO_4) regulation according to the following mechanisms. Ca-sensing receptors (CaR) located on the surface of the PTG detect sub-basal Ca levels (hypocalcemia) and stimulate the production and secretion of PTH through a complex intracellular pathway (4). In the kidneys, high levels of PTH induce two distinct responses: (a) production of CTL (1,25 dihydroxyvitamin D) via the hydroxylation of 25-hydroxyvitamin D (5); and (b) increased Ca reabsorption in the renal tubules (1). Increased PTH levels, in concert with CTL, stimulate increased bone cell (osteoblasts and osteoclasts) proliferation; however, prolonged increases in PTH inhibit osteoblastic synthesis of bone collagen and other bone matrix protein, resulting in net bone resorption and subsequent transfer of Ca from bone to the plasma (6). CTL, in turn, inhibits PTH secretion by inhibiting PTG growth, and increases intestinal Ca absorption (1-4). The resulting net transfer of Ca from the kidneys, bone and intestines to the plasma increases plasma Ca to basal levels (normocalcemia). High Ca levels (hypercalcemia) produce the opposite response in each organ.

Phosphate regulation, even though not as well studied, occurs in tandem with Ca regulation, as both ions are controlled by the same hormones (7). Supra-normal phosphate levels (hyperphosphatemia) stimulate PTH secretion, which causes increased bone resorption (net transfer of phosphate to plasma) and reduced renal phosphate reabsorption (increased renal PO_4

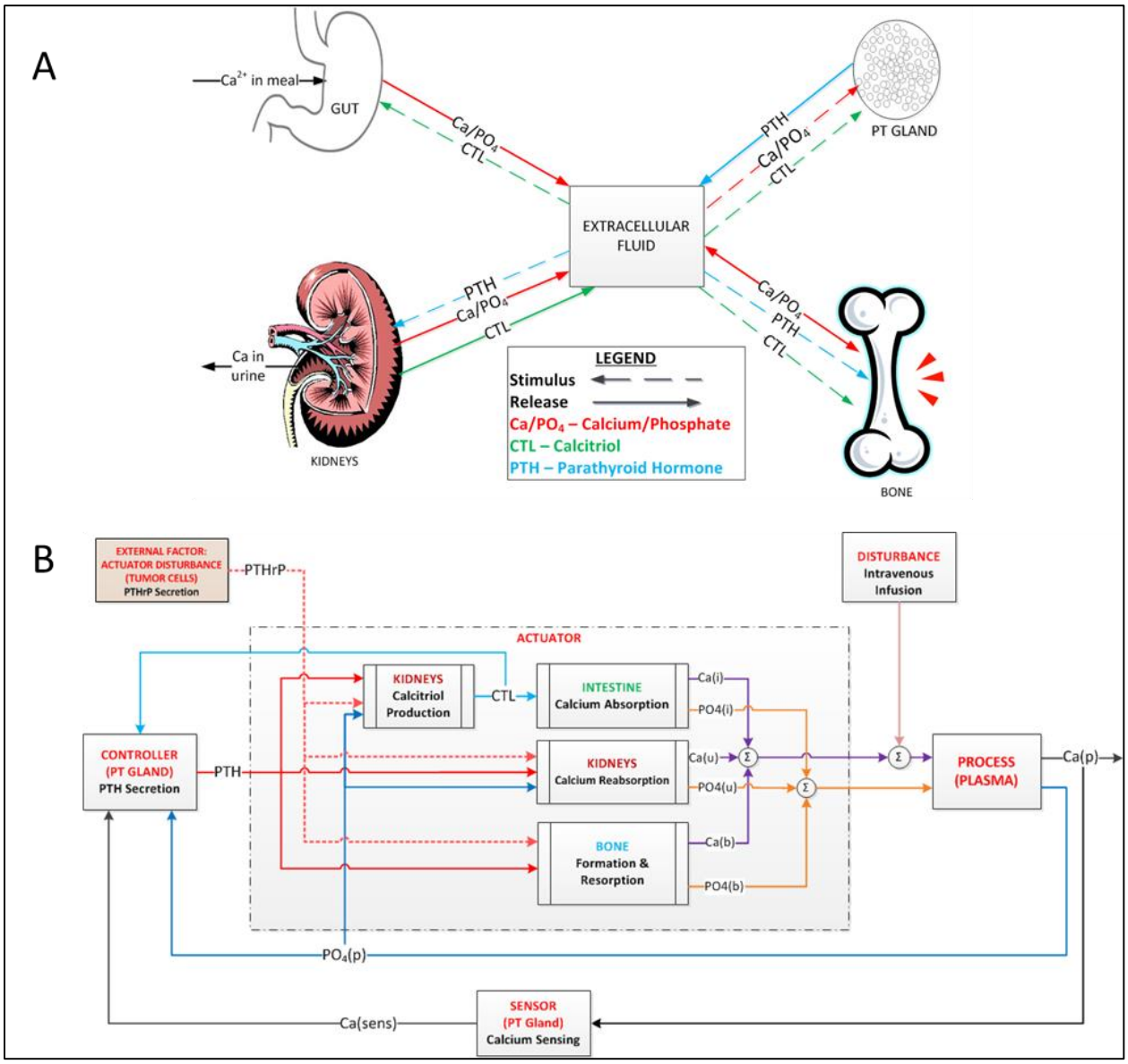

Figure 2.1. Diagrams of Ca regulation.

(A) Schematic of physiological components and mechanisms involved in Ca homeostasis. (B) Corresponding engineering control system block diagram representation of plasma calcium regulation.

excretion). CTL production is induced by the high PTH levels, but inhibited by hyperphosphatemia (8); the net effect is a reduction in CTL levels, leading to reduced intestinal PO_4 absorption (7). The overall result is a return to normal plasma PO_4 levels (normophosphatemia).

Engineering control systems (such as a residential home's HVAC system) consist of four basic elements: (a) the *sensor* receives relevant information about the variable of interest (*room*

temperature) from (b) the controlled *process (the room in question),* and transmits this information to (c) the *controller (the wall-mounted thermostat),* which determines and sends appropriate corrective action signals to (d) the *actuator* (*the compressor and fan*) for implementation on the process (9). The biological control system responsible for Ca regulation may be represented similarly by identifying the physiological equivalents of each engineering control system component as follows: (a) the sensor is the Ca-sensing receptor, CaR; (b) the controlled process is the plasma Ca and PO_4 pools; (c) the controller is the PTG; finally (d) the actuators are the kidneys, bone and intestines. This leads to the block diagram representation of Ca regulation in Figure 2.1B, where each block represents a control system component connected by lines representing the information emanating from and conveyed to each component, according to the mechanistic description of the physiological processes represented by the block in question.

From this perspective, we observe that computational modeling of human Ca regulation in the literature has been cast in the form of a series of graphical interpolations (10) or a single monolithic system of differential equations (11, 12). Alternatively, organizing the complete Ca regulatory system into interconnected functional components produces a modular representation that is easier to validate with clinical data module-by-module; it also results in an overall system that is easier to analyze holistically and from which greater fundamental insight can be derived.

2.2. Materials and Methods

The dynamic behavior of PTH, CTL, bone cell proliferation, ECF Ca and phosphate are modeled as a system of nonlinear ordinary differential equations derived from material balances applied to each component sub-processes as depicted in Figure 2.1B. The resulting equations, relevant parameters, and initial conditions, are summarized in Tables 1 and 2. A detailed description of each component sub-process along with the general assumptions and other considerations follow.

1) All hormones and ions are uniformly distributed in the ECF and their concentrations are identical to that in the plasma.
2) Consistent with receptor theory and physiological dose-response characteristics (13, 14), the rates of secretion, production or proliferation, and all hormone/ion dependencies, are described by the logistic function, $H(x)$ given in Eqn. (1). The input variable, x is the stimulus used to elicit the response, H; A_x and B_x are, respectively, the minimum and maximum rates; S_x is the midpoint (the value of x corresponding to a half-maximal response); m_x is the slope of the curve at S_x.

3) Phosphate regulation is based on the description in reference (12).
4) The effect of calcitonin (CTN) is ignored since its role in Ca regulation is not as important as that of PTH and of CTL (1, 2).
5) Least squares optimization is employed in parameter estimation.
6) All model simulations are carried out using MATLAB® and Simulink®.
7) Component defects are implemented as first-order dynamic changes over time in the relevant parameter values.

Table 2.2. Model Equations

Logistic Equation

$$H(x) = (A_x - B_x)/\left[1 + \left({}^{x}/_{S_x}\right)^{m_x}\right] + B_x \quad (1)$$

Process – *Plasma*

$$dCa_{(p)}/dt = Ca_{(i)} + Ca_{(b)} - Ca_{(u)} - Ca_{(d)} \quad (2)$$

$$dPO_{4(p)}/dt = PO_{4(i)} + PO_{4(b)} - PO_{4(u)} - PO_{4(ic)} \quad (3)^*$$

Sensor – *Ca-sensing receptor (CaR) on PTG*

$$Ca_{(s)} = K_{sens}Ca_{(p)} \quad (4)$$

Controller – *Parathyroid Gland (PTG)*

$$dPTH/dt = H\left(Ca_{(s)}\right)PTG - k_{PTH}PTH \quad (5)$$

$$\frac{dPTG}{dt} = \frac{\lambda_{PTG}}{PTG_0}\begin{Bmatrix}(PTG_{max} - PTG)[\varphi_{PTG}T^{-}_{PTG} + (1-\varphi_{PTG})] \\ -PTG[\varphi_{PTG}T^{+}_{PTG} + (1-\varphi_{PTG})]\end{Bmatrix} \quad (6)^*$$

$$T^{\pm}_{PTG} = 1 \pm tanh[\lambda_{CTL}(CTL - CTL_0)] \quad (7)$$

Actuator - *Intestines*

$$Ca_{(i)} = \frac{Ca_{meal}}{V}(H(CTL) + \lambda_{Cai}) \quad (8)$$

$$PO_{4(i)} = \lambda_{PO4i}PO_{4meal} \quad (9)$$

Actuator - *Kidneys*

$$dCTL/dt = [H_1(PTH) + H(PTHrP)]H(PO_4) - k_{CTL}CTL \quad (10)$$

$$Ca_{(u)} = \frac{GFR}{V}\begin{Bmatrix}Ca_{(p)}[0.1 - 0.09H_2(PTH)], & Ca_{(p)} \le Ca_{thr} \\ (\alpha_{Cau}Ca_{(p)} + \beta_{Cau}), & Ca_{(p)} > Ca_{thr}\end{Bmatrix} \quad (11)$$

$$PO_{4(u)} = \frac{GFR}{V}\alpha_{PO4u}PO_{4(p)} \quad (12)$$

Actuator - *Bone*

$$Ca_{(b)} = \sigma_{Cab}\begin{Bmatrix}(1-\lambda_{Cab}) + \lambda_{Cab}\left[H(OC)\left({}^{RANKL}/_{OC}\right)^{\gamma_{Cab}}\right] \\ -\frac{Ca_{(p)}}{Ca_{(p)0}}\left[(1-\lambda_{Cab}) + \lambda_{Cab}\left(\frac{OB}{OB_0}\right)\right]\end{Bmatrix} \quad (13)^*$$

$$\pi_P = \lambda_b\left(\frac{PTH + PTHrP}{PTH_0}\right)\Big/\left[\lambda_b\left(\frac{PTH + PTHrP}{PTH + PTHrP - PTH_0}\right) + PS\right] \quad (14)^*$$

$$PO_{4(b)} = \lambda_{PO4b}Ca_{(b)} \quad (15)$$

$$dPO_{4(ic)}/dt = k_{aPO4ic}PO_{4(p)} - k_{bPO4ic}PO_{4(ic)} \quad (16)^*$$

Model Disturbance – *PTHrP production*

$$dPTHrP/dt = V(R_{PTHrP} - k_{PTHrP}PTHrP) \quad (17)$$

Table 2.3. Parameter Estimates

Parameter	Value	Units	Parameter	Value	Units
$Ca_{(p)0}$	1.715E+01	mmol	φ_{PTG}	8.500E-01	Unitless
CTL_0	1.260E+03	pmol	$A_{Ca(s)}$	4.641E+02	pmol.hr^{-1}
OB_0	7.282E-04	pM cells	$A_{Ca(s)}$	6.276E+03	pmol.hr^{-1}
$PO_{4(ic)0}$	4.516E+04	mmol	$m_{Ca(s)}A$	-3.000E+01	Unitless
$PO_{4(p)0}$	1.680E+01	mmol	$m_{Ca(s)}B$	-2.500E+02	Unitless
PTG_0	5.000E-01	Unitless	$m_{Ca(s)}m$	-1.500E+02	Unitless
PTH_0	5.526E+01	pmol	$m_{Ca(s)}S_1$	1.800E+01	mmol
$\mathrm{Ca_{meal}}$	9.158E-01	mmol.hr^{-1}	$m_{Ca(s)}S_2$	1.500E+01	mmol
$\mathrm{Ca_{thr}}$	3.108E+01	mmol	A_{CTL}	4.150E-01	Unitless
GFR	6.000E+00	L.hr^{-1}	B_{CTL}	0.000E+00	Unitless
$\mathrm{k_{a,PO4ic}}$	5.180E+01	hr^{-1}	m_{CTL}	-8.416E+00	Unitless
$\mathrm{k_{b,PO4ic}}$	1.927E-02	hr^{-1}	S_{CTL}	1.306E+03	pmol
$\mathrm{k_{CTL}}$	8.660E-02	hr^{-1}	$A_{1,PTH}$	3.228E+00	hr^{-1}
$\mathrm{k_{PTH}}$	3.199E+01	hr^{-1}	$B_{1,PTH}$	1.000E+00	hr^{-1}
$\mathrm{k_{PTHrP}}$	6.932E+00	hr^{-1}	$m_{1,PTH}$	-2.000E+01	Unitless
$\mathrm{K_{sens}}$	1.000E+00	Unitless	$S_{1,PTH}$	9.823E+01	pmol
$\mathrm{PO_{4,meal}}$	5.695E-01	mmol.hr^{-1}	$A_{2,PTH}$	1.045E+00	Unitless
PS	1.500E+02	Unitless	$B_{2,PTH}$	0.000E+00	Unitless
$\mathrm{PTG_{max}}$	1.000E+00	Unitless	$m_{2,PTH}$	-6.520E+00	Unitless
V	1.400E+01	L	$S_{2,PTH}$	5.186E+01	pmol
α_{Cau}	3.146E-01	Unitless	A_{PO4}	1.034E+00	Unitless
α_{PO4u}	5.545E-02	Unitless	B_{PO4}	4.182E-01	Unitless
β_{Cau}	-5.710E+00	mmol	m_{PO4}	1.242E+01	Unitless
γ_{Cab}	6.038E-01	Unitless	S_{PO4}	1.860E+01	mmol
λ_{b}	2.907E+00	Unitless	A_{OC}	1.271E+00	Unitless
λ_{Cab}	1.500E-01	Unitless	B_{OC}	9.951E-01	Unitless
λ_{Cai}	1.500E-01	Unitless	m_{OC}	-1.188E+00	Unitless
λ_{CTL}	2.143E-03	pmol^{-1}	S_{OC}	9.615E-01	pM cells/pM cells
λ_{PO4b}	4.640E-01	Unitless	A_{PTHrP}	-4.630E-01	hr^{-1}
λ_{PO4i}	7.000E-01	Unitless	B_{PTHrP}	5.280E-01	hr^{-1}
λ_{PTG}	7.500E-02	hr^{-1}	S_{PTHrP}	1.534E+00	pM
π_{P}	-	Unitless	m_{PTHrP}	5.888E+00	Unitless
σ_{Cab}	7.973E-01	hr^{-1}	R_{PTHrP}	1.04E+01 to 3.0E+01	pMhr^{-1}

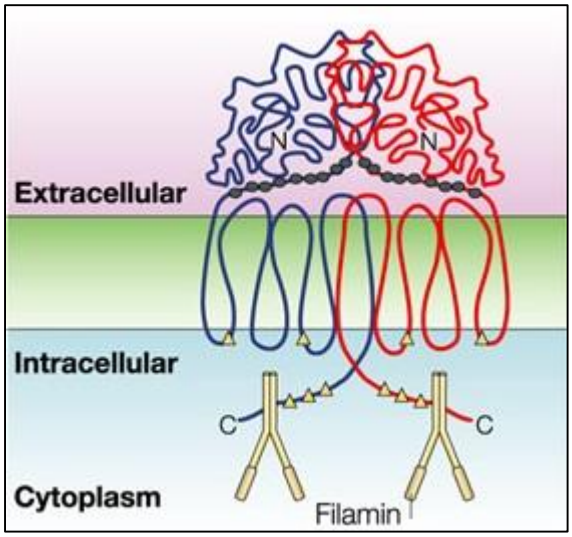

Figure 2.2. Model of the Ca-sensing receptor (CaR).

The extracellular portion of the CaR detects Ca and other agonists and transmits the signal to G-proteins embedded to the intracellular surface of the PT cell and connected to the CaR at the points labelled C. This figure is copied from (15)- Hofer.

2.2.1. Sensor: G protein-coupled Calcium-Sensing Receptors (CaR)

Ca regulation begins with the detection of Ca ions that bind to an amino-terminal domain located on the surface of the calcium-sensing receptor (CaR) (Fig. 2.2). The CaRs are attached to the surface of the PT cell via coupling to G-proteins which transmit the detected Ca signal to the cell (16). In some families, hereditary mutations of the CaR gene result in Familial Benign Hypocalciuric Hypercalcemia (FBH)—a loss-of function mutation, characterized by elevated PTH, low Ca excretion and mild-to-high hypercalcemia; or Autosomal Dominant Hypoparathyroidism (ADH)—a gain-of-sense mutation, characterized by low PTH, high urinary Ca excretion and, hypocalcemia (17).

In our model, the two processes of CaR sensing of plasma Ca, $Ca_{(p)}$, and G-protein transmission of the signal, are combined and represented by a single, linear static relationship between $Ca_{(p)}$ and the sensor output, $Ca_{(s)}$, where the constant of proportionality is the sensor gain, K_{sens}. For a healthy individual, K_{sens} is unity; for those with genetic mutations in the CaR, the gain-of-function mutation is represented as an increase in K_{sens} for ADH, or for FBH, missense mutation is represented as a decrease in K_{sens}.

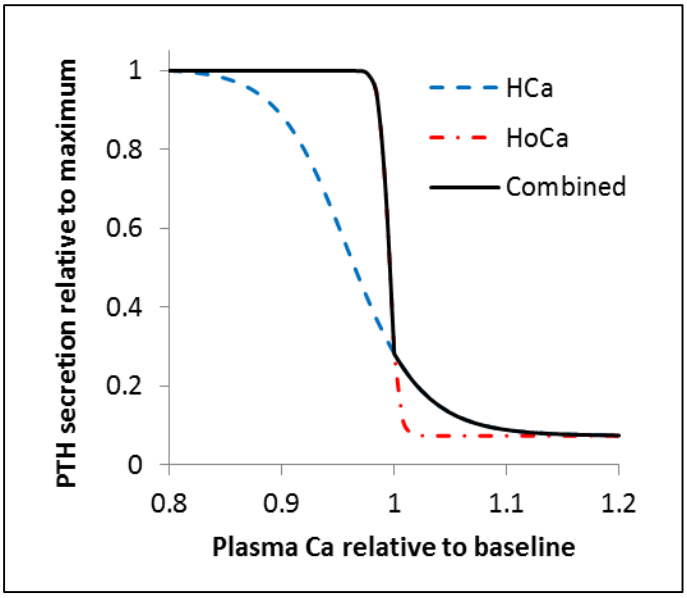

Figure 2.3 The Ca-PTH curve.
PTH secretory response to plasma Ca. during both hypercalcemia (HCa) and hypocalcemia (HoCa). Our model captures the asymmetry with the indicated 'Combined' curve

2.2.2. Controller: The Parathyroid Glands

PT cells have a two-fold response to changes in $Ca_{(p)}$: (i) cellular proliferation and (ii) increased PTH production (4), jointly resulting in an overall increase in PTH secretion. Brown (18) first proposed a reverse sigmoid relationship to represent the combined Ca-mediated PTG response. However, as shown in Figure 2.3, the change in PTH as a function of $Ca_{(p)}$ is asymmetric: generally higher under conditions of hypocalcemia (Figure 2.3 - HoCa) and lower under hypercalcemia (Figure 2.3 - HCa) (1, 4, 19). We use a model proposed in reference (20) to capture this asymmetry. Estimates of the unknown parameters in the response function, $H\left(Ca_{(s)}\right)$, are determined from published clinical data on PTH responses to induced hypo- and hypercalcemia in healthy subjects (21-23).

Increased levels of CTL are known to inhibit PT cellular proliferation both *in vivo* and *in vitro* (24) – a form of regulatory negative feedback. Although the mechanism by which this occurs is not yet fully understood (25), a cell-surface receptor-like mechanism has been proposed (4). The overall inhibition of PT cellular proliferation by CTL is therefore represented as in reference (11). Additionally, consistent with the literature (3, 19), the half-life of PTH in the plasma (related to k_{PTH}, the rate of PTH decay) is set at 1.3 minutes.

2.2.3. Actuator

2.2.3.1. Kidneys: Calcitriol Production

Circulating vitamin D_3 undergoes 25-hydroxylation, a loosely regulated process in the liver, forming 25-hydroxyvitamin D_3 (25-OH-D_3). In the kidneys, PTH from the controller and circulating PO_4 regulate the renal hydroxylation of 25-hydroxyvitamin D_3 (25-OH-D_3) to form the physiologically active CTL (1, 25-dihydroxyvitamin D_3) (5, 8). In the model, we assume an infinite supply of CTL precursors, so that hepatic hydroxylation may be ignored. On the other hand, we represent renal hydroxylation as a product of the PTH- and PO_4-dependent logistic functions, estimating the associated parameters from clinical data (26-28). Additionally, a CTL half-life of 8 hours (29) was used to determine the CTL elimination rate.

2.2.3.2. Kidneys – Renal Calcium Reabsorption

"Ca excretion" in the kidneys is defined as the difference between the filtered load—non-protein-bound Ca (i.e., soluble Ca)—and the amount reabsorbed. Filtered Ca is computed as the difference between total plasma Ca and insoluble Ca. About 80% to 90% of the filtered Ca is reabsorbed by processes linked to sodium reabsorption (30), and approximately 10% of the filtered Ca is further reabsorbed by PTH-dependent processes (1). Additionally, Ca reabsorption is limited by the capacity of the renal tubules (1). The net effect is a maximum tubular reabsorptive capacity for calcium (31), represented as "Ca threshold" (Ca_{thr}), the concentration of $Ca_{(p)}$ above which there is no additional renal reabsorption. Finally, for normal bodily function, a minimum Ca excretion rate of approximately 1mmol/day is necessary (1).

Renal excretion is represented in the model by a piecewise continuous curve where below the Ca threshold, tubular Ca reabsorption is 90% passive and 10% PTH-dependent and above the threshold, Ca excretion is independent of PTH levels and varies linearly with $Ca_{(p)}$ levels. Parameter values are determined from literature data (31).

2.2.3.3. Intestines – Calcium Absorption

The rate of Ca absorption which matches the rate of renal excretion at steady state (1), is regulated through both active and passive pathways. Passive absorption via the paracellular pathway accounts for 8% to 23% of total absorption, while transcellular active absorption is CTL-dependent (1, 30, 32). Therefore, we assume that passive absorption accounts for an average of

15% of total intestinal Ca absorption. Parameter values for CTL-dependent active absorption are determined from data published by Heaney et al (33).

2.2.3.4. Bone Cell Proliferation, Formation, and Resorption

The bone cell proliferation model used in this work is based on reference (34). To incorporate that bone model into our overall model, the PTH and PTHrP concentrations in the fractional PTH receptor occupation expression (π_P) were normalized as shown in Eqn. (14). Finally, the model linking bone cell proliferation to calcium flux is taken from reference (12) with parameters estimated using clinical data (35).

2.2.4. Model disturbance: PTH-related peptide (PTHrP) production

In order to capture tumor-related effects on Ca regulation adequately, PTHrP production must be included in the model. PTHrP is important in many physiological processes *in utero* and neonatally, including Ca control, (36) but has no effect on calcium control in the healthy adult (3). However, its production by some cancerous cells causes abnormal responses in the Ca regulatory system (37) (Figure 2.1B). While PTHrP activates PTH receptors, thus effecting responses identical to those of PTH in the kidneys and bone, it stimulates less CTL production than does PTH (3, 27).

Estimates of unknown parameters associated with plasma PTHrP levels are based on the following data: PTHrP has a half-life of 2-8 minutes (38); average basal PTHrP level in healthy subjects is 1.34pM (39), and varies between the range 2.4-51.2pM in patients with Humoral Hypercalcemia of Malignancy (HHM) (40). In addition, since PTHrP action is identical to that of PTH in the bone and renal tubules but dissimilar in CTL production, PTHrP concentration is added to the PTH concentration term in (i) the PTH-mediated CTL secretion term, $H_2(PTH)$ in eqn. (11), and (ii) the fractional PTH receptor occupation expression (π_P) in eqn. (14); finally, an independent term for PTHrP-mediated CTL production is added in eqn. (10).

2.2.5. Process: ECF Calcium and Phosphate

$Ca_{(p)}$ and $PO_{4(p)}$ concentrations in the ECF are determined from the net ion transfer rates from the kidneys, intestines, bone and any "disturbances" introduced via intravenous infusions.

2.3. Results

In what follows, the basic model is first validated against clinical data from healthy subjects. Subsequently, the utility of the validated model is demonstrated through a systematic comparison of model predictions of various Ca-related pathologies against corresponding physiological data of patients with relevant pathologies.

An important attribute of the model is its ability to predict the dynamic responses of CTL, renal Ca excretion, bone cell proliferation (CB ratio) and other such physiological variables that are often unavailable for direct measurement but which provide additional insight into the overall performance of the Ca regulatory system. For ease of comparison the simulation results are presented not in their usual clinical units but as changes relative to healthy baseline values.

2.3.1. Model Validation

The datasets used for model validation are from clinically induced hypo- and hypercalcemia in healthy subjects, in response to infusions of sodium EDTA, sodium citrate, or calcium gluconate. The corresponding model simulations are obtained by representing the experimental stimulus as an appropriate $Ca_{(p)}$ disturbance with magnitude and duration matching those of the clinical infusion. The results are shown in Figure 2.4.

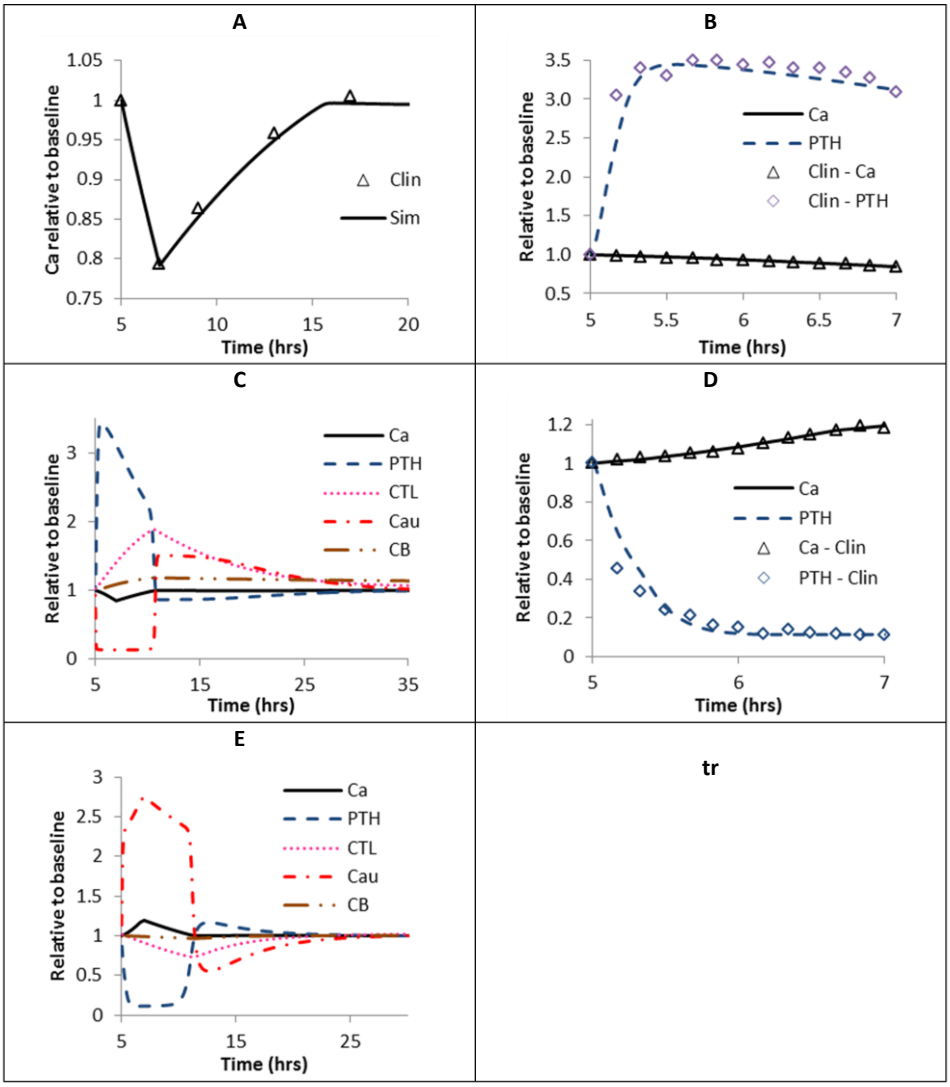

Figure 2.4. Response of healthy subjects to induced hypo- and hypercalcemia:

(A) Calcium response to 2-hr infusion of sodium EDTA (37); (B) Ca and PTH response during 2-hr infusion of sodium citrate (19); (C) Model prediction of Ca, PTH, CTL, urinary Ca and CB ratio response during and after 2-hr infusion of sodium citrate; (D) Ca and PTH response during 2-hr infusion of calcium gluconate (20); (E) Model predictions of Ca, PTH, CTL, urinary Ca and CB ratio response during and after 2-hr infusion of calcium gluconate.

Figure 2.4A shows scaled measurements of the average plasma Ca response of a group of healthy patients to a 2-hour infusion of sodium EDTA followed by a 10-hour recovery (35), with the corresponding model simulation superimposed. Similarly, as shown in Figure 2.4B, we are able to predict the PTH response during a 2-hr sodium citrate infusion (21) accurately. In response to the same sodium citrate infusion, Figure 2.4C shows the corresponding dynamic profiles of CTL, renal Ca excretion ($Ca_{(u)}$), and CB ratio; quantities not reported in the study possibly because

they are unmeasurable. Induced hypocalcemia causes an initial rapid increase in PTH with a corresponding increase in CTL and reduced Ca excretion. Upon removal of the disturbance, the subsequent increase in plasma Ca causes a gradual reduction in PTH with a consequent increase in renal excretion, $Ca_{(u)}$. Owing to its slower dynamics, CTL levels continue to rise long after PTH levels have peaked. Once normocalcemia is achieved, the inhibitory effect of high CTL levels on PTH secretion dominates the Ca-dependent PTH secretory response thus causing PTH to fall to sub-basal levels until CTL returns to baseline. Finally, PTH induces increased bone cell proliferation (CB ratio) resulting in net bone resorption; because bone cell proliferation is a slow process, the CB ratio takes a long time to return to basal levels.

In response to hypercalcemia induced by 2-hr calcium gluconate infusions in healthy subjects (22), Figure 2.4D shows how our model simulation accurately predicts clinical observations of PTH and Ca. Figure 2.4E shows our model prediction of the associated responses of the clinically unreported Ca excretion, CTL and CB profiles during infusion and recovery. The increased Ca inhibits PTH secretion leads to lower CTL secretion, greater Ca excretion, and negligible bone cell proliferation.

With the preceding results validating both our proposed modeling approach and the resulting model of Ca regulation itself, we are now in a position to use the modeling framework to investigate Ca-related pathologies as control system component defects. Understanding a particular pathology in terms of an appropriate control system component failure provides a unique perspective from which effective treatment procedure (targeted to the identified component defect) may be postulated and subsequently tested.

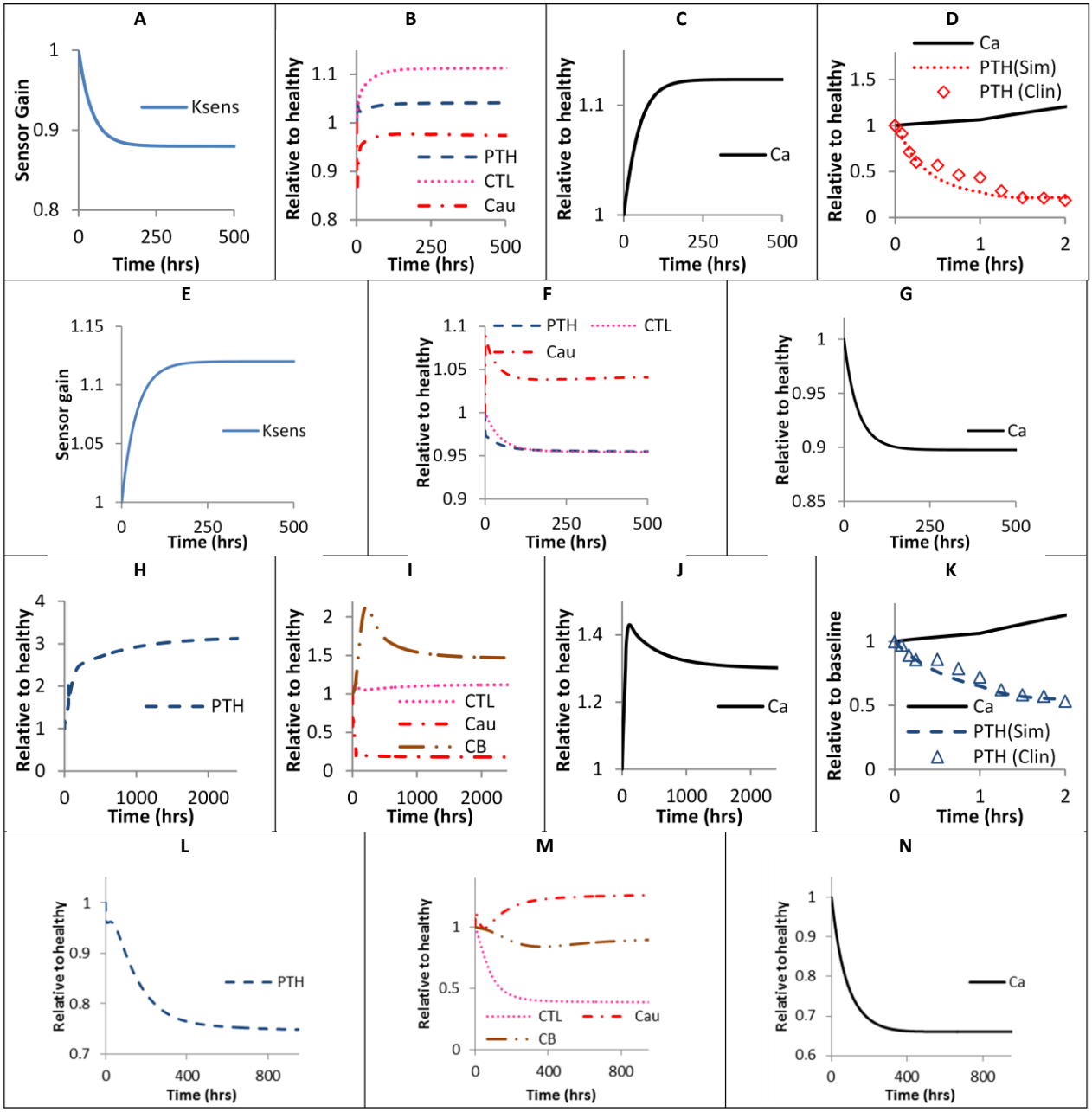

Figure 2.5. Simulations of pathologies as ECS component defects:
(A – D) FBH (Sensor defect) – Reduction in sensor gain. (A) Sensor gain change trajectory; (B) PTH, CTL, urinary Ca (Cau) responses; (C) Plasma Ca. (D) Model prediction and clinical observation of Ca and PTH response to 2-hr clinical infusion of calcium gluconate in FBH (39). **(E– G)** ADH (Sensor defect) – Increase in sensor gain. (E) Sensor gain change trajectory; (F) PTH, CTL, urinary Ca (Cau) responses; (G) Plasma Ca response. **(H – K)** PHPT (Controller defect) – Increase in PTH secretion. (H) PTH change trajectory; (I) CTL, urinary Ca and CB ratio responses; (J) Plasma Ca response. (K) Model prediction and clinical observation of Ca and PTH response to 2-hr clinical infusion of calcium gluconate in PHPT (39). **(L – N)** HoPT (Controller defect) – Decrease in PTH secretion. (L) PTH change trajectory; (M) CTL, urinary Ca, CB ratio responses; (N) Plasma Ca.

2.3.2. Model Utility: Investigation of Diseased States as Control System Component Defects

2.3.2.1. Familial Benign Hypercalcemia (FBH) and Autosomal Dominant Hypoparathyroidism (ADH) - (Sensor Defects)

FBH, characterized by elevated PTH, low Ca excretion and mild-to-high hypercalcemia (17), is due to a missense mutation of the CaR gene. From a control system perspective, therefore, FBH arises from a sensor defect. To investigate the phenomenon within our control system framework, the loss of receptor sensitivity characteristic of FBH is represented by a 12% reduction in the sensor gain,K_{sens}, occurring gradually over time according to the trajectory indicated in Figure 2.5A. A simulation of the consequences of this alteration is shown in Figures 2.5B-C. The reduced CaR sensitivity causes higher PTH secretion which in turn induces increased CTL secretion (indicating increased intestinal Ca absorption) and hypocalciuria (Figure 2.5B) leading to an overall increase in $Ca_{(p)}$ (Figure 2.5C), precisely as observed in FBH patients (17). Additionally, so that our simulation results match clinical data of induced hypercalcemia in FBH subjects (Figure 2.5D) (41), we increased the maximum (B_{Ca}) and minimum (A_{Ca}) PTH secretory rate parameters in $H(Ca_{(s)})$. Such increases are indicative of PTG growth and are consistent with clinical findings of enlarged PTGs in some cases of FBH (17, 42).

Conversely, but in conceptually similar fashion, low PTH, hypercalciuria and hypocalcemia, the pathophysiology associated with ADH, a gain-of-function mutation of the CaR gene, can be reproduced from the control system model by simulating the sensor defect as increased sensitivity of the CaR. A 12% increase in K_{sens} occurring gradually as indicated in Figure 2.5E results in an expected reduced PTH secretion which in turn causes a similar reduction in CTL levels and increased Ca excretion (Figure 2.5F) ultimately causing a reduction in $Ca_{(p)}$ (Figure 2.5G).

2.3.2.2. Primary Hyperparathyroidism (PHPT) and Hypoparathyroidism (HoPT) - (Controller Defects)

In PHPT, adenomatous or hyperplastic PTGs secrete excess PTH that induces increased renal Ca reabsorption, bone resorption and intestinal Ca absorption, leading to hypercalcemia (2, 43). Because the PTG is the controller in the control system framework, PHPT therefore arises from a controller defect. This phenomenon is represented in our model by increasing B_{Ca} and A_{Ca} and reducing the slope ($m_{Ca_{(s)}}$) to achieve a 3-fold increase in PTH levels at steady-state (Figure 2.5H). The result is an increase in CTL levels, a reduction in renal excretion and a significant

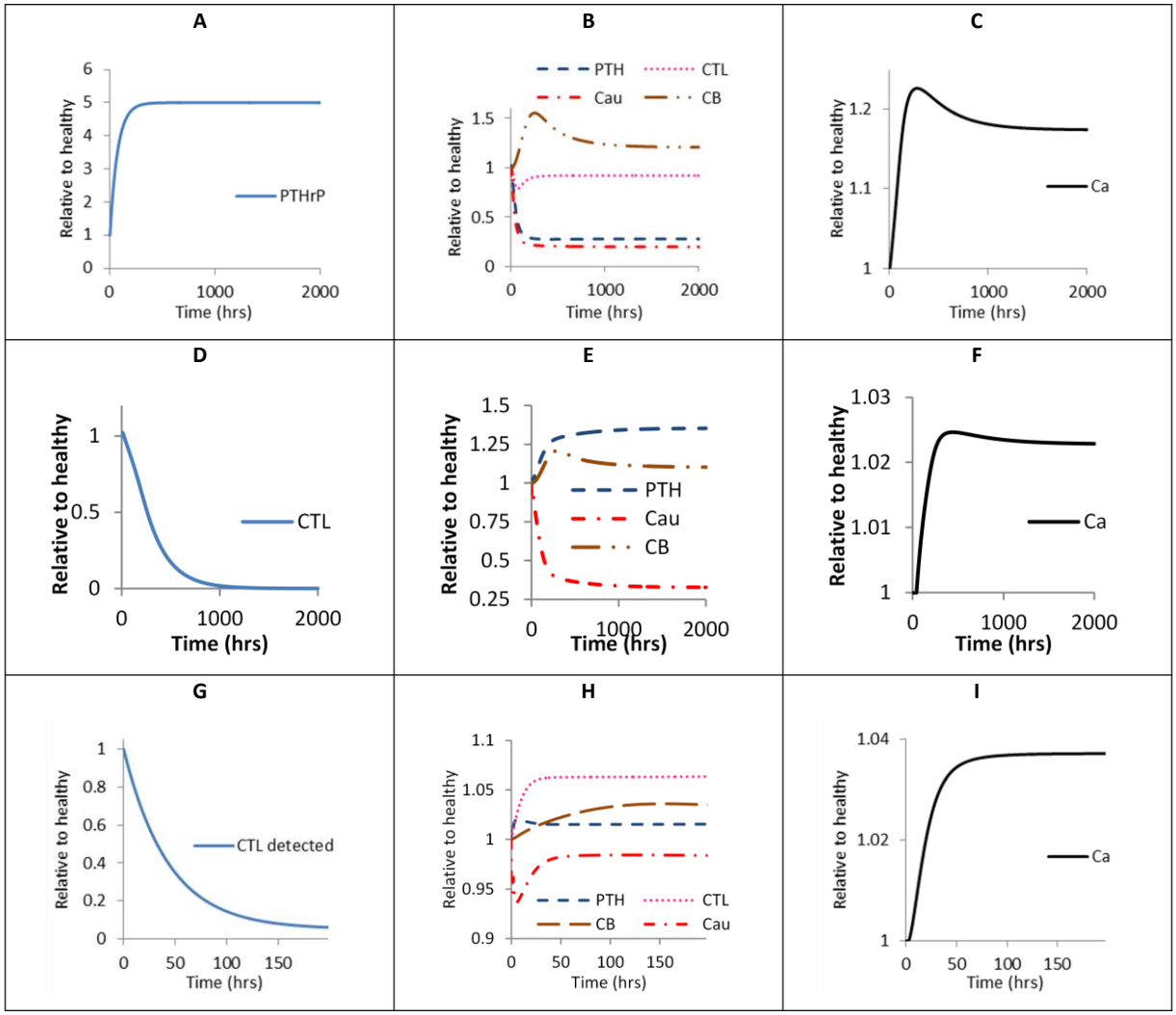

Figure 2.6. Simulations of pathologies as component defects in the ECS Ca model .

(A – C) HHM (Process disturbance) – PTHrP production. (A) PTHrP; (B) PTH, CTL, urinary Ca and CB responses; (C) Plasma Ca response; **(D – F)** Vitamin D deficiency (Actuator defect) – No production of CTL. (D) CTL; (E) Calciotropic response of PTH, urinary Ca and CB ratio; (F) Plasma Ca response. **(G – I)** CTL missense in the PTG (Controller defect). (G) Detected CTL in the PTG; (H) Calciotropic response of PTH, CTL, urinary Ca and CB ratio; (I) Plasma Ca response.

increase in CB ratio (higher bone resorption) (Figure 2.5I) and ultimately, a 30% increase in $Ca_{(p)}$ (Figure 2.5J).

Conversely, HoPT, characterized by inappropriately low or no PTH secretion, reduced CTL, hypercalciuria and hypocalcemia (44) is reproduced in simulating by decreasing A_{Ca} and B_{Ca} to obtain a 25% decrease in PTH from initial basal levels (Figure 2.5L). The result is lower CTL secretion, increased Ca excretion and a lower CB ratio (net bone formation) (Figure 2.5M), all combining to produce a 30% reduction in $Ca_{(p)}$ (Figure 2.5N).

2.3.2.3. Humoral Hypercalcemia of Malignancy (HHM) - (External Factor: Actuator Disturbance)

HHM arises because of tumorous secretion of PTHrP, which induces increased bone resorption and reduced Ca excretion leading to hypercalcemia. The resulting hypercalcemia causes reduced PTH secretion, which in turn leads to lower CTL levels (45). Since PTHrP from tumor cells affect processes in the actuator, from a control system perspective, HHM occurs due to an external factor disturbing the actuator. The phenomenon is introduced in our framework through the addition of PTHrP-secreting tumor cells (Figure 2.1B) and is simulated by increasing the PTHrP production rate, R_{PTHrP}, to obtain a five-fold increase in PTHrP levels (Figure 2.6A). The result is lower PTH and CTL levels, reduced renal Ca excretion and increased CB ratio (net bone resorption) (Figure 2.6B), with the net effect of an increase in plasma Ca levels (Figure 2.6C).

2.3.2.4. Vitamin D deficiency (VDD) - (Actuator Defects)

Vitamin D deficiency causes a reduction in the production of CTL which in turn results in increased PTH secretion, bone resorption and normocalcemia (46). This phenomenon corresponds to a defect in the very first of the four actuator blocks in Figure 2.1B, simulated in our model, by reducing the production of CTL in the kidneys to zero as shown in Figure 2.6D, essentially decommissioning this actuator. The consequent elimination of the inhibitory effect of CTL on PTH secretion causes a 40% increase in PTH levels which leads to (i) increased Ca reabsorption in the kidneys and (ii) net bone resorption through a 10% increase in the CB ratio (Figure 2.6E), with an overall effect of a marginal increase (2%) in plasma Ca levels (Figure 2.6F).

2.4. Discussion and Conclusions

Based on the premise that effective regulation of physiological processes is achieved by biological control systems that possess direct analogs with engineering control systems (ECS), we proposed a modeling and analysis framework for plasma calcium regulation in the form of an ECS. Such an approach achieves two important objectives: (i) the collection of complex sub-processes subtending Ca regulation can be organized into interconnected functional modules, thereby facilitating modeling and analysis of the entire system; and (ii) pathologies can be understood in terms of ineffective regulation caused by identifiable component defects/failures. The unknown parameters within each functional block were estimated using data from relevant clinical tests of healthy subjects; and the overall model was validated with additional clinical data

from induced hypo- and hypercalcemia. We have shown that the resulting model is capable of predicting both short- and long-term physiological changes in the Ca homeostatic environment, under both healthy and pathological conditions.

The PTH oversecretion characteristic of PHPT is implemented by an increase in the maximum (B_{Ca}) and minimum (A_{Ca}) PTH secretory rate parameters. Our simulation results for PHPT (Figures 2.5H-K) are consistent with the general clinical observations of the disease (2, 43), except that the hypocalciuria predicted by our model is consistent with less than 25% of PHPT cases (47). In order to predict the PTH response to clinically induced hypercalcemia (2-hr calcium gluconate infusion) in PHPT subjects (Figure 2.5K) (41) more accurately, it was necessary also to reduce the hypercalcemic slope ($m_{Ca(s)}A$). The relative change to the slope is therefore an indicator of decreased PTH secretory response to changes in $Ca_{(p)}$ in PHPT compared to the healthy model (41, 48) and possibly an indicator of the degree of PHPT.

In their review, Diaz et al., (4) hypothesized that a cell-surface receptor-like mechanism drives CTL-mediated PTH secretion; therefore, we investigated the effect of a missense in this receptor on Ca regulation by implementing a 95% reduction in the PTG-detected CTL (Figure 2.6G)—a controller defect. The resulting calciotropic response—increased PTH, CTL and CB ratio, reduced urinary Ca and hypercalcemia (Figure 2.6H–I)—is similar to that resulting from a decrease in K_{sens} (FBH). However, the magnitude of the effect is markedly lower for CTL-missense. This finding suggests that the pathological effects of receptor defects (Ca or CTL) on the PTG are similar, differing only in the magnitude of the respective effects on PTH secretion. Note, therefore, that our ECS model of Ca regulation makes it possible to differentiate pathologies that may otherwise be confounded.

While qualitatively accurate in general, quantitatively, the model predictions of pathological conditions do not always match all clinical observations of Ca, PTH, CTL, urinary Ca, and/or CB ratio as precisely. This is likely due to the fact that our model simulations of pathologies are based on individual component defects in the 'healthy' model (i) without accounting for the possible effects of external hormones/ions on Ca regulation under pathological conditions; and (ii) assuming that the pathologies in question manifest as defects isolated to a single component with no "interactions" from or on other sub-processes.

Nevertheless, taken together, we have demonstrated how the control engineering framework provides an efficient means for organizing the various physiological sub-processes constituting calcium regulation and facilitates a fundamental understanding of this complex physiological

process. The resulting mathematical model adequately predicts the short- and long-term dynamic characteristics of the Ca regulatory system in both healthy and pathological states. The model provides novel insights into Ca regulation by generating results about physiological variables that are currently unmeasurable. Furthermore, the framework facilitates the testing of hypotheses about mechanisms underlying the emergence of known pathologies. Currently, we are using the model to explore the differential diagnosis of Ca-related pathologies with similar pathophysiologies; as well as, to identify potential sites for therapeutic intervention in different Ca-related pathologies.

2.5. References

1. **Parfitt AM** 1993 Calcium homeostasis. Heidelberg, Allemagne: Springer
2. **Kovacs WJ, Ojeda SR** 2012 Textbook of Endocrine Physiology. 6th ed. Oxford: Oxford University Press
3. **Mundy GR, Guise TA** 1999 Hormonal control of calcium homeostasis. Clinical chemistry 45:1347-1352
4. **Diaz R, Fuleihan GE-H, Brown EM** 2010 Parathyroid Hormone and Polyhormones: Production and Export. In: Comprehensive Physiology: John Wiley & Sons, Inc.
5. **Jones G, Strugnell SA, DeLuca HF** 1998 Current understanding of the molecular actions of vitamin D. Physiological Reviews 78:1193-1231
6. **Haynes DR, Findlay DM** 2006 Bone Resorption. In: Wiley Encyclopedia of Biomedical Engineering: John Wiley & Sons, Inc.
7. **Bergwitz C, Juppner H** 2010 Regulation of phosphate homeostasis by PTH, vitamin D, and FGF23. Annual Review of Medicine 61:91-104
8. **Simboli-Campbell M, Jones G** 1991 Dietary phosphate deprivation increases renal synthesis and decreases renal catabolism of 1,25-dihydroxycholecalciferol in guinea pigs. Journal of nutrition 121:1635-1642
9. **Ogunnaike BA, Ray WH** 1994 Process Dynamics, Modeling, and Control. Oxford ; New York: Oxford University Press
10. **Járos GG, Coleman TG, Guyton AC** 1979 Model of short-term regulation of calcium-ion concentration. Simulation 32:193-204
11. **Raposo JF, Sobrinho LG, Ferreira HG** 2002 A minimal mathematical model of calcium homeostasis. Journal of Clinical Endocrinology and Metabolism 87:4330-4340
12. **Peterson MC, Riggs MM** 2010 A physiologically based mathematical model of integrated calcium homeostasis and bone remodeling. Bone 46:49-63
13. **DeLean A, Munson PJ, Rodbard D** 1978 Simultaneous analysis of families of sigmoidal curves: application to bioassay, radioligand assay, and physiological dose-response curves. American Journal of Physiology 235:E97-102
14. **Gibaldi M, Perrier D** 1982 Pharmacokinetics. New York: M. Dekker
15. **Hofer AM, Brown EM** 2003 Extracellular calcium sensing and signalling. Nature Reviews Molecular Cell Biology 4:530-538
16. **Chattopadhyay N, Mithal A, Brown EM** 1996 The calcium-sensing receptor: a window into the physiology and pathophysiology of mineral ion metabolism. Endocrine Reviews 17:289-307
17. **Yano S, Brown EM** 2005 The Calcium Sensing Receptor. In: Molecular Biology of the Parathyroid: Springer US; 44-56
18. **Brown EM** 1983 Four-parameter model of the sigmoidal relationship between parathyroid hormone release and extracellular calcium concentration in normal and abnormal parathyroid tissue. Journal of Clinical Endocrinology and Metabolism 56:572-581
19. **Schmitt CP, Schaefer F, Bruch A, Veldhuis JD, Schmidt-Gayk H, Stein G, Ritz E, Mehls O** 1996 Control of pulsatile and tonic parathyroid hormone secretion by ionized calcium. Journal of Clinical Endocrinology and Metabolism 81:4236-4243

20. **Shrestha RP, Hollot CV, Chipkin SR, Schmitt CP, Chait Y** 2010 A mathematical model of parathyroid hormone response to acute changes in plasma ionized calcium concentration in humans. Mathematical Biosciences 226:46-57
21. **Ramirez JA, Goodman WG, Gornbein J, Menezes C, Moulton L, Segre GV, Salusky IB** 1993 Direct in vivo comparison of calcium-regulated parathyroid hormone secretion in normal volunteers and patients with secondary hyperparathyroidism. Journal of Clinical Endocrinology and Metabolism 76:1489-1494
22. **Goodman WG, Veldhuis JD, Belin TR, Van Herle AJ, Juppner H, Salusky IB** 1998 Calcium-sensing by parathyroid glands in secondary hyperparathyroidism. Journal of Clinical Endocrinology and Metabolism 83:2765-2772
23. **Haden ST, Brown EM, Hurwitz S, Scott J, El-Hajj Fuleihan G** 2000 The effects of age and gender on parathyroid hormone dynamics. Clinical Endocrinology 52:329-338
24. **Nygren P, Larsson R, Johansson H, Ljunghall S, Rastad J, Akerstrom G** 1988 1,25(OH)2D3 inhibits hormone secretion and proliferation but not functional dedifferentiation of cultured bovine parathyroid cells. Calcified tissue international 43:213-218
25. **Sugimoto T, Ritter C, Slatopolsky E, Morrissey J** 1988 Effect of 1,25-dihydroxyvitamin D3 on phospholipid metabolism in cultured bovine parathyroid cells. Endocrinology 122:2387-2392
26. **Horwitz MJ, Tedesco MB, Sereika SM, Hollis BW, Garcia-Ocana A, Stewart AF** 2003 Direct comparison of sustained infusion of human parathyroid hormone-related protein-(1-36) [hPTHrP-(1-36)] versus hPTH-(1-34) on serum calcium, plasma 1,25-dihydroxyvitamin D concentrations, and fractional calcium excretion in healthy human volunteers. Journal of Clinical Endocrinology and Metabolism 88:1603-1609
27. **Horwitz MJ, Tedesco MB, Sereika SM, Syed MA, Garcia-Ocana A, Bisello A, Hollis BW, Rosen CJ, Wysolmerski JJ, Dann P, Gundberg C, Stewart AF** 2005 Continuous PTH and PTHrP infusion causes suppression of bone formation and discordant effects on 1,25(OH)2 vitamin D. Journal of bone and mineral research : the official journal of the American Society for Bone and Mineral Research 20:1792-1803
28. **Rix M, Andreassen H, Eskildsen P, Langdahl B, Olgaard K** 1999 Bone mineral density and biochemical markers of bone turnover in patients with predialysis chronic renal failure. Kidney International 56:1084-1093
29. **Kurbel S, Radic R, Kotromanovic Z, Puseljic Z, Kratofil B** 2003 A calcium homeostasis model: orchestration of fast acting PTH and calcitonin with slow calcitriol. Medical hypotheses 61:346-350
30. **Parfitt AM, Kleerekoper M** 1980 The divalent ion homeostatic system: physiology and metabolism of calcium, phosphorus, magnesium and bone. In: Maxwell M, Kleeman CR eds. Clinical Disorders of Fluid and Electrolyte Metabolism. 3rd ed. New York: McGraw-Hill; 269-398
31. **Peacock M, Nordin BE** 1968 Tubular reabsorption of calcium in normal and hypercalciuric subjects. Journal of Clinical Pathology 21:353-358
32. **McCormick CC** 2002 Passive diffusion does not play a major role in the absorption of dietary calcium in normal adults. Journal of Nutrition 132:3428-3430

33. **Heaney RP, Barger-Lux MJ, Dowell MS, Chen TC, Holick MF** 1997 Calcium absorptive effects of vitamin D and its major metabolites. Journal of Clinical Endocrinology and Metabolism 82:4111-4116
34. **Lemaire V, Tobin FL, Greller LD, Cho CR, Suva LJ** 2004 Modeling the interactions between osteoblast and osteoclast activities in bone remodeling. Journal of theoretical biology 229:293-309
35. **Parfitt AM** 1969 Study of parathyroid function in man by EDTA infusion. Journal of Clinical Endocrinology and Metabolism 29:569-580
36. **Rodda CP, Caple IW, Martin T** 1992 Role of PTHrP in fetal and neonatal physiology. Parathyroid Hormone Related Protein: Normal Physiology and Its Role in Cancer:169-196
37. **Mundy GR, Oyajobi B, Padalecki S, Sterling JA** 2009 Hypercalcemia of Malignancy. In: Clinical Endocrine Oncology: Blackwell Publishing, Ltd; 561-566
38. **Ratcliffe WA, Abbas SK, Care AD** 1993 Clearance of exogenous parathyroid hormone-related protein in pregnant, non-pregnant and fetal sheep, goats and pigs. Journal of Endocrinology 138:459-465
39. **Dobnig H, Kainer F, Stepan V, Winter R, Lipp R, Schaffer M, Kahr A, Nocnik S, Patterer G, Leb G** 1995 Elevated parathyroid hormone-related peptide levels after human gestation: relationship to changes in bone and mineral metabolism. Journal of Clinical Endocrinology and Metabolism 80:3699-3707
40. **Grill V, Ho P, Body JJ, Johanson N, Lee SC, Kukreja SC, Moseley JM, Martin TJ** 1991 Parathyroid Hormone-Related Protein: Elevated Levels in both Humoral Hypercalcemia of Malignancy and Hypercalcemia Complicating Metastatic Breast Cancer. Journal of Clinical Endocrinology & Metabolism 73:1309-1315
41. **Khosla S, Ebeling PR, Firek AF, Burritt MM, Kao PC, Heath H, 3rd** 1993 Calcium infusion suggests a "set-point" abnormality of parathyroid gland function in familial benign hypercalcemia and more complex disturbances in primary hyperparathyroidism. Journal of Clinical Endocrinology and Metabolism 76:715-720
42. **Carling T, Szabo E, Bai M, Ridefelt P, Westin G, Gustavsson P, Trivedi S, Hellman P, Brown EM, Dahl N, Rastad J** 2000 Familial Hypercalcemia and Hypercalciuria Caused by a Novel Mutation in the Cytoplasmic Tail of the Calcium Receptor. Journal of Clinical Endocrinology & Metabolism 85:2042-2047
43. **Rubin MR, Bilezikian JP, McMahon DJ, Jacobs T, Shane E, Siris E, Udesky J, Silverberg SJ** 2008 The natural history of primary hyperparathyroidism with or without parathyroid surgery after 15 years. Journal of Clinical Endocrinology and Metabolism 93:3462-3470
44. **Rubin MR, Sliney J, Jr., McMahon DJ, Silverberg SJ, Bilezikian JP** 2010 Therapy of hypoparathyroidism with intact parathyroid hormone. Osteoporosis international : a journal established as result of cooperation between the European Foundation for Osteoporosis and the National Osteoporosis Foundation of the USA 21:1927-1934
45. **Clines GA** 2011 Mechanisms and treatment of hypercalcemia of malignancy. Current Opinion in Endocrinology, Diabetes, and Obesity 18:339-346
46. **Holick MF** 2005 The vitamin D epidemic and its health consequences. Journal of Nutrition 135:2739S-2748S

47. **Younes NA, Shafagoj Y, Khatib F, Ababneh M** 2005 Laboratory screening for hyperparathyroidism. International Journal of Clinical Chemistry 353:1-12
48. **Malberti F, Farina M, Imbasciati E** 1999 The PTH-calcium curve and the set point of calcium in primary and secondary hyperparathyroidism. Nephrology, Dialysis, Transplantation 14:2398-2406

3. Modeling Phosphate Control and Chronic Kidney Disease

Plasma phosphate plays an important role in chronic kidney disease (CKD), as such, a more detailed description of phosphate regulation is required than the minimal representation provided in Chapter 2; therefore this chapter serves as a continuation of Chapter 2. Note that the updated Ca—phosphate model is only used in simulations associated with kidney disease; all other pathologies discussed in this research are simulated using the previous model.

3.1. Phosphate Control

Phosphate regulation occurs in tandem with Ca regulation as they are both regulated through the actions of PTH and CTL. In hyperphosphatemia, the high plasma PO_4 levels cause the increased production and secretion of fibroblast growth factor-23 (FGF-23) from the osteocytes and osteoblasts in the bone. Both high PO_4 and increasing FGF-23 induce increased PTH secretion from the PTG. In the kidneys, both FGF-23 and PTH reduce PO_4 reabsorption in the renal tubules. Additionally, there is a net reduction in CTL levels as CTL production is stimulated by high PTH levels but is inhibited by both hyperphosphatemia and FGF-23. The fall in CTL levels results in decreased phosphate absorption in the intestines. Increased phosphate excretion and reduced intestinal absorption lead to decline in plasma PO_4 to basal levels. The converse is true for hypophosphatemia (1).

A detailed description of the mechanisms of phosphate regulation, as depicted in Figure 3.1 is presented below. The combined Ca-PO_4 regulatory system, shown in Figure 3.2, is then validated using the same

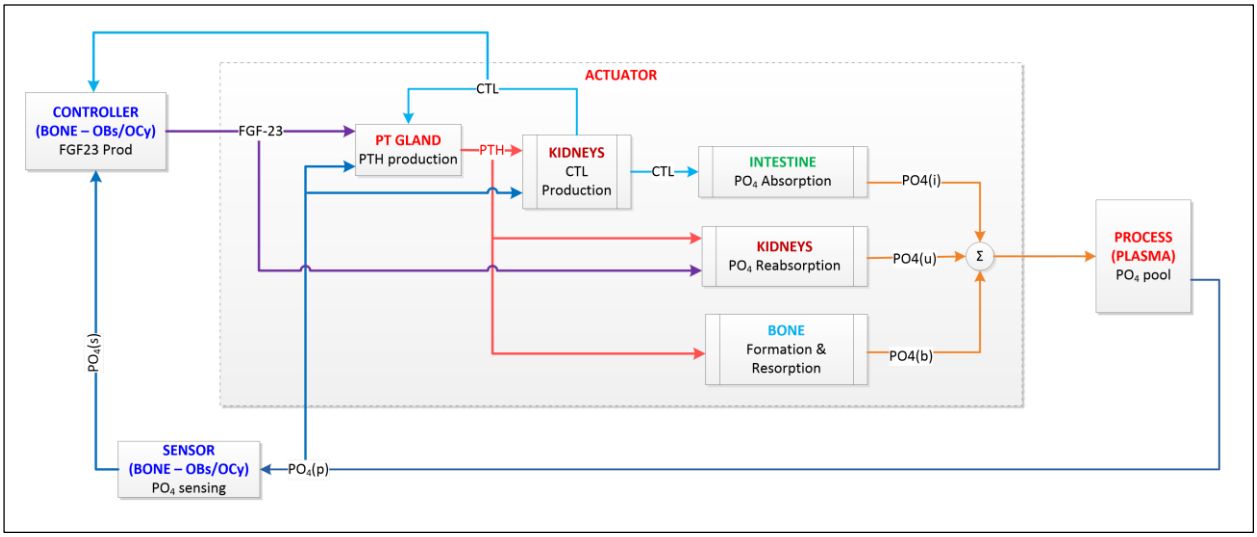

Figure 3.1. Engineering control system block diagram of plasma phosphate regulation

datasets of clinically induced hypo- and hypercalcemia in health and disease, as presented in Chapter 2. The general assumptions outlined in Chapter 2, are employed in the updated model as well:

1) All hormones and ions are uniformly distributed in the ECF and their concentrations are identical to that in the plasma.
2) Consistent with receptor theory and physiological dose-response characteristics (2, 3), the rates of production and secretion, and all hormone/ion dependencies, are described by the logistic function, $H(x)$ given in Table 2.1. The input variable, x is the stimulus used to elicit the response, H; A_x and B_x are, respectively, the minimum and maximum rates; S_x is the midpoint (the value of x corresponding to a half-maximal response); m_x is the slope of the curve at S_x.
3) Parameter estimation and model simulation are carried out using MATLAB® and Simulink®.
4) Component defects are implemented as first-order dynamic changes over time in the relevant parameter values.

3.1.1. Sensor: Osteoblasts/Osteocytes

Phosphate ions are detected by the osteoblasts and osteocytes in the bone through a yet unknown mechanism (4). As with the Ca-sensing receptor, we assume a linear relationship between the process variable, $PO_{4(p)}$, and the phosphate sensor output, $PO_{4(s)}$; the constant of proportionality is the phosphate sensor gain, $K_{PO4,sens}$, where a value of unity is assumed.

3.1.2. Controller: Osteoblasts/Osteocyte

Since the impact of PO_4 and CTL on FGF-23 secretion is greater and more prolonged than PTH (5-7) and since PTH regulates both PO_4 and CTL levels (1, 8), we assume that FGF-23 synthesis and secretion is adequately described by both PO_4- and CTL-dependence. As such, the FGF-23 production and secretory term is an addition of two logistic functions for both PO_4 and CTL. Parameter values for these expressions are estimated from published clinical data (9, 10).

There are two immunometric assays commonly used in the measurement of human FGF-23. The "C-terminal" assay measures both the intact FGF-23 peptide and carboxyl terminal (C-terminal) fragments with results reported in reference units (RU)/mL. The "intact" assay detects the intact FGF-23 peptide and its measurement units are pg/mL (9). However, there is no correlation between the two assays in determining FGF-23 levels in the physiologic range (9, 11) and the range of FGF-23 in health and disease is hard to come by due to insufficient data. We therefore use the healthy baseline for the intact peptide, 35 pg/mL (9) and a normalized range of 0.7-7 consistent with the literature (6, 7, 9). Finally, the FGF-23 elimination rate was determined from a half-life of 58 minutes (12).

3.1.3. Actuator

3.1.3.1. Parathyroid Glands

FGF-23 and CTL suppress PTH mRNA synthesis (13-15) while the stability of the transcription product (PTH mRNA) is strengthened at low Ca levels and high phosphate levels (16). We therefore updated the PTH balance equation, described in Chapter 2 (Eqn. 5), to include a logistic function for both PO_4- and FGF-dependent PTH production. Parameters for the phosphate and FGF-23 dependent functions are estimated from the literature (17).

3.1.3.2. Kidneys – Calcitriol Production

Owing to the lack of clinical data describing the effect of FGF-23 on CTL, we assumed that our representation of PO_4-dependent CTL production, $H_1(PO_4)$, incorporates the FGF-23 effect because: i) both FGF-23 and PO_4 inhibit 1α-hydroxylase synthesis during CTL production (8, 18); and, ii) FGF-23 is stimulated due to increases in PO_4 levels (1).

3.1.3.3. Kidneys – Renal phosphate Reabsorption

In the literature, there is no consensus regarding the actual site and mechanism of action of FGF-23 in the kidneys; however, it has a similar mechanism to PTH in inhibiting phosphate reabsorption (19). As such, we assumed equal weighting of the normalized concentrations of PTH and FGF-23 and use a logistic expression which takes the sum of the normalized concentrations of PTH and FGF-23 as input, thus we have $H(FGF + PTH)$.

More than 80% of the phosphate filtered in the glomerulus is reabsorbed in the proximal tubules and less than 10% in the distal segments of the nephron (20-23). Additionally, as with renal Ca absorption, there is a maximum tubular phosphate absorption rate beyond which, phosphate excretion increases linearly with plasma phosphate levels (24). Therefore, we use a piecewise continuous function to represent phosphate excretion. Below the threshold, excretion is dependent on FGF-23 and PTH while above the threshold, excretion is hormone independent. The value of the threshold and parameters for active and passive reabsorption are estimated using data from the literature (25).

3.1.3.4. Intestines – Calcium Absorption

Seventy percent of daily dietary phosphate intake is absorbed in the intestines (26) and the average phosphate intake is 30-50 mmol/day in humans (1). Seventy percent of this absorption occurs via a non-

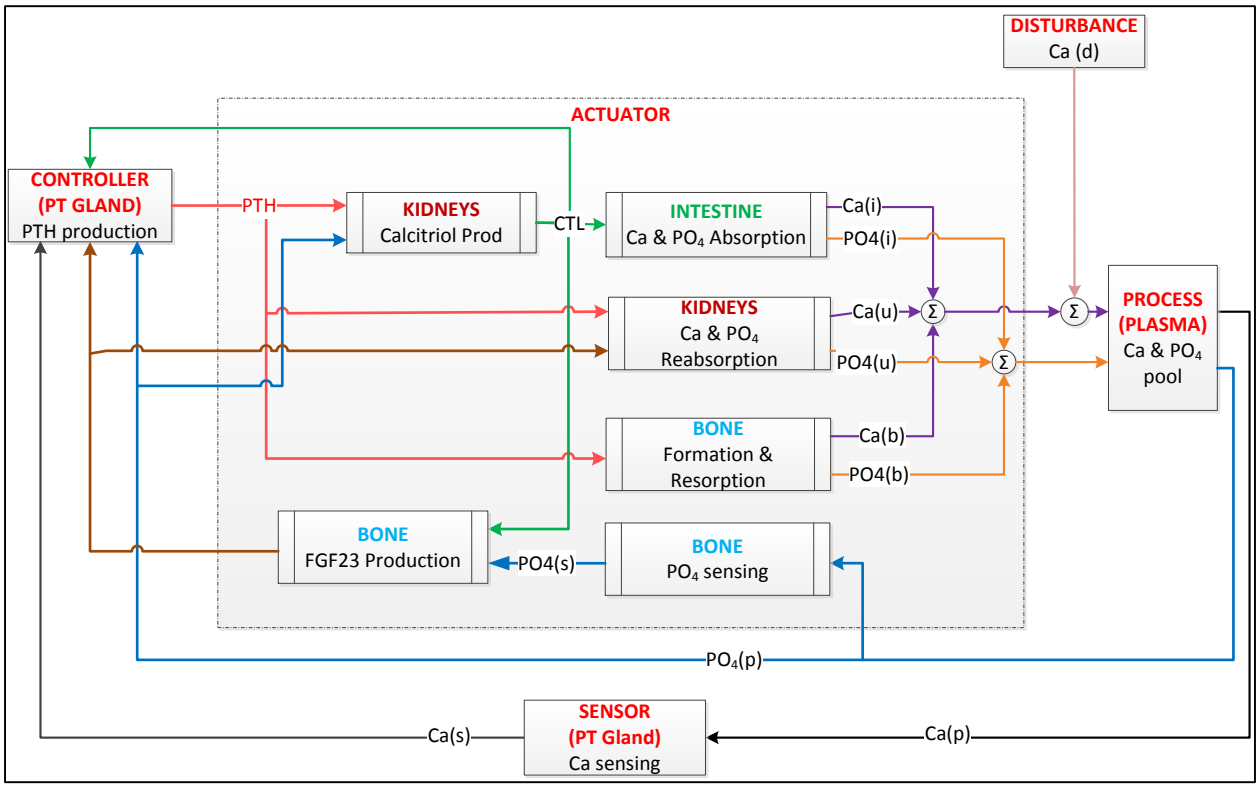

Figure 3.2. The engineering control system block diagram representation of combined plasma calcium and phosphate regulation.

saturable paracellular pathway, while the remainder occurs through a Vitamin D-dependent transcellular pathway (1, 27, 28). Therefore, we assume a daily PO_4 intake of 40 mmol/day, and use a logistic expression to describe the CTL-dependent absorption; the parameters values are estimated from the literature (29).

3.1.3.5. Bone Cell Proliferation, Formation and Resorption

Phosphate transfer between the bone and plasma is assumed to be proportional to Ca transfer and a ratio of 0.464 is used as described in the literature (30).

3.1.4. Process: ECF Calcium and Phosphate

Plasma phosphate concentration is determined using the net ion transfer rates from the kidneys, intestines, and bone.

3.2. Chronic Kidney Disease

Like the pathologies presented in Chapter 2, kidney disease originates from a defect in one organ–the kidney. As such, kidney disease is considered an *actuator defect*. During the progression from kidney disease to chronic kidney disease (CKD), the control system response to prolonged waste accumulation in the plasma leads to defects in several of the other regulatory subprocesses, namely PTH and CTL production, and even the process itself. Therefore, in modeling CKD, multiple changes within different component blocks are required. A detailed mathematical description of the key changes in the updated model is presented below followed by validation with clinical data. The updated expressions for CKD are given in the Appendix.

Renal failure: In CKD, the decline in function of the renal tubules is manifested in reductions in: the glomerular filtration rate (GFR); the hormone-dependent portion of Ca/PO_4 reabsorption; and CTL production. An independent term—renal failure (RF) — is introduced to indicate the fractional decline in renal function. RF is proportional to GFR (the clinical measure of renal failure), which is unitless and varies from 1 to 0.1.

Ca/PO4 excretion: We multiply the hormone-dependent Ca and PO_4 reabsorption by the factor, RF; because, in the absence of sufficient data, we assume that the change in reabsorption is proportional to the decline in renal function.

Circulating CTL: We assume that circulating CTL decreases proportionally with the loss in renal function; as such, we amend the CTL secretory term in the CTL production equation to include RF.

Ca/PO4 Precipitation: In the healthy body, calcium phosphate (found in bone) solubility is very low (~ $7x10^{-5}$ M) while plasma Ca levels are 2-3 orders of magnitude higher. In order to maintain such high levels of plasma Ca, plasma PO_4^{3-} concentration is very low and phosphate ions exist in the form of HPO_4^{2-} and the solubility of $CaHPO_4$ is 2 x 10^{-3}M (31). In their 1966 study, Hebert et al., showed that increasing plasma phosphate concentrations caused a reduction in plasma Ca levels via $CaHPO_4$ formation rather than through simultaneous calcium excretion (32).

Taken together, we assume that only $CaHPO_4$ is formed during hyperphosphatemia and that the plasma Ca/PO_4 threshold, beyond which $CaHPO_4$ begins to form, is the healthy baseline. With increasing plasma PO_4 levels, the excess PO_4 forms $CaHPO_4$ and plasma Ca is lowered according to the stoichiometric ratio.

Secondary Hyperparathyroidism: In order to account for the PTG hyperplasia that occurs during CKD, the same model as used in PHPT is employed for SHPT (increasing the maximum and minimum PTH secretory rates and reducing hypercalcemic slope).

3.3. Model Validation

3.3.1. Ca/PO4 Regulation

In this section, the results from the more comprehensive Ca-PO_4 model—denoted as the *"Combined"* model—are compared with both the clinical dataset and the results from the previous model— denoted as *"Model (1)"*. As the dynamics of Ca control were discussed in the previous sections, the focus of this section will be on the observable differences between the two models as well as the dynamics of the *combined* model as it relates to phosphate control.

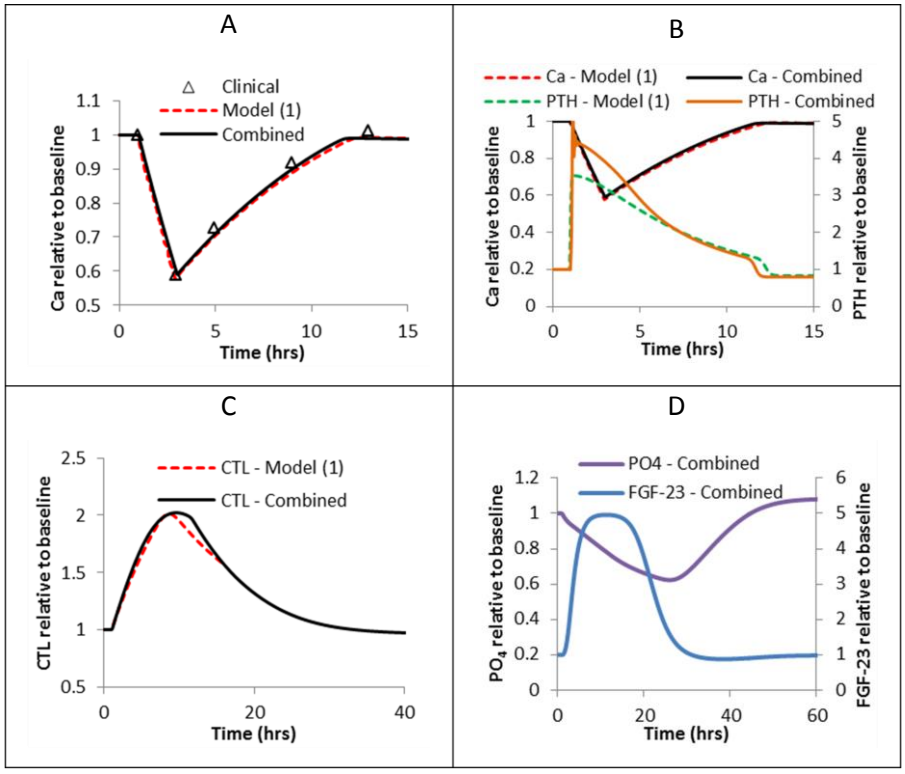

Figure 3.3. Calciotropic response, for both models, to induced hypocalcemia (2-hr infusion of sodium EDTA (33)) in healthy subjects:
(A) Calcium. Model predictions of calciotropic responses: (B) Ca and PTH; (C) CTL and, (D) Phosphate and FGF-23

The dynamic profiles of Ca, PTH and CTL from both models (Figure 3.3A-C) are identical in the simulation of a 2-hour infusion of sodium EDTA followed by a 10-hour recovery (33). However, owing to the impact of plasma phosphate and FGF-23 on PTH secretion, which was incorporated in the *combined* model, the maximum PTH reached is higher in the *combined* model than in *Model (1)* (Figure 3.3B). Additionally, the dynamics of plasma phosphate and FGF-23 are now available from the combined model. The increase in PTH induces CTL production which in turn causes FGF-23 production Figure 3.3C-D. Both FGF-23 and PTH cause increased phosphate excretion resulting in lower plasma phosphate (Figure 3.3D). Although the low phosphate levels inhibit FGF-23 formation, there is net FGF-23 secretion due to the greater effect of increasing CTL levels. The profiles in Figure 3.3A-D indicate the variations in settling times of the different hormones/ions. Ca and PTH return to basal levels within 10 hrs (Figure 3.3B), CTL and FGF-23 returns to steady-state within 35 hrs (Figure 3.3C-D) and phosphate has the slowest dynamics with a settling time > 40hrs (Figure 3.3D). This observation underscores the fact that plasma calcium is tightly regulated whereas plasma phosphate is loosely controlled.

Again, the calcium and PTH responses to hypocalcemia and hypercalcemia (Figures 3.4A-B) induced by 2-hr sodium citrate infusion (34) and 2-hr calcium gluconate infusions (35) respectively, in healthy

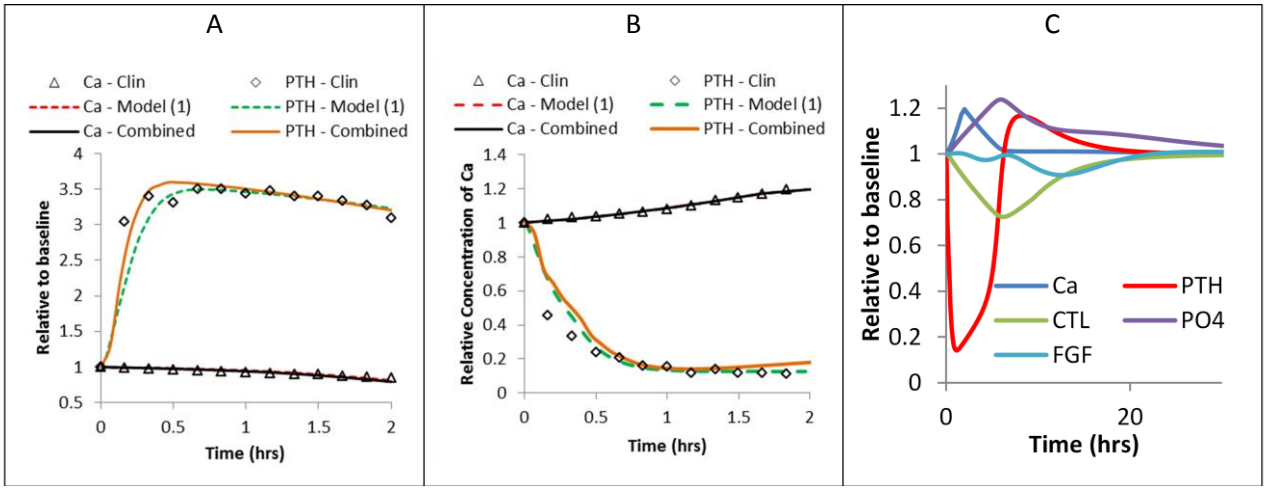

Figure 3.4. Ca and PTH response during 2-hr infusion of:

(A) sodium citrate (Ramirez) and (B) calcium gluconate (35); (C) Model predictions of Ca, PTH, CTL, urinary Ca and CB ratio response during and after 2-hr infusion of calcium gluconate (35).

subjects are identical in both models and are similar to the clinical data. Further analysis of the biochemical profiles intra- and post-infusion leads to some interesting observations (Figure 3.4C). The hypercalcemia-induced decrease in PTH causes a decrease in CTL secretion. The decreasing PTH leads to increasing renal phosphate reabsorption, while the low CTL reduces intestinal phosphate absorption. The net effect of phosphate retention and low intestinal absorption is an increase in plasma phosphate. As PTH levels increase, there is a corresponding increase in renal phosphate excretion thus lowering plasma PO_4 levels.

The diverging increases and decreases in phosphate and CTL levels cause FGF-23 levels to fluctuate over the response period (Figure 3.4C). Initially, there is a net zero effect of the increase in PO_4 and decrease in CTL on FGF-23 secretion; however, as time progresses, the effect of decreasing CTL on FGF-23 production dominates resulting in a fall in FGF-23 levels. As phosphate levels increase to a maximum, the PO_4 effect dominates CTL-inhibition, leading to an increase in FGF-23 levels. Once the nadir of CTL and the crest of phosphate levels have passed, the net effect of the lowering PO_4 and the, still sub-basal but, increasing, CTL is a further decrease in FGF-23 levels. As plasma PO_4 and CTL approach basal levels, their combined effect causes an increase in FGF-23 back to baseline levels.

The calciotropic response to calcium gluconate in subjects with primary hyperparathyroidism is shown in Figure 3.5. The PTH profiles during infusion are identical in both models, and comparable to the clinical data. The intra- and post-infusion response profiles to hypercalcemia are slightly different in PHPT (Figure 3.5B) than in healthy subjects (Figure 3.4C). Since PTH levels are already high in PHPT, PTH-induced phosphate excretion is slightly higher than in healthy subjects. The hypercalcemia-induced

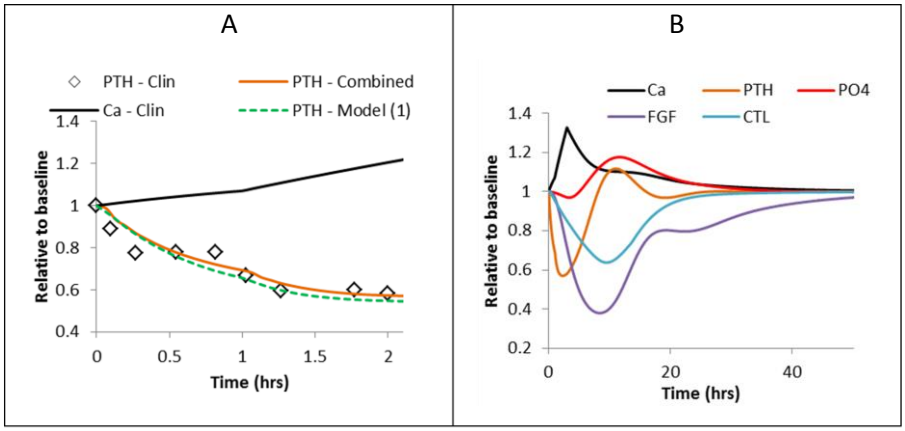

Figure 3.5. Model prediction and clinical observation of Calciotropic response to 2-hr clinical infusion of calcium gluconate in PHPT subjects.

(A) Ca and PTH; (B) Ca, PTH, CTL, phosphate and FGF-23

decrease in PTH causes a similar decrease in CTL that leads to lower intestinal phosphate absorption and ultimately, an initial decrease in plasma phosphate levels. No such decrease was observed in the predictions for the healthy subjects (Figure 3.4C). At the same time, FGF-23 levels are reduced due to lower CTL- and phosphate levels, thus contributing to the reduced phosphate excretion (Figure 3.5B). As PTH levels increase there is still a reduction in FGF-23 levels, the net effect of PTH and FGF-23 is a continued reduction in renal phosphate excretion, which contributes to increasing plasma phosphate levels, even with a continued reduction in intestinal absorption due to lowering CTL. Plasma phosphate reaches a maximum as CTL and FGF-23 pass their minimum because the now-increasing FGF-23 and the near-basal PTH cause an increase in renal excretion thus lowering plasma PO_4. At the same time, CTL returns to basal levels thus countering the loss of plasma PO_4 through increasing intestinal absorption.

3.3.2. Chronic Kidney Disease

We validate our CKD model using clinical data of plasma biochemistries in two sets of patients (36). The first set is a cohort of 113 patients with CKD who were not undergoing dialysis nor taking phosphate binders. This cohort was divided into four groups according to their renal function (measured by GFR). The second set is a control group of 89 healthy volunteers. For our simulations, we simulate the plasma biochemistries of the healthy group to use as our reference point. We then simulate each of the CKD groups by reducing the renal function from the healthy reference to the reported value.

Figure 3.6A-D shows our prediction of plasma Ca, PTH, PO_4 and CTL compared to the clinical data. In general, our model predicts the profile of all four plasma biochemistries very well.

In accounting for Ca loss due to $CaHPO_4$ formation in CKD, we assumed that the amount of Ca lost from the plasma is equivalent to the stoichiometric amount used to form $CaHPO_4$ (i.e. 1 mole Ca/ mole $CaHPO_4$). However, in reproducing clinical presentations of Ca in CKD, we found that this only holds for renal function decline down to 40%. Below 40%, the fraction of plasma Ca used in $CaHPO_4$ formation declines, as is shown in Figure 3.6E. Therefore, we adjusted the factor to account for this deviation. This deviation may be due to the fact that at lower renal function ($RF < 60\%$), hypocalcemia becomes prevalent, as such, only small amounts of Ca can be precipitated from the plasma.

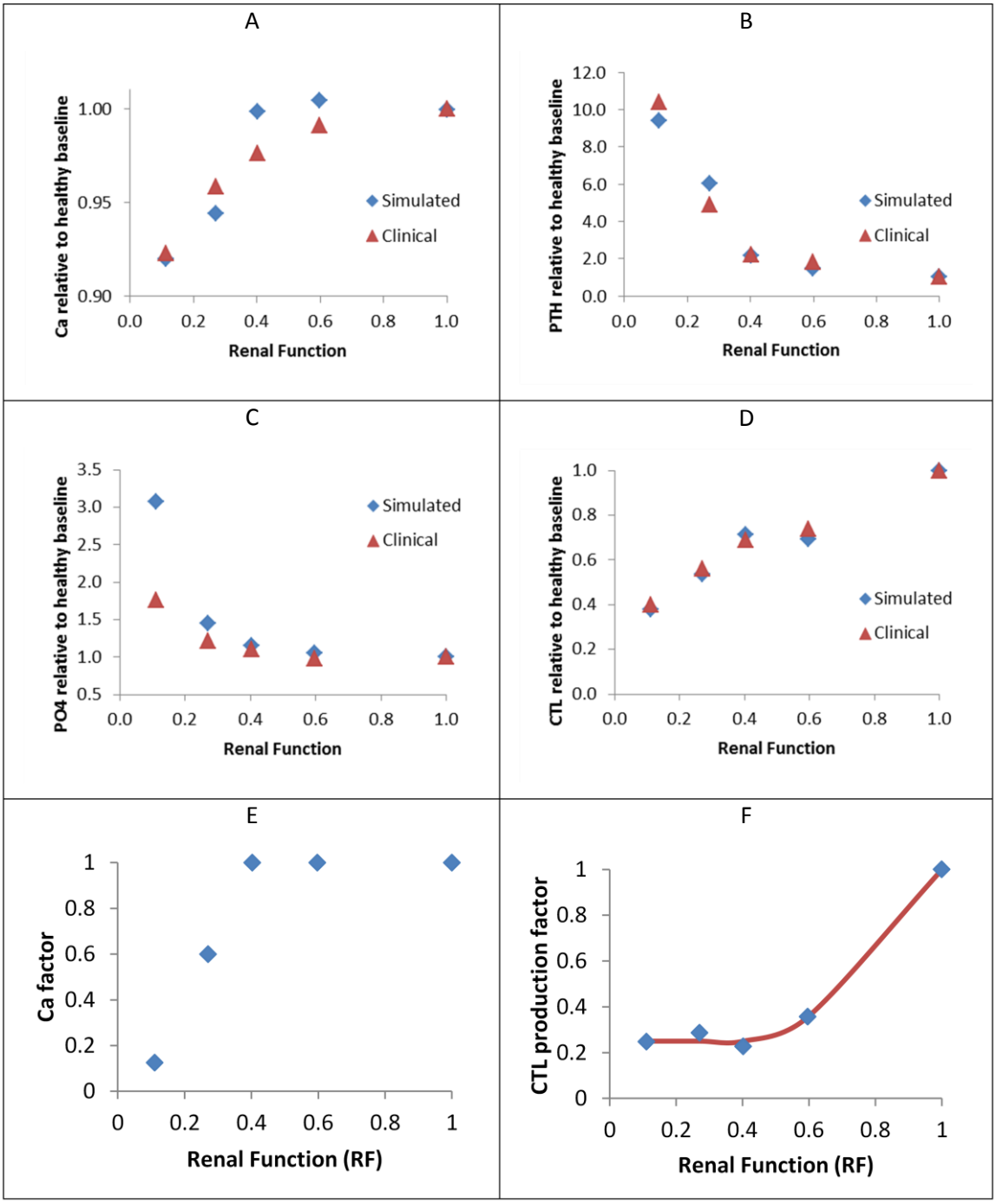

Figure 3.6. Comparison of Simulated results and clinical observations of plasma biochemistry changes among patients with varied severity of kidney disease (as determined by a decline in renal function/GFR) (36).
All biochemistries are presented relative to the healthy basal levels: (A) Ionized Calcium; (B) PTH; (C) Phosphate; (D) Calcitriol. (E) The precipitation of Ca salts during CKD progression is indicated by the Ca factor. (E) CTL production in CKD progression declines according to the CTL production factor.

At very low renal function ($RF < 0.3$), the model overestimates plasma PO_4 (Figure 3.6C which may occur due to unaccounted changes in PO_4 regulation. Owing to insufficient data, the effect of FGF-23 on

renal phosphate reabsorption is lumped with PTH, therefore, any change in FGF-23 effect on the renal tubules during CKD is unaccounted for.

In preliminary studies we found that our simulation results for CTL levels in different stages of CKD did not match the clinical data when using a proportional relationship between declining renal function (RF) and circulating CTL levels. Therefore, we multiplied the CTL production rate by a factor ($r_{CTL,deg}$). Figure 3.6F shows the relationship between $r_{CTL,deg}$ and declining renal function, the factor decreases proportionally with renal function down to $RF = 40\%$; below this, the factor remains at a constant value. Therefore, a sigmoid function can be used to represent the relationship between $r_{CTL,deg}$ and RF.

The disproportionate decrease in CTL levels compared to the decline in renal function may be due to the net effects of hyperphosphatemia and metabolic acidosis in inhibiting CTL synthesis (8, 37-40) as well as the reduced metabolic clearance of CTL in CKD (41).

Figure 3.7 shows the simulation results of progressive decline in renal function. For each simulation, the renal function is gradually reduced from the healthy reference down to the desired value. Each data point represents the steady-state end-point at each renal function.

Normocalcemia and normophosphatemia persists down to ~ 50% renal function, below this, hypocalcemia and hyperphosphatemia appear (Figure 3.7A). Below 50% RF, hyperphosphatemia increases disproportionately to the decrease in plasma Ca. As discussed before, there may be alterations in the PO_4 regulation—during later stages of CKD—that are not accounted for in our model.

Below 70% renal function, circulating PTH starts increasing, while CTL decreases (Figure 3.7B). The fall in CTL occurs due to the loss in capacity for CTL production in the renal tubules. This suggests that the healthy kidneys have a "buffer" or excess capacity of approximately 30% to produce CTL. As renal function declines, the capacity of production of CTL also declines, thus reducing circulating CTL. There is a further decrease in CTL levels at approximately 30% renal function, which coincides with the dramatic increase in plasma PO_4. The declining CTL has less inhibitory effect on the PTG, thus PTH synthesis and secretion increases and is reflected in PTH levels. The rate of increase of PTH becomes steeper below 50% renal function because both hypocalcemia and hyperphosphatemia appear.

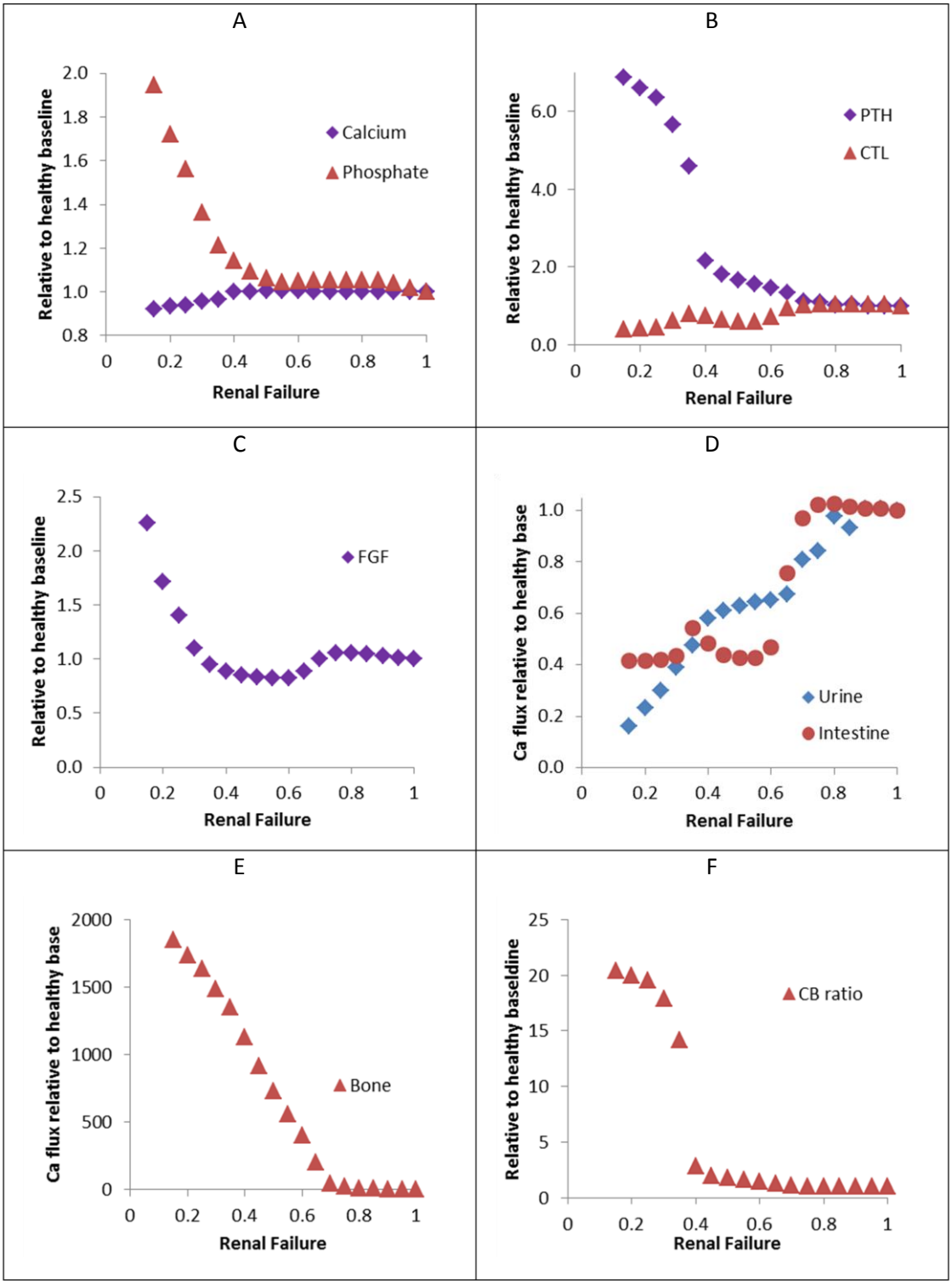

Figure 3.7. Simulated results of calciotropic response to progressive decline in renal function:

(A) Ionized Ca and Phosphate; (B) PTH and CTL; (C) FGF; (D) Renal Ca excretion and Intestinal Ca absorption; (E) Ca transfer from bone to plasma; (F) bone osteoclast-to-osteoblast (CB) ratio.

The results of FGF-23 (FGF), osteoclast-to-osteoblast ratio (CB ratio) and Ca flux from the bone, urine

and intestine are readily available from the model and can be used to provide greater insight into the progression of CKD. Between normal RF and 50% RF, the profile of FGF-23 (Figure 3.7C) is identical to that of CTL; below 50%, the profile follows that of plasma PO_4. FGF-23 synthesis is induced by both CTL and PO_4; however CTL has a greater effect, therefore the decline in CTL levels causes a similar decrease in FGF-23 levels between 70% to 50% renal function. As the extent of hyperphosphatemia increases, PO_4 induces FGF-23 synthesis resulting in increased FGF-23 levels.

Upon initial decline of renal function (100% to 80%) there is no change in Ca flux in the kidneys (Figure 3.7D), this suggests that there is a 20% excess capacity for renal excretion. On further decline of renal function, there are two piecewise linear regions of decline in Ca excretion, the difference in slopes is due to the effect of PTH on renal reabsorption. Between 80% and 40% renal function, PTH levels are slightly high (up to 2X normal), thus only a fraction of PTH-dependent renal reabsorption occurs, as a result, the decline in Ca excretion is less than the decline in renal function. However, below 40% renal function, when PTH levels are very high (> 4X normal), PTH-dependent renal reabsorption is maximum, thus only PTH-independent Ca excretion occurs, thus the decline is directly proportional to the decline in GFR.

As expected, intestinal Ca flux varies with CTL levels (Figure 3.7D), however, the effect of CTL is diminished below 60% renal function even though minimum CTL is observed at 20% renal function. This suggests the existence of a CTL threshold, below which no transcellular (i.e. CTL-dependent) Ca absorption occurs. A similar observation is made from the work done by Heaney et al., in exploring the Ca absorptive effect of Vitamin D metabolites (42).

Bone Ca flux (Figure 3.7E) and the osteoblast-to-osteoclast (CB) ratio (Figure 3.7F) provide interesting insight into the mechanism of CKD progression. Since the bone model takes only plasma PTH as input, then any change in CB ratio is attributed to PTH. Therefore, as with PTH, CB ratio remains normal down to a renal function of ~70%; between 70% and 40% RF, there is marginal increase in CB ratio (up to 2.5X normal) (Fig. 3.7F). Below 40% renal function, CB ratio increases dramatically, from 2.5X to ~ 20X normal. On the other hand, below 70% renal function the Ca flux from bone increases linearly up to ~ 3 orders of magnitude greater than basal levels. It is this dramatic increase in bone flux that maintains normocalcemia between 70% and 50% renal function when there is significant decrease in intestinal Ca flux.

Rix et al., observed a decline in total body bone mineral density correlating with declining renal function (36). The group found that the measured biochemical markers of bone turnover (formation and resorption) all showed a strong negative correlation with GFR and the serum levels of these markers were

significantly increased in the group of patients with advanced stages of renal failure. This finding supports our simulation results of significantly increased bone Ca flux and CB ratio for RF less than 40%.

In summary, compared to Ca regulation, plasma PO_4 is loosely controlled and is therefore not a major player in certain Ca-related pathologies; modeling these pathologies require a detailed model of Ca regulation and only a minimal model of PO_4 regulation. However, in order to investigate the role of phosphate levels in some Ca-related pathologies, a more detailed description of PO_4 regulation is required. The updated Ca-PO_4 model provides a more complete description of phosphate regulation with additional insight into the calciotropic responses of CTL and PTH and the heretofore unmentioned protein FGF-23. Additionally, the ease with which PO_4 control was incorporated in the model emphasizes the flexibility of our approach in modifying and adding component blocks or even entire systems. The updated model offers the potential to explore more complex Ca-PO_4-related pathologies and our simulation of CKD provides the opportunity to explore potential therapeutic sites in the pathology.

3.4. References

1. **Bergwitz C, Juppner H** 2011 Phosphate Homeostasis Regulatory Mechanisms. Pediatric Bone: Biology & Diseases:141-161
2. **DeLean A, Munson PJ, Rodbard D** 1978 Simultaneous analysis of families of sigmoidal curves: application to bioassay, radioligand assay, and physiological dose-response curves. American Journal of Physiology 235:E97-102
3. **Gibaldi M, Perrier D** 1982 Pharmacokinetics. New York: M. Dekker
4. **Yamashita T, Yoshioka M, Itoh N** 2000 Identification of a novel fibroblast growth factor, FGF-23, preferentially expressed in the ventrolateral thalamic nucleus of the brain. Biochemical and Biophysical Research Communications 277:494-498
5. **Gutiérrez OM, Smith KT, Barchi-Chung A, Patel NM, Isakova T, Wolf M** 2012 (1-34) Parathyroid Hormone Infusion Acutely Lowers Fibroblast Growth Factor 23 Concentrations in Adult Volunteers. Clinical Journal of the American Society of Nephrology 7:139-145
6. **Nishida Y, Taketani Y, Yamanaka-Okumura H, Imamura F, Taniguchi A, Sato T, Shuto E, Nashiki K, Arai H, Yamamoto H** 2006 Acute effect of oral phosphate loading on serum fibroblast growth factor 23 levels in healthy men. Kidney International 70:2141-2147
7. **Vervloet MG, van Ittersum FJ, Büttler RM, Heijboer AC, Blankenstein MA, ter Wee PM** 2011 Effects of dietary phosphate and calcium intake on fibroblast growth factor-23. Clinical Journal of the American Society of Nephrology 6:383-389
8. **Jones G, Strugnell SA, DeLuca HF** 1998 Current understanding of the molecular actions of vitamin D. Physiological reviews 78:1193-1231
9. **Burnett SAM, Gunawardene SC, Bringhurst FR, Jüppner H, Lee H, Finkelstein JS** 2006 Regulation of C-Terminal and Intact FGF-23 by Dietary Phosphate in Men and Women. Journal of Bone and Mineral Research 21:1187-1196
10. **Collins MT, Lindsay JR, Jain A, Kelly MH, Cutler CM, Weinstein LS, Liu J, Fedarko NS, Winer KK** 2005 Fibroblast Growth Factor-23 Is Regulated by 1α, 25-Dihydroxyvitamin D. Journal of Bone and Mineral Research 20:1944-1950
11. **Ito N, Fukumoto S, Takeuchi Y, Yasuda T, Hasegawa Y, Takemoto F, Tajima T, Dobashi K, Yamazaki Y, Yamashita T** 2005 Comparison of two assays for fibroblast growth factor (FGF)-23. Journal of Bone and Mineral Metabolism 23:435-440
12. **Ito N, Fukumoto S, Takeuchi Y, Takeda S, Suzuki H, Yamashita T, Fujita T** 2007 Effect of acute changes of serum phosphate on fibroblast growth factor (FGF) 23 levels in humans. Journal of Bone and Mineral Metabolism 25:419-422
13. **Naveh-Many T, Silver J** 2005 Regulation of Parathyroid Hormone Gene Expression by 1,25-Dihydroxyvitamin D. In: Molecular Biology of the Parathyroid: Springer US; 84-94
14. **Krajisnik T, Björklund P, Marsell R, Ljunggren Ö, Åkerström G, Jonsson KB, Westin G, Larsson TE** 2007 Fibroblast growth factor-23 regulates parathyroid hormone and 1α-hydroxylase expression in cultured bovine parathyroid cells. Journal of Endocrinology 195:125-131
15. **Ben-Dov IZ, Galitzer H, Lavi-Moshayoff V, Goetz R, Kuro-o M, Mohammadi M, Sirkis R, Naveh-Many T, Silver J** 2007 The parathyroid is a target organ for FGF23 in rats. Journal of Clinical Investigation 117:4003-4008

16. **Kilav R, Silver J, Naveh-Many T** 2005 Regulation of Parathyroid Hormone mRNA Stability by Calcium and Phosphate. In: Molecular Biology of the Parathyroid: Springer US; 57-67
17. **Estepa JC, Aguilera-Tejero E, Lopez I, Almaden Y, Rodriguez M, Felsenfeld AJ** 1999 Effect of phosphate on parathyroid hormone secretion in vivo. Journal of Bone and Mineral Research 14:1848-1854
18. **Bai X-Y, Miao D, Goltzman D, Karaplis AC** 2003 The autosomal dominant hypophosphatemic rickets R176Q mutation in fibroblast growth factor 23 resists proteolytic cleavage and enhances in vivo biological potency. Journal of Biological Chemistry 278:9843-9849
19. **Bergwitz C, Juppner H** 2010 Regulation of phosphate homeostasis by PTH, vitamin D, and FGF23. Annual review of medicine 61:91-104
20. **Berndt T, Knox F** 1992 Renal regulation of phosphate excretion. The kidney: Physiology and pathophysiology:2511-2532
21. **Silve C, Friedlander G** 2000 Renal regulation of phosphate excretion. The kidney: physiology and pathophysiology Philadelphia: Lippincott, Williams & Wilkins 2:1885-1904
22. **Suki W, Lederer E, Rouse D** 2000 Renal transport of calcium, magnesium and phosphate. The kidney 6th ed Philadelphia: Saunders:538-543
23. **Bonjour J-P, Caverzasio J** 1984 Phosphate transport in the kidney: Springer
24. **Bijvoet O** 1976 The importance of the kidneys in phosphate homeostasis. Phosphate metabolism, kidney and bone Armour Montagu, Paris:421-474
25. **Thompson DD, Hiatt HH** 1957 Renal reabsorption of phosphate in normal human subjects and in patients with parathyroid disease. Journal of Clinical Investigation 36:550
26. **Bonjour J-P, Fleisch H** 1980 Tubular adaptation to the supply and requirement of phosphate. In: Renal Handling of Phosphate: Springer; 243-264
27. **Lee D, Walling MW, Corry DB** 1986 Phosphate transport across rat jejunum: influence of sodium, pH, and 1, 25-dihydroxyvitamin D3. American Journal of Physiology-Gastrointestinal and Liver Physiology 251:G90-G95
28. **Peterlik M, Wasserman R** 1978 Effect of vitamin D on transepithelial phosphate transport in chick intestine. American Journal of Physiology-Gastrointestinal and Liver Physiology 234:G379-G388
29. **Katai K, Miyamoto K-i, Kishida S, Segawa H, Nii T, Tanaka H, Tani Y, Arai H, Tatsumi S, Morita K** 1999 Regulation of intestinal Na+-dependent phosphate co-transporters by a low-phosphate diet and 1, 25-dihydroxyvitamin D3. Biochemical Journal 343:705
30. **Raposo JF, Sobrinho LG, Ferreira HG** 2002 A minimal mathematical model of calcium homeostasis. Journal of Clinical Endocrinology and Metabolism 87:4330-4340
31. **Talmage RV, Talmage DW** 2006 Calcium homeostasis: solving the solubility problem. Journal of musculoskeletal & neuronal interactions 6:402-407
32. **Hebert LA, Lemann Jr J, Petersen JR, Lennon E** 1966 Studies of the mechanism by which phosphate infusion lowers serum calcium concentration. Journal of Clinical Investigation 45:1886
33. **Parfitt AM** 1969 Study of parathyroid function in man by EDTA infusion. Journal of Clinical Endocrinology and Metabolism 29:569-580
34. **Ramirez JA, Goodman WG, Gornbein J, Menezes C, Moulton L, Segre GV, Salusky IB** 1993 Direct in vivo comparison of calcium-regulated parathyroid hormone secretion in normal volunteers and patients with secondary hyperparathyroidism. Journal of Clinical Endocrinology and Metabolism 76:1489-1494

35. **Goodman WG, Veldhuis JD, Belin TR, Van Herle AJ, Juppner H, Salusky IB** 1998 Calcium-sensing by parathyroid glands in secondary hyperparathyroidism. Journal of Clinical Endocrinology and Metabolism 83:2765-2772
36. **Rix M, Andreassen H, Eskildsen P, Langdahl B, Olgaard K** 1999 Bone mineral density and biochemical markers of bone turnover in patients with predialysis chronic renal failure. Kidney International 56:1084-1093
37. **Lemann Jr J, Litzow J, Lennon E** 1966 The effects of chronic acid loads in normal man: further evidence for the participation of bone mineral in the defense against chronic metabolic acidosis. Journal of Clinical Investigation 45:1608
38. **Hsu CH** 2006 Calcitriol Metabolism and Action in Chronic Renal Disease. In: Calcium and Phosphate Metabolism Management in Chronic Renal Disease: Springer; 105-130
39. **Hsu CH, Patel SR, Young EW, Vanholder R** 1991 Effects of purine derivatives on calcitriol metabolism in rats. American Journal of Physiology 260:F596-F601
40. **Hsu C, Patel S** 1990 The effect of polyamines, methyl guanine, and guanidinosuccinic acid on calcitriol metabolism. Journal of Laboratory and Clinical Medicine 115:69-73
41. **Hsu CH, Patel SR, Young EW** 1992 Mechanism of decreased calcitriol degradation in renal failure. American Journal of Physiology-Renal Physiology 262:F192-F198
42. **Heaney RP, Barger-Lux MJ, Dowell MS, Chen TC, Holick MF** 1997 Calcium absorptive effects of vitamin D and its major metabolites. Journal of Clinical Endocrinology and Metabolism 82:4111-4116

4. A Model-Based Approach to Diagnosing Primary Hyperparathyroidism

From preliminary simulations, we observed that simulations results of intravenous Ca infusion in the models of the different Ca-pathologies suggested divergent calciotropic responses (plasma Ca, PTH, CTL and urinary Ca) in the different pathologies. As such, this chapter details the research into identifying an effective method to differentiate the hypercalcemia-causing pathologies that are most common, and often confounded due similarities in clinical presentations.

4.1. Introduction

The two most common pathologies, accounting for ninety-percent (90%) of hypercalcemia cases are primary hyperparathyroidism (PHPT) and hypercalcemia of malignancy (HHM). Other less common causes of hypercalcemia include, familial benign hypocalciuric hypercalcemia (FBH) and Vitamin D intoxication (1).

PHPT is characterized by a secretion of excess PTH due to adenoma or hyperplasia of one or more parathyroid gland(s) (PTGs) with the only cure being surgical removal of the affected gland(s) (2). In a majority of patients (70-80%) the condition is asymptomatic and is most commonly discovered through incidental finding of elevated PTH along with normocalcemia or elevated serum calcium (Ca) (2-4) or, in rare cases, low-normal PTH (5). FBH, a missense-mutation of the calcium-sensing receptor (CaR), presents similar characteristics to PHPT, namely, hypercalcemia with high-normal PTH (6) and is ultimately isolated from PHPT through a review of family history (2). HHM is caused by the secretion of PTH-related protein (PTHrP) from cancerous cells and has a similar pathophysiology to PHPT (7). However, unlike in PHPT, PTH and CTL are suppressed and osteoclastic and osteoblastic activities are decoupled in HHM (8-10).

There is no standardized test for differentially diagnosing the causes of hypercalcemia (11); however, the biochemical investigation steps include: measurement of plasma Ca (on two separate occasions), PTH, PTHrP, and urinary Ca along with a review of family history of FBH (2). For PHPT, both pre-operative serum Ca and PTH generally increase with increasing adenoma weight, yet these biochemical parameters cannot accurately predict parathyroid adenoma size (12, 13). However, given that Ca-mediated PTH suppressibility decreases with adenomatous growth (14, 15), several studies have proposed PTH suppressibility through intravenous (IV) Ca infusion as a means of identifying different stages of PHPT (11, 16). Furthermore, PTH suppression through oral Ca loading is suggested as a good measure for differential diagnosis (17-19). However, these tests were limited to specific cases (such as normocalcemic

PHPT in osteoporosis) (19), or only used analysis of too few calciotropic biochemistries (Ca, PTH, calcitonin and gastrin) (17, 18).

The aim of this chapter is to explore the effects of short-term Ca loading on FBH, PHPT, and HHM and determine if such a method is effective in the differential diagnosis of these three diseases, and identifying the extent of PHPT progression. This approach is similar to the IV glucose test for determining insulin secretion and resistance (20) now used in the diagnosis of diabetes.

4.2. Materials and Methods

4.2.1. Clinical datasets

Group characteristics and PTH suppressibility data were taken from two previous clinical studies (14, 16).

Khosla et al., (1993) (14): 11 FBH patients (3 male, 8 females; ages 24-49); 7 females with PHPT (ages 29-75); and 12 normal volunteers (3 male, 9 females; ages 25-57).

Zhao et al. (2011), (16): 1) 20 healthy volunteers (aged 50.7±3.7 years) with normal serum Ca and PTH; 2) 17 patients with "Mild" PHPT (aged 49.6±3.6 years) characterized by elevated serum intact PTH and mild elevation of fasting total Ca (2.5-2.75 mM) and confirmed PHPT; and, 3) 73 patients of undetermined (ND) PHPT status (aged 42.2 ± 1.7 years) with normal plasma Ca levels and elevated PTH, unconfirmed PHPT and no evidence of secondary HPT.

4.2.2. Model simulations

A detailed description of the healthy and pathology models used in this work is given in Chapter 2; only the adjusted model parameters for the current simulations are discussed herein. All parameters are initially estimated by an ad-hoc method to determine the optimum range; subsequently the final values are improved using least squares estimation. Following this, each model is simulated with the relevant Ca loading until the post-infusion steady state is achieved. The calciotropic response of Ca, PTH, CTL and urinary Ca are then analyzed.

Calcium loading or calcium disturbance ($Ca_{(d)}$): Identical infusion rates and times, for each dataset, are implemented in each model through the disturbance block. For the Khosla et al., (1993) datasets (Healthy, FBH, PHPT) and HHM, we use three (3) different Ca loadings: 1) as described in their work (14), one hour infusion of 0.025 mmol elemental Ca/kg followed by 0.05 mmol elemental Ca/kg for the second hour; then two modified loadings: 2) 30-minute infusion of 0.025 mmol elemental Ca/kg; and, 3) 60-minute infusion of 0.025 mmol elemental Ca/kg. The loading implemented in the Zhao et al., (2011)

datasets (Healthy, ND and Mild PHPT) is as described in the paper (16), two hour infusion of 4 mg elemental Ca/kg per hr.

Healthy: Each model is first initialized using the baseline serum Ca and PTH provided in each study for the relevant groups (14, 16). Ca loading is then implemented, as described above, and the PTH secretory rate parameters (hypercalcemic slope ($m_{Ca(s)}A$) and minimum and maximum PTH secretory rates ($A_{Ca(s)}$ and $B_{Ca(s)}$)) are estimated such that the simulated PTH response matches the clinical data. These parameters then serve as a reference for the other pathology groups within the relevant clinical study.

FBH (sensor defect): The missense mutation of the CaR associated with FBH is implemented as a sensor defect—a decrease in sensor gain (K_{sens}). Using the healthy model as a basis, K_{sens} is decreased from 1 to 0.88, such that simulated ionized Ca at steady-state is identical to the reported baseline serum ionized Ca. $A_{Ca(s)}$ and $B_{Ca(s)}$ are then estimated such that the steady-state serum PTH matches the reported baseline. Finally, Ca loading is simulated and the estimates of $m_{Ca(s)}A$ and $A_{Ca(s)}$ corrected to match the clinical PTH response profile.

HHM (actuator disturbance): We implement a four-fold increase in the circulating PTHrP levels, consistent with clinical presentation (21), by adjusting the PTHrP production rate in the PTHrP production block,. Once steady-state is achieved, Ca loading is then applied.

PHPT (controller defect): For PHPT cohorts (14, 16) in both studies, the PHPT model is first initialized using the reported group baseline serum Ca and PTH. The minimum and maximum secretory rate parameters ($A_{Ca(s)}$ and $B_{Ca(s)}$) and the PTH secretory slope midpoints ($m_{Ca(s)}S_1$ and $m_{Ca(s)}S_2$) are then estimated such that the steady-state PTH and Ca are the same as the reported baseline values. Finally, Ca loading is implemented and the parameters related to hypercalcemia—minimum PTH secretory rate ($A_{Ca(s)}$), PTH secretory slope hypercalcemic midpoint ($m_{Ca(s)}S_2$) and hypercalcemic slope ($m_{Ca(s)}A$)—are optimized using the group PTH response data.

For individual patients, since no PTH baseline data is given, each model is initialized using the individual baseline serum Ca and the group baseline PTH provided. Ca loading is applied to the model and parameters related to hypercalcemia (as noted above) are estimated using the individual patient PTH response data.

4.2.3. Performance Analysis

Along with the comparison of intra- and post-infusion response profiles of Ca, PTH, CTL and urinary Ca, the following expressions are computed to aid in our analysis:

1) The *rise/fall time* ($T_{r/f,x,\%}$) is the time taken (post-infusion) for the hormone/ion (x = Ca, PTH or CTL) response to rise (r) or fall (f) to a predetermined fraction of its final value. We use 10% for all analyses except when determining shorter observation times, in which case 25% is used.
2) The *urinary Ca ratio* $\left(uCa_t = \frac{AUC\ Cau_{+t}}{AUC\ Cau_{-t}}\right)$ is the ratio of the amount of Ca excreted in a period of time t hours after and t hours prior to the start of infusion.
3) *PTH suppression* $\left(PTH_{supp} = \frac{PTH_{base} - PTH_{min}}{PTH_{base}} \times 100\%\right)$ is measure of the observed reduction in PTH compared to baseline PTH concentrations.

4.3. Results

Unless otherwise stated, all simulation results are normalized using pre-infusion baseline values provided to account for differences in biochemical characteristics across the different groups. For convenience, the estimated minimum PTH secretory rates and hypercalcemic slopes are reported relative to the relevant study's healthy values and are thus denoted as $A_{Ca(s),r}$ and $m_{Ca(s)}A_r$, respectively. We equate PHPT progression with increasing PTG mass, therefore, for the PHPT cohort in reference (14), we consider PHPT progressing from patient #1 to #7 since the PTG mass increases from patient #1 to #7. From our simulations, the responses for PHPT Patients 3 and 4 are identical to the PHPT group mean. Therefore, we consider responses for PHPT#3 or #4 to be synonymous with the group mean response. Additionally, for ease of presentation, where necessary, only responses for Patients 1, 4 and 7 are displayed, indicating early, mid and late stage PHPT, respectively.

4.3.1. Model Predictions

Figure 4.1 shows our model simulations of clinical PTH response to 2-hr Ca loading for all groups and individual patients in both studies. The model predictions are better for the group data (Fig.4.1A, D – F) than for individual PHPT patient data (Fig. 4.1B and C). This is due to variability in individual patient data and differences in response times (the time taken for an observable PTH change in response to Ca loading). PHPT patients # 1, 2, 4 and 6 show less variability compared to patients 3, 5 and 7 (Fig. 4.1B and C). The response times for PHPT# 1, 4 and 7 were 10, 30 and 45 minutes, respectively (Fig. 4.1B and C) which is greater than the 5 minutes observed in Patients # 3, 5 and 6. On the other hand, PHPT#2 seemed to respond within 10 minutes of infusion but the PTH secretion at 15 and 30 minutes returned to basal and resumed responding thereafter (Fig. 4.1B).

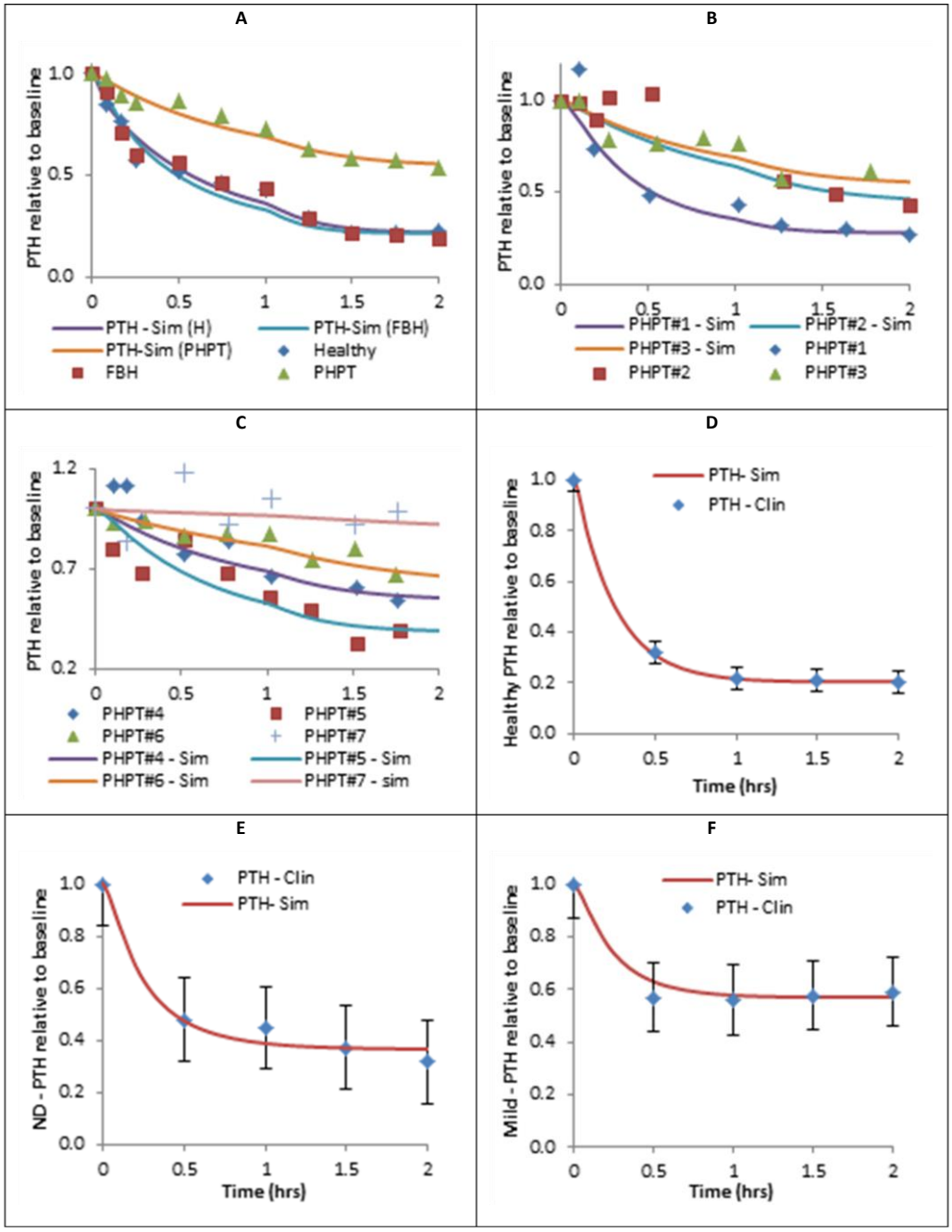

Figure 4.1. PTH suppression from Ca loading

Model simulations vs. clinical data. Khosla et al., dataset (Khosla, 1993) – (A) Groups: Healthy, FBH, PHPT; (B – C) Individual PHPT patients. Zhao et al., dataset (Zhao, 2011) – Groups: (D) Healthy; (E) Undetermined (ND); (F) Mild PHPT.

4.3.1.1. PTH suppression

Figure 4.2 shows the response profiles for 2-hr Ca loading for both clinical studies. When comparing Healthy, FBH, PHPT and HHM, the lowest suppression at ~24% is observed in HHM (Fig. 4.2A) since

baseline PTH levels are already near minimum (22). For PHPT#1, the first hour PTH response profile was identical to the FBH and Healthy groups but eventual PTH suppression was 6% lower (Fig. 4.2A). PTH suppression decreases within the PHPT group, greatest in PHPT#1 and least in #7. Additionally, from Table 4.1, PTH suppression in HHM (24%) lies within the range of advanced stages of PHPT (8-33%), Patients 6 and 7. These suppression levels indicate that the PTG ability to respond to induced

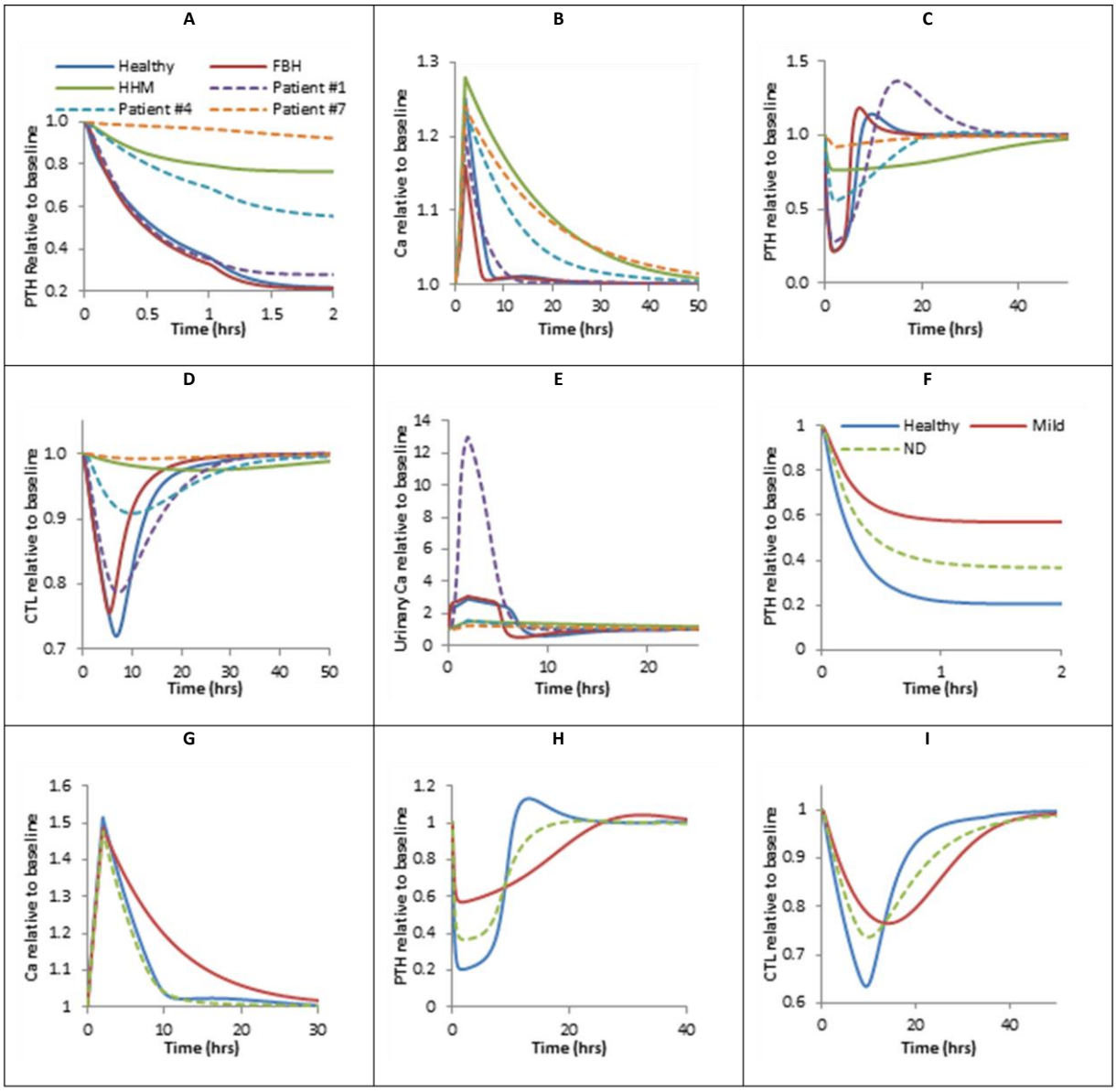

Figure 4.2. Model groups and individuals intra- and post- infusion profiles.

(A-E) Calciotropic response of Healthy, FBH, HHM and PHPT Patients #1, 4 and 7 based on 2-hr infusion of Ca gluconate as described in the reference (14): (A) 2-hr PTH response. Intra- and post-infusion response of: (B) Ca; (C) PTH; (D) CTL; and, (E) urinary Ca.

(F-I) Calciotropic response of Healthy, Mild and ND groups based on 2-hr infusion of Ca gluconate as described in the reference (16). (F) 2-hr PTH response. Intra- and post-infusion response of: (G) Ca (H) PTH, (I) CTL.

hypercalcemia is greatest in Healthy and FBH individuals, decreases with increasing PTG adenoma mass in PHPT and, is least in HHM.

4.3.1.2. Ca, PTH, CTL and urinary Ca excretion response profiles

The settling time, (the time it takes, post-infusion, to return to within 2% of basal levels) varies across all 4 groups for Ca, PTH and CTL. For plasma Ca (Fig. 4.2B), the settling time occurs between 3-5 hours for FBH and Healthy groups, varies from 10-48 hours within the PHPT group and is about 48 hours for HHM. In FBH and Healthy, PTH settling times are similar at 13-15 hours, the PHPT group ranges from 17- 28 hours and HHM is 48 hours (Fig. 4.2C). Interestingly, when returning to steady-state, the Healthy and FBH groups and PHPT#1 overshoot their basal levels, which accounts for their long settling times. Therefore, considering the PTH rise time ($T_{r,PTH,0.1}$) we see shorter times 3.5hr, 5.2hr, and 7.2hr for FBH, Healthy and PHPT#1, respectively, but no significant differences between PTH settling and rise times in later stages of PHPT or in HHM (comparison not shown). The PTH overshoot in Healthy, FBH and PHPT#1 (Fig. 4.2C) indicates the sensitivity of the PTG to changing Ca levels, which decreases as PHPT progresses (14, 15) and is ineffective in HHM.

Due to its slower dynamics, the maximum CTL suppressibility occurred within 2-6 hours post-infusion for Healthy, FBH, and PHPT groups versus within 2 hours post-infusion for PTH. However, since circulating PTH induces CTL secretion, CTL suppression follows the same trend as PTH (Fig. 4.2D).

Table 4.4. Parameter estimates and correlation with parathyroid function and mass

	PTH Suppression (%)	$m_{Ca(s)}A_r$	$A_{Ca(s),r}$	PTH Rise time (hrs) ($T_{r,PTH,0.1}$)	Urinary Ca ratio (uCa_4)	Measured PTG mass (mg)	Predicted PTG mass (mg)
Zhao et al., 2011							
Healthy	79%	1	1.0	8.1	3.1	-	-
ND	63%	0.85	1.5	11.7	10.4	-	44
Mild	43%	0.95	3.6	20.9	6.1	-	161
Khosla et al., 1993							
Healthy	78%	1.0	1	5.2	2.6	32.5	-
FBH	78%	1.88	1.2	3.5	2.8	-	-
HHM	24%	1.00	1.0	48.3	1.4	-	-
PHPT #1	72%	1.45	5	7.4	8.7	110	239
PHPT #2	54%	0.62	8	13.2	1.7	250	407
PHPT #3	44%	0.67	10	16.3	1.4	330	419
PHPT #4	44%	0.67	10	16.3	1.4	590	419
PHPT #5	61%	0.90	7	11.3	2.8	620	351
PHPT #6	33%	0.35	11	19.1	1.2	3840	4004
PHPT #7	8%	0.05	12	25.8	1.2	7670	7588

CTL suppression is greatest in the Healthy and FBH groups and both groups have similar levels of suppression (24% - 28%). CTL suppression decreases with PHPT progression, from 21% in Patient #1 to negligible (1%) in Patient #7 and, likewise, is negligible in HHM (3%).

PTH is one of the principal drivers of urinary Ca excretion. As such, urinary Ca profiles (Fig. 4.2E) follow the trend of the PTH response, rising to maximum excretion at 2 hours with an eventual return to basal excretion. There is an approximate 3-fold increase in excretion rate in Healthy and FBH and a negligible increase in HHM and PHPT, in general. However, PHPT#1 showed a significant increase (~ 13X basal) in Ca excretion which we attribute to PTH falling to within the "healthy" range and is discussed below.

Figures 4.2F-I show the simulation results for clinical data presented in reference (16). PTH suppression was greatest in the Healthy group (79%) and decreases from the ND to Mild groups, 63% and 43%, respectively. The post-infusion Ca and PTH profiles show that the Mild group has a slower settling time than the Healthy and ND groups (Figs. 4.2G and H). Although the ND and Healthy groups had identical Ca profiles (Fig. 4.2G), $T_{r,PTH,0.1}$ was shorter and the overshoot greater in the Healthy group (Fig. 4.2H). These results indicate a successive decrease in PTG function from Healthy to ND to mild.

The profile of urinary Ca ratio is shown in Figure 4.3A; there is a minimal increase in Ca excretion within 2-10 hours of infusion in mid-stage PHPT (1.2-1.4), late-stage PHPT (1.1-1.2) and HHM (1.3-1.4). Meanwhile, there are dramatic increases in the FBH group (1.2-2.8) and the Healthy group (2.0-2.6). The largest increase in urinary Ca ratio is observed in PHPT#1 varying from 4.9-8.7 times the pre-infusion amounts. The maximum ratio occurs at the 4-hr mark for PHPT#1, FBH and Healthy models, indicating that most of the Ca load is excreted within 4 hours of start of infusion. There is a dramatic increase in uCa_t between 2 and 4-hours for both FBH and PHPT#1 which is attributable to the generally high total Ca excretion observed in the 4-hr vs. 2-hr from the start of Ca infusion (Fig. 4.2E).

4.3.1.3. Ca, PTH and CTL rise/fall times

In Figure 4.3B, Ca, PTH and CTL $T_{r/f,0.1}$ follow the same trend across the different pathologies and within the PHPT group. The Ca fall time and PTH and CTL rise times are shortest in the Healthy and FBH groups, longer and increasing with PHPT progression and longest in HHM. As the PTG is the controller in the Ca regulatory system, all processes within the actuator (CTL production and Ca transfer to/from plasma) are directly or indirectly triggered by PTH. Given the rapid renal tubular reabsorption response (Fig. 4.2E) to circulating PTH levels, the Ca fall times $T_{f,Ca,0.1}$ for the Healthy and FBH groups and PHPT#1 are similar to the PTH rise times, $T_{r,PTH,0.1}$, (+/- 0.3hrs) (Fig. 4.3B). However, as PHPT

progresses, $T_{f,Ca,0.1}$ becomes progressively longer than $T_{r,PTH,0.1}$ (Fig. 4.3B) due to the minimal changes in renal Ca excretion (Fig. 4.2E) in the later stages of PHPT. However, $T_{r,CTL,0.1}$ is much longer (~1.5 to 4X) than $T_{r,PTH,0.1}$ (Fig. 4.3B) due to the slower CTL dynamics.

For the 2-hr infusion in the healthy group, $T_{f,Ca,0.1}$ and $T_{r,PTH,0.1}$ differed by only 0.4 hours (Fig. 4.3B). A similar observation is made for the 30- and 60-min infusions for the Healthy group (Fig 4.3C-D). Likewise, the models of FBH and PHPT#1 exhibit similar trends for the 2-hr (Fig 4.3B) and the 30-min and 60-min infusions (Fig 4.3C-D). However, the differences in Ca fall time and PTH rise time become noticeable as PHPT progresses and also in HHM (Fig. 4.3B). Also, $T_{r,PTH,0.1}$ is shorter than $T_{f,Ca,0.1}$ as PHPT progresses from PHPT#2 to #7 (~ 4 to 14hrs); however $T_{r,PTH,0.1}$ is longer than $T_{f,Ca,0.1}$ in HHM (Fig. 4.3B). Taken together, we can use the Ca fall time and PTH rise time from intravenous Ca infusion to differentiate FBH, PHPT and HHM as well as to identify the extent of PHPT progression. The observation time for each subject will vary depending on the underlying pathology. The observation time may be shortened by increasing the threshold from 10% to 25% or by reducing the infusion time. When we compare the PTH fall time for a threshold of 25% vs. 10% and 30-min Ca infusion, we observe reductions of 0.3hrs, 0.9hrs, 1.3hrs and 8hrs for FBH, PHPT#1, PHPT#4 and HHM, respectively (results not shown).

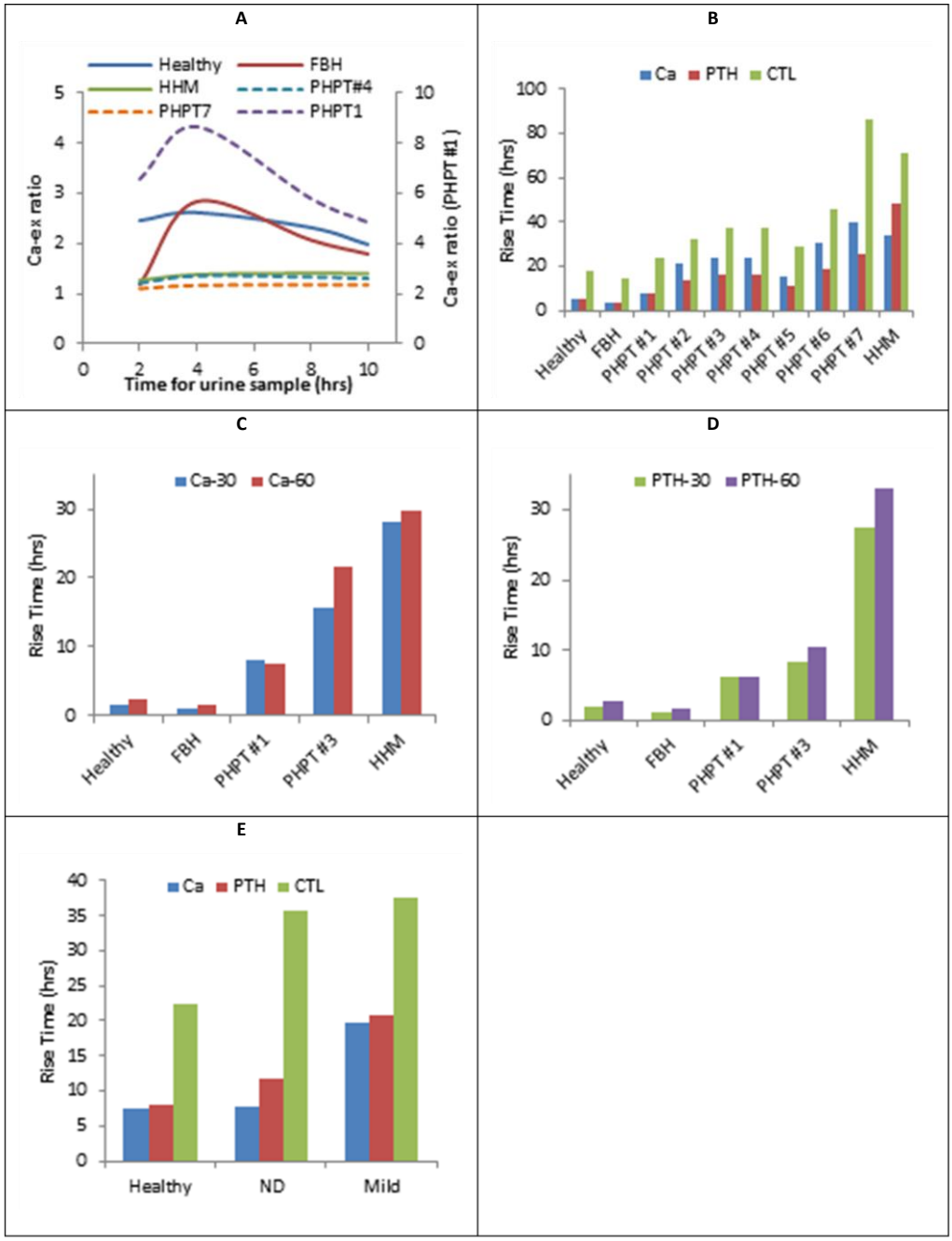

Figure 4.3. Simulation Results.

(A) Urinary Ca excretion ratio for Healthy, FBH, HHM and PHPT#1,4 &7; (B) Ca fall time and , PTH and CTL rise times for Healthy, FBH, HHM and PHPT#1-7 based on 2-hr Ca loading as described in (14). (C) Ca fall time and, PTH and CTL rise times for Healthy, ND and Mild based on 2-hr Ca loading as described in (16). (D) Ca fall time for Healthy, FBH, HHM and PHPT#1 and #3 based on 30 and 60 minute Ca loading. (E) PTH rise time Healthy, FBH, HHM and PHPT#1 and #3 based on 30 and 60 minute Ca loading

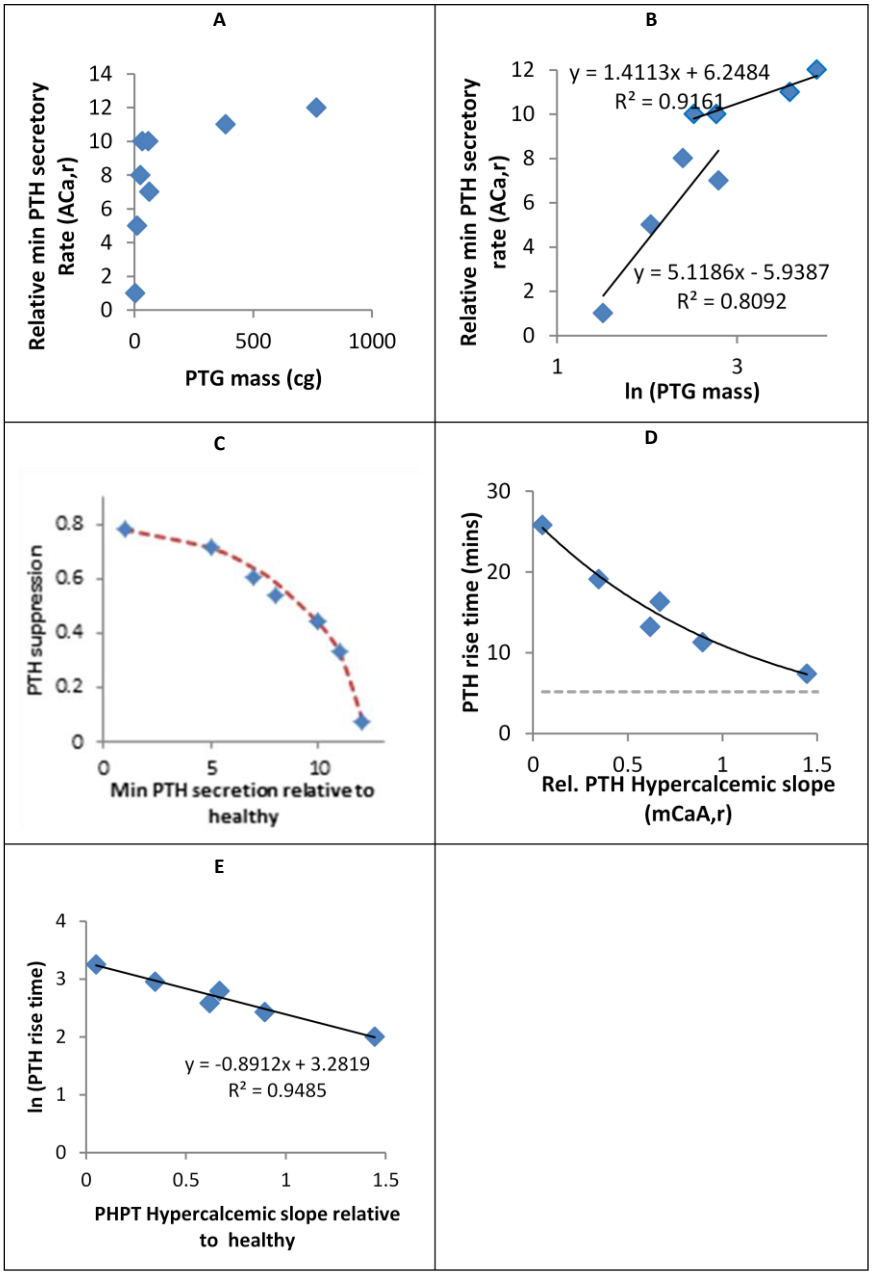

Figure 4.4. Analysis of parathyroid function.

(A) Minimum PTH secretion vs. PTG adenoma mass. (B) Semi-log plot of PTG mass and minimum PTH secretion. (C) PTH suppression vs. minimum PTH secretion. The dashed line represents our approximation of the data. (D) PTH rise time vs. hypercalcemic slope. The dashed line represents the PTH rise time for the healthy model. (E) Semi-log plot of PTH rise time vs. hypercalcemic slope, the line indicates the equation of best fit to the data.

4.4. Discussion

4.4.1. Minimum PTH secretory rate and PTG

The minimum PTH secretory rate, $A_{Ca(s),r}$ increases with increasing PTG mass and has two distinct regions (Fig. 4.4A-B). From the semi-log plot in Fig 4.4B, we see that the slope of the line, indicating the rate of change of $A_{Ca(s),r}$ with respect to PTG mass is higher in the early- to mid-stages of PHPT and lower in the later stages. This indicates that the amount of PTH secreted per unit mass of gland decreases as PHPT progresses. A similar observation was found in secondary HPT where larger PT hyperplastic glands did not secrete more whole PTH per unit mass than smaller hyperplastic ones (23). Since PTH suppression decreases with increasing PTG mass (15) and has a direct correlation with minimum PTH secretory rate (Fig. 4.4C), we propose that the above relationship in Fig. 4.4B can be used to estimate PTG mass in PHPT *a priori*. However, our analysis is based on limited post-surgical data and the relationship can be improved further with additional data of Ca loading and post-surgical PTG mass in PHPT subjects.

We observe that, for PHPT, ACa_r increases with increasing PTG mass (Figs. 4.4A-B). Additionally, PTH suppression decreases with increasing ACa_r, (Fig. 4.4C). This is expected because 1) PTH suppression decreases with PTG mass (15) and, 2) from its definition, PTH suppression is dictated by the minimum PTH secretory rate. Therefore, we propose the following expression, as depicted in Fig. 4.4C, to describe their relationship:

$$ACa_r = \sqrt{{ACa_{r,max}}^2 \left(1 - \frac{{PTH_{supp}}^2}{{PTH_{supp,max}}^2}\right)}$$

4.4.2. Ca-dependent PTH secretory slope and PTG behavior

The estimated hypercalcemic slopes ($m_{Ca(s)}A_r$) decrease in PHPT as PTG mass increases (Table 4.1) and there is an exponential decrease in PTH rise time as $m_{Ca(s)}A_r$ increases (Fig. 4.4D-E). Taken together, we purport that the PTH rise time increases with increasing gland size. Previous studies have shown that, in PHPT, there is evidence of altered signaling between the CaR and PT cells (24); and decreased CaR and Ca-sensing protein mRNA expression (25-29), yet no correlation between this loss in mRNA expression and PTG adenoma mass (25, 26). However, there is no evidence of CaR mutation in PHPT (30, 31). Given these observations, we hypothesize that the slope ($m_{Ca(s)}$) in the Ca-dependent PTH secretory term, is a measure of the combined effect of Ca signaling between the CaR and PT cells and the calciotropic response of the PTH production and secretory sequence. Therefore, the decreasing $m_{Ca(s)}A_r$ during PHPT progression points to the declining signaling and PTH production/secretory response in hypercalcemia, contributing to increasing PTH rise times.

4.4.3. Ca excretion and its indication in pathologies

As presented in our previous work Chapter 2, the PHPT model results in hypocalciuria at steady-state, which is observed in less than 25% of cases (32). In order to account for hypercalciuria in PHPT, we would need to decrease the estimated renal Ca threshold (Ca_{thr})—the Ca level at which Ca excretion is independent of circulating PTH. In the absence of sufficient data for renal excretion in PHPT, we retain the estimates from our healthy model. However, partial renal resistance to PTH activity has been noted in cases of PHPT (33, 34), therefore, a reduction in Ca_{thr} may indicate that, in PHPT, the high PTH levels cause PTH-desensitivity in the renal tubules. Additionally, we purport that the efficiency of handling excess Ca loading through renal Ca excretion decreases as PHPT progresses as evidenced by uCa_4 in PHPT# 1 (8.7) vs. PHPT#2-7 (1.7 to 1.2) in Table 4.1. This is primarily due to the elevated circulating PTH levels and our assumed PTH-desensitivity in the renal tubules, especially in the later stages.

We theorize that the urinary Ca excretion response for PHPT#1 (Fig. 4.2E) is indicative of the initial development of PHPT. In the early stage, induced hypercalcemia suppresses PTH to within the "healthy" range where the renal tubules are still sensitive to PTH. As such, urinary Ca reabsorption is reduced resulting in increased excretion. In addition, between the 5-10 hr marks the Healthy and FBH groups undershoot basal Ca excretion coinciding with their respective PTH overshoot. However, there is no such undershoot for PHPT#1; because, PTH has now returned to PHPT (supra-healthy) levels, thus forcing Ca excretion back to pre-infusion levels.

4.4.4. Predictions for Zhao et al., (2011) dataset

Using our findings, we can confirm the detection of early stage PHPT in the undetermined (ND) clinical group in Zhao et al (16). PTH suppression was greatest in the Healthy group, lower in the ND and least in the Mild PHPT group (Fig. 4.2F). On the other hand, the estimated $A_{Ca(s),r}$ increased from the Healthy to the ND to the Mild group (Table 4.1). There is an anomaly in the hypercalcemic slopes as the $m_{Ca(s)}A_r$ for the Mild cohort was greater than that of the ND group (Table 4.1). This may be attributed to the long sampling time (30 minutes) (16). A comparison of the Ca, PTH and CTL $T_{r/f,0.1}$ shows that the times for all three components increased from Healthy to ND to Mild (Fig. 4.3E). Finally, the 4-hr urinary Ca ratio is higher in ND than in both the Healthy and Mild groups (Table 4.1). Taken as a whole, we see that the characteristics of the ND group are similar to that of early stage PHPT from the Khosla et al., (1993) dataset analysis. Furthermore, using the equation in Fig. 5B, we estimate that the average PTG mass in the ND and Mild groups are 44 mg and 161 mg, respectively.

Notwithstanding the analysis provided by our simulation of the clinical data, there are a few caveats to be noted. First, Khoo et al., (2007) noted that dynamic changes in PHPT calciotropic response may occur in the presence of secondary contributing factors (35). As such, the accuracy of our estimated model parameters are dependent on the calciotropic responses to IV Ca loading and any external factors impacting Ca regulation at the time of testing. Secondly, For the Zhao et al., (2011) dataset, given the short half-life of PTH (< 5 mins) (36, 37), the frequency of sampling in the second dataset (30 minutes) (16) and the fact that full PTH suppression may occur within the first 20 minutes in some individuals (36, 38), PTH may be significantly suppressed in all three groups by the 30-minute mark. Thus, data points within the 30-minute sampling period are necessary for a more representative PTH response profile and a more accurate estimate of $m_{Ca(s)}A$. Finally, PTH dynamics vary across race, gender and age groups (39-41), we developed the relationship between PTG mass and ACa_r using data from a mid-western US population (14) and applied the results to a mainland Chinese population. Although our results confirmed the conclusions of the study by Zhao et al. (16), it may be best to use group-specific data in determining and applying predictive relationships for PTG adenoma mass

In conclusion, the two major indicators of parathyroid function in our simulations are the minimum PTH secretory rate and the hypercalcemic slope, both of which dictate calciotropic response. Through a systematic review of PTH suppression, minimum PTH secretory rate, hypercalcemic slope, urinary Ca ratio and PTH rise time from 30-min IV Ca loading, we can isolate FBH, PHPT and HHM from each other. In the case of PHPT, we can also identify the stage of progression and predict the PTG mass. The analysis requires no additional information or patient history; it will prove useful in early detection of PHPT. Additionally, we propose using population-specific data in determining the predictive relationships for PTG adenoma mass.

4.5. References

1. **Kovacs WJ, Ojeda SR** 2012 Textbook of Endocrine Physiology. 6th ed. Oxford: Oxford University Press
2. **Fraser WD** 2009 Hyperparathyroidism. Lancet 374:145-158
3. **Bilezikian JP, Potts JT, Fuleihan GE, Kleerekoper M, Neer R, Peacock M, Rastad J, Silverberg SJ, Udelsman R, Wells SA** 2002 Summary statement from a Workshop on Asymptomatic Primary Hyperparathyroidism: A perspective for the 21st century. Journal of Bone and Mineral Research 17:N2-N11
4. **Monchik J, Gorgun E** 2004 Normocalcemic hyperparathyroidism in patients with osteoporosis. Surgery 136:1242-1246
5. **Hollenberg AN, Arnold A** 1991 Hypercalcemia with low-normal serum intact PTH: a novel presentation of primary hyperparathyroidism. American Journal of Medicine 91:547-548
6. **Yano S, Brown EM** 2005 The Calcium Sensing Receptor. In: Molecular Biology of the Parathyroid: Springer US; 44-56
7. **Clines GA, Guise TA** 2005 Hypercalcaemia of malignancy and basic research on mechanisms responsible for osteolytic and osteoblastic metastasis to bone. Endocrine-Related Cancer 12:549-583
8. **Schilling T, Pecherstorfer M, Blind E, Leidig G, Ziegler R, Raue F** 1993 Parathyroid hormone-related protein (PTHrP) does not regulate 1, 25-dihydroxyvitamin D serum levels in hypercalcemia of malignancy. Journal of Clinical Endocrinology & Metabolism 76:801-803
9. **Nakayama K, Fukumoto S, Takeda S, Takeuchi Y, Ishikawa T, Miura M, Hata K, Hane M, Tamura Y, Tanaka Y, Kitaoka M, Obara T, Ogata E, Matsumoto T** 1996 Differences in bone and vitamin D metabolism between primary hyperparathyroidism and malignancy-associated hypercalcemia. Journal of Clinical Endocrinology & Metabolism 81:607-611
10. **Stewart AF, Vignery A, Silverglate A, Ravin ND, Livolsi V, Broadus AE, Baron R** 1982 Quantitative bone histomorphometry in humoral hypercalcemia of malignancy: uncoupling of bone cell activity. Journal of Clinical Endocrinology & Metabolism 55:219-227
11. **Titon I, Cailleux-Bounacer A, Basuyau JP, Lefebvre H, Savoure A, Kuhn JM** 2007 Evaluation of a standardized short-time calcium suppression test in healthy subjects: interest for the diagnosis of primary hyperparathyroidism. European Journal of Endocrinology 157:351-357
12. **Randhawa PS, Mace AD, Nouraei SA, Stearns MP** 2007 Primary hyperparathyroidism: do perioperative biochemical variables correlate with parathyroid adenoma weight or volume? Clinical Otolaryngology 32:179-184
13. **McCarron DA, Muther RS, Lenfesty B, Bennett WM** 1982 Parathyroid function in persistent hyperparathyroidism: relationship to gland size. Kidney International 22:662-670
14. **Khosla S, Ebeling PR, Firek AF, Burritt MM, Kao PC, Heath H, 3rd** 1993 Calcium infusion suggests a "set-point" abnormality of parathyroid gland function in familial benign hypercalcemia and more complex disturbances in primary hyperparathyroidism. Journal of Clinical Endocrinology and Metabolism 76:715-720
15. **Malberti F, Farina M, Imbasciati E** 1999 The PTH-calcium curve and the set point of calcium in primary and secondary hyperparathyroidism. Nephrology, Dialysis, Transplantation 14:2398-2406

16. **Zhao L, Zhang M, Zhao H, Sun L, Li J, Tao B, Wang W, Ning G, Liu J** 2011 PTH inhibition rate is useful in the detection of early-stage primary hyperparathyroidism. Clinical Biochemistry 44:844-848
17. **Hagag P, Revet-Zak I, Hod N, Horne T, Rapoport M, Weiss M** 2003 Diagnosis of normocalcemic hyperparathyroidism by oral calcium loading test. Journal of Endocrinological Investigation 26:327-332
18. **Bevilacqua M, Dominguez LJ, Righini V, Valdes V, Vago T, Leopaldi E, Baldi G, Barrella M, Barbagallo M** 2006 Dissimilar PTH, gastrin, and calcitonin responses to oral calcium and peptones in hypocalciuric hypercalcemia, primary hyperparathyroidism, and normal subjects: a useful tool for differential diagnosis. Journal of Bone and Mineral Research 21:406-412
19. **Monchik J, Lamberton R, Roth U** 1992 Role of the oral calcium-loading test with measurement of intact parathyroid hormone in the diagnosis of symptomatic subtle primary hyperparathyroidism. Surgery 112:1103
20. **DeFronzo RA, Tobin JD, Andres R** 1979 Glucose clamp technique: a method for quantifying insulin secretion and resistance. American Journal of Physiology-Endocrinology And Metabolism 237:E214
21. **Grill V, Ho P, Body JJ, Johanson N, Lee SC, Kukreja SC, Moseley JM, Martin TJ** 1991 Parathyroid Hormone-Related Protein: Elevated Levels in both Humoral Hypercalcemia of Malignancy and Hypercalcemia Complicating Metastatic Breast Cancer. Journal of Clinical Endocrinology & Metabolism 73:1309-1315
22. **Takeuchi Y, Fukumoto S, Nakayama K, Tamura Y, Yanagisawa A, Fujita T** 2002 Parathyroid hormone-related protein induced coupled increases in bone formation and resorption markers for 7 years in a patient with malignant islet cell tumors. Journal of Bone and Mineral 17:753-757
23. **Kakuta T, Tanaka R, Kanai G, Miyamoto Y, Inagaki M, Suzuki H, Fukagawa M, Saito A** 2008 Relationship Between the Weight of Parathyroid Glands and Their Secretion of Parathyroid Hormone in Hemodialysis Patients With Secondary Hyperparathyroidism. Therapeutic Apheresis and Dialysis 12:385-390
24. **Corbetta S, Mantovani G, Lania A, Borgato S, Vicentini L, Faglia G, Di Blasio AM, Spada A** 2000 Calcium-sensing receptor expression and signalling in human parathyroid adenomas and primary hyperplasia. Clinical Endocrinology 52:339-348
25. **Farnebo F, Höög A, Sandelin K, Larsson C, Farnebo L-O** 1998 Decreased expression of calcium-sensing receptor messenger ribonucleic acids in parathyroid adenomas. Surgery 124:1094-1099
26. **Farnebo F, Enberg U, Grimelius L, Bäckdahl M, Schalling M, Larsson C, Farnebo L-O** 1997 Tumor-specific decreased expression of calcium sensing receptor messenger ribonucleic acid in sporadic primary hyperparathyroidism. Journal of Clinical Endocrinology & Metabolism 82:3481-3486
27. **Kifor O, Moore F, Wang P, Goldstein M, Vassilev P, Kifor I, Hebert S, Brown E** 1996 Reduced immunostaining for the extracellular Ca2+-sensing receptor in primary and uremic secondary hyperparathyroidism. Journal of Clinical Endocrinology & Metabolism 81:1598-1606
28. **Gogusev J, Duchambon P, Hory B, Giovannini M, Goureau Y, Sarfati E, Drüeke TB** 1997 Depressed expression of calcium receptor in parathyroid gland tissue of patients with hyperparathyroidism. Kidney International 51:328-336

29. **Yano S, Sugimoto T, Tsukamoto T, Chihara K, Kobayashi A, Kitazawa S, Maeda S, Kitazawa R** 2003 Decrease in vitamin D receptor and calcium-sensing receptor in highly proliferative parathyroid adenomas. European Journal of Endocrinology 148:403-411
30. **Hosokawa Y, Pollak MR, Brown EM, Arnold A** 1995 Mutational analysis of the extracellular Ca(2+)-sensing receptor gene in human parathyroid tumors. Journal of Clinical Endocrinology & Metabolism 80:3107-3110
31. **Cetani F, Pinchera A, Pardi E, Cianferotti L, Vignali E, Picone A, Miccoli P, Viacava P, Marcocci C** 1999 No Evidence for Mutations in the Calcium-Sensing Receptor Gene in Sporadic Parathyroid Adenomas. Journal of Bone and Mineral Research 14:878-882
32. **Younes NA, Shafagoj Y, Khatib F, Ababneh M** 2005 Laboratory screening for hyperparathyroidism. International Journal of Clinical Chemistry 353:1-12
33. **Maruani G, Hertig A, Paillard M, Houillier P** 2003 Normocalcemic primary hyperparathyroidism: evidence for a generalized target-tissue resistance to parathyroid hormone. Journal of Clinical Endocrinology & Metabolism 88:4641-4648
34. **Özbey N, Erbil Y, Ademoğlu E, Özarmağan S, Barbaros U, Bozbora A** 2006 Correlations between vitamin D status and biochemical/clinical and pathological parameters in primary hyperparathyroidism. World Journal of Surgery 30:321-326
35. **Khoo T-K, Baker C, Abu-Lebdeh H, Wermers R** 2007 Suppressibility of Parathyroid Hormone in Primary Hyperparathyroidism. Endocrine Practice 13:785-789
36. **Schmitt CP, Schaefer F, Bruch A, Veldhuis JD, Schmidt-Gayk H, Stein G, Ritz E, Mehls O** 1996 Control of pulsatile and tonic parathyroid hormone secretion by ionized calcium. Journal of Clinical Endocrinology and Metabolism 81:4236-4243
37. **Mundy GR, Guise TA** 1999 Hormonal control of calcium homeostasis. Clinical Chemistry 45:1347-1352
38. **Shrestha RP, Hollot CV, Chipkin SR, Schmitt CP, Chait Y** 2010 A mathematical model of parathyroid hormone response to acute changes in plasma ionized calcium concentration in humans. Mathematical Biosciences 226:46-57
39. **Fuleihan G, Gundberg CM, Gleason R, Brown EM, Stromski ME, Grant FD, Conlin PR** 1994 Racial differences in parathyroid hormone dynamics. Journal of Clinical Endocrinology and Metabolism 79:1642-1647
40. **Cosman F, Nieves J, Morgan D, Shen V, Sherwood D, Parisien M, Lindsay R** 1999 Parathyroid hormone secretory response to EDTA-induced hypocalcemia in black and white premenopausal women. Calcified Tissue International 65:257-261
41. **Haden ST, Brown EM, Hurwitz S, Scott J, El-Hajj Fuleihan G** 2000 The effects of age and gender on parathyroid hormone dynamics. Clinical Endocrinology 52:329-338

5. Potentiation of the calcium-sensing receptor across the spectrum of primary hyperparathyroidism

Having shown that it is possible to identify the various stages of primary hyperparathyroidism, the objective of this chapter is to explore the benefits of increasing the sensitivity of the calcium-sensing receptor across the spectrum of primary hyperparathyroidism.

5.1. Introduction

Increased parathyroid activity and oversecretion of parathyroid hormone (PTH) stemming from an adenomatous or hyperplastic growth of the PTG is termed primary hyperparathyroidism (PHPT) (1). This excessive secretion of PTH induces an increase in the calciotropic responses of the kidneys, bone and intestines resulting in: elevated CTL levels, thus higher intestinal calcium (Ca) absorption; increased bone resorption, thus lower bone mineral density (BMD); and, reduced Ca excretion. The net transfer of Ca from the bone, intestines and kidneys to the plasma gives rise to hypercalcemia (2).

The only cure for PHPT is surgical removal of the affected gland(s); however, medical treatment is considered for those that do not meet the criteria, or are unsuitable, for surgery (1). Current treatments include: hormone replacement therapy and bisphosphonates, which reduce plasma Ca and bone resorption; (3, 4) and calcimimetics (5).

Calcimimetics are a class of drugs that potentiate the effects of ionized Ca in parathyroid cells (6) through positive allosteric modulation of the Ca-sensing receptor (CaR) (7). The compounds, without triggering any functional activity in the CaR (7, 8), bind to the CaR thus enhancing signal transduction in the receptor thereby increasing receptor sensitivity to plasma Ca. In clinical studies, cinacalcet (CNC), a second-generation calcimimetic, has been shown: to upregulate CaR expression and decrease PTH levels in uremic rats (9); and, to inhibit PT cellular proliferation and prevent PTG weight and/or volume increases in partially nephrectomized rats (10). In humans, CNC has been proven to provide long-term reductions in serum PTH, Ca and phosphate levels across the entire spectrum of PHPT severity and in secondary hyperparathyroidism (SHPT) (11-14). However, in severe cases of PHPT, CNC has been reported to reduce or normalize serum Ca but modestly reduces or, in some cases has no effect on PTH levels (15-17).

To date, there has been no published literature on *in silico* studies of CaR activation in various stages of PHPT. Therefore, given that we can identify the extent of PHPT, we seek to explore the impact of increasing CaR sensitivity on Ca-regulation across the spectrum of PHPT. Additionally, we model CNC

therapy as reported in the literature (18) and, from this, develop a method to determine the optimum CNC dose *a priori*. The results of the study are reported herein.

5.2. Materials and Methods

5.2.1. Clinical datasets

Clinical data of Ca-related plasma biochemistries in PHPT subjects are taken from two studies (18, 19). The relevant group mean baseline ± SEM, or range, are reported below. Due to the similarity of the Ca and PTH values for the 30mg, 40mg and 50mg CNC cohorts in the study, data for the combined CNC group is used (18).

1. *Khosla et al., (19)*: seven patients with PHPT; serum Ca, 2.60 ± 0.05 mM; serum ionized Ca, 1.46 ± 0.02 mM; PTH, 9.31 ± 1.51 pM.
2. *Shoback et al., (18)*: 16 patients with PHPT; serum Ca, 10.6 (9.4 –12.7) mg/dL; PTH, 102 (67–186) pg/mL.

5.2.2. Model simulations

PHPT severity: In Chapter 4, we found that: the hypercalcemic slope ($m_{Ca(s)}A$) decreases with PHPT progression; the minimum PTH secretory rate (ACa) increases with PHPT progression and ACa approaches a maximum value. As such we used the estimated parameters for Patients 1, 4 and 7 (19) (reported as early-, mid- and late-stage PHPT). Additionally, we interpolated between the ranges of ACa and $m_{Ca(s)}A$ to get a better distribution of PHPT severity. Reported values of ACa are relative to that of the healthy model.

Calciotropic response to CaR activation: The CaR is represented by the sensor in the ECS diagram and the characteristic function is given by Eqn. (5.1). Plasma Ca ($Ca_{(p)}$) is detected by the sensor (CaR) which transmits the signal ($Ca_{(sens)}$) to the cell. The sensitivity of the CaR is indicated by the sensor gain (K_{sens}), which for the normal CaR in PHPT is unity.

$$Ca_{(sens)} = K_{sens}Ca_{(p)} \tag{5.1}$$

Each model of PHPT is first simulated with an initial K_{sens} of unity until steady-state is reached, at which point K_{sens} is increased and simulation continues until a new steady-state is reached. The steady-state values for Ca, PTH, urine Ca (Cau), calcitriol (CTL) and osteoblast-to-osteoclast (CB) ratio, at both the initial and final steady-states are recorded. This procedure is repeated for all changes in K_{sens} in

increments of 0.1 up to $K_{sens} = 2$. However, for late-stage PHPT, K_{sens} is increased in increments of: i) 0.1 up to a K_{sens} of 2; ii) 0.25 up to a K_{sens} of 3; and, iii) 0.5 up to a K_{sens} of 4.

Cinacalcet (CNC) therapy in PHPT:

The mechanisms involved in CNC lowering of PTH can be lumped as follows: i) CNC dissolution in the gastrointestinal (GI) tract; ii) CNC transfer to the plasma; ii) CNC activation of CaR; and, finally, iv) PTG response to increased sensitivity of the CaR.

The maximum reduction in PTH in the CNC cohort was approximately 47% (18), which coincides with the observed PTH suppression in early PHPT (Patient 1) (19). As such, ACa, and $m_{Ca(s)}A$ were initially chosen to be the same as early stage PHPT, the final values are determined using least squares estimation to match the Ca and PTH data provided. CaR sensitivity was studied for this model, as described above.

Cinacalcet in the GI tract and plasma: We approximate the processes of CNC dissolution in the GI tract and transfer to the plasma as a series reaction and estimate the cinacalcet profile in the plasma, $CNC_{(p)}$, using Equation (5.2). The parameters are defined as follows: $CNC_{gi,0}$ is the initial dose of CNC ingested in the GI tract at time, $t = 0$; $k_{CNC_{gi}}$ is the rate of transfer from the GI tract to the plasma and k_{CNC_p} is the rate of removal of CNC from the plasma. $k_{CNC_{gi}}$ and k_{CNC_p} are estimated such that the maximum CNC in plasma occurs at 4 hours post-dose (20).

$$CNC_{(p)} = \frac{k_{CNC_{gi}} CNC_{gi,0}}{k_{CNC_p} - k_{CNC_{gi}}} \left(e^{-k_{CNC_{gi}} t} - e^{-k_{CNC_p} t} \right) \quad 5.2$$

Plasma CNC activation of the CaR: The reported maximum PTH reduction, for the 30mg, 40mg and 50mg doses of CNC, at Day 1, are taken from the literature (18). The corresponding K_{sens} for each PTH reduction was recorded and a relationship between CNC dose and K_{sens} developed.

The plasma CNC profile and results from CNC activation of the CaR are used to simulate CNC therapy in PHPT.

5.3. Results

For ease of comparison, and unless otherwise stated, all simulation results are normalized using baseline values.

5.3.1. Calciotropic response to activation of the Ca-sensing receptor:

The increases in K_{sens} cause decreases in PTH, CTL, CB ratio and Ca across all stages of PHPT (Fig. 5.1A-C). However, only in early-stage PHPT is there any significant change in urinary Ca excretion (Fig. 5.1A). In early-stage PHPT (Fig. 5.1A), as K_{sens} increases, PTH levels decrease to a minimum of 51% of baseline. The downturn in PTH-stimulated synthesis of CTL precursors in the kidneys leads to a corresponding decline in CTL levels down to a minimum of 71% of basal levels. In the bone, the lower circulating PTH reduces bone cell proliferation such that a maximum decline of 21% is observed in the CB ratio. Finally, the falling PTH causes a complementary reduction in renal Ca reabsorption leading to an overall increase in Ca excretion up to 21% above basal levels. The combined effect of these changes in Ca regulation, is a reduction in circulating ionized Ca down to 85% of baseline.

For both early and mid-stage PHPT, the maximal effect of K_{sens} on PTH level—and by extension, CTL, CB, Cau and plasma Ca—is observed near a K_{sens} of 1.5 leading to a corresponding maximum change in CTL, CB, Cau and plasma Ca (Fig. 5.1A-B). This maximal effect will be explored in detail later. On the other hand, up to a $K_{sens} = 4$, no maximal effect of K_{sens} on PTH level is observed in late-stage PHPT; however, at this K_{sens}, the changes in plasma Ca, CTL,CB and Cau are minimal (Fig. 5.1C).

In both early and mid-stage PHPT, the rate-of-change of all variables (Ca, PTH, CTL, Cau and CB) with respect to a change in K_{sens} increases to a maximum at a K_{sens} of 1.1 and decreases thereafter, with no observable change beyond a K_{sens} of 1.5. For late-stage PHPT, the derivative of all variables increases to a maximum at 1.1 and decreases thereafter reaching a minimum beyond a K_{sens} of 4. The rate of change of PTH with respect to K_{sens}, for early- and mid-stage PHPT, increases up to 3 and 1.9, respectively at a $K_{sens} = 1.1$ and decreases to zero between a K_{sens} of 1.1 and 1.5 (Fig. 5.1D). Yet, for late-stage PHPT, the rate of change of PTH increases up 0.25 at a K_{sens} of 1, decreases to 0.06 between a K_{sens} range of 1.1 and 2, decreases to 0 thereafter (not shown). These findings indicate that the responses in the CaR-mediated PTH suppressing mechanisms are greater upon initial activation (sensitization) and moderately increase with further activation. However, for late-stage PHPT, there is moderate increase in the CaR-mediated PTH secretory mechanisms beyond initial activation.

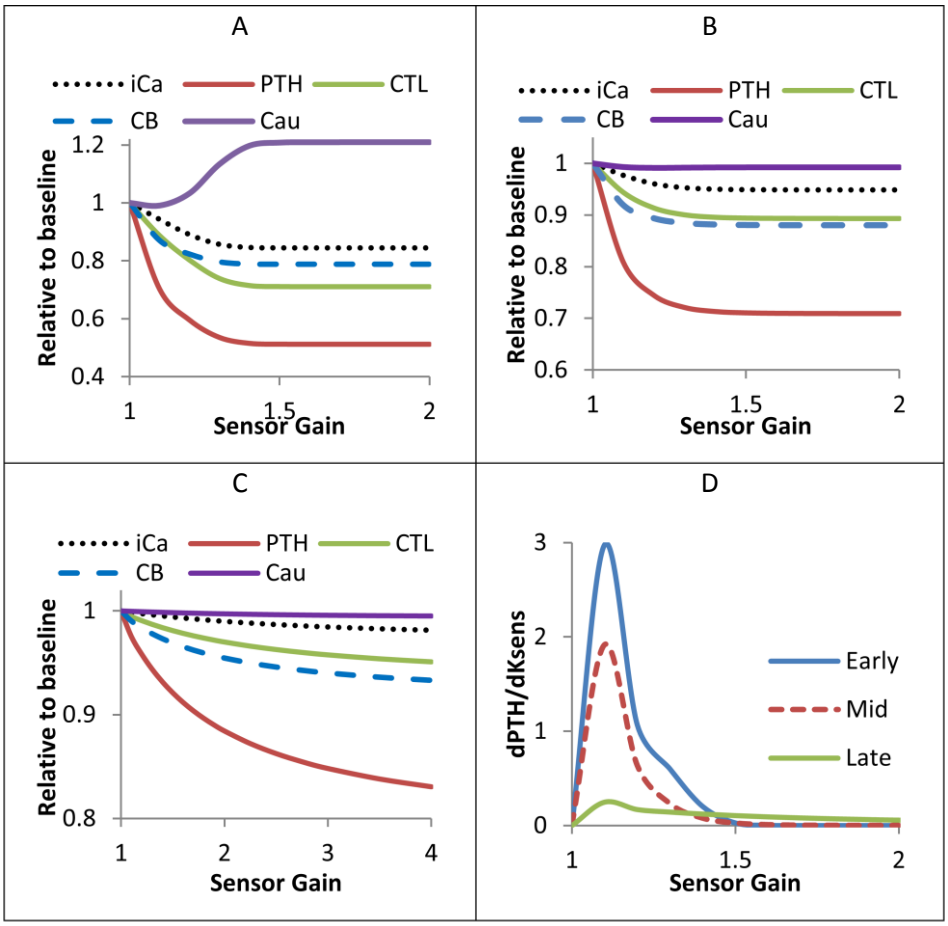

Figure 5.1. Simulated calciotropic response (ionized Ca, PTH, CTL, urinary Ca (Cau) and CB ratio) to changes in sensor gain in:

(A) Early-, (B) Mid-, and (C) Late-stage PHPT. (D) Comparison of the rate of change of PTH with respect to changes in sensor gain in Early-, Mid- and Late-stage PHPT.

The maximum change in PTH levels, due to increasing K_{sens}, decreases with the severity of the pathology, and by extension, the maximum changes in CTL, CB, Cau and Ca also fall with PHPT progression. For a K_{sens} of 2, the changes in PTH levels are 49%, 29% and 12% in early-, mid- and late-stage PHPT, respectively, with the corresponding changes in plasma Ca being 16%, 5% and 1%, respectively (Fig. 5.1A-C).

Given that there is a maximum PTH change with increasing K_{sens} in PHPT, we looked at the impact of K_{sens} changes across all the PHPT models. Figures 5.2A-B show the maximum observed change in PTH and Ca with incremental changes in K_{sens} for varying minimum PTH secretory rates (A_{Ca}). In general, for all models, there is a threshold value of K_{sens} beyond which any further increase will result in no observable change in PTH and Ca levels. This threshold value decreases as A_{Ca} increases. The maximum change in PTH (and Ca) with the corresponding threshold K_{sens} are 45% (14%) at 1.6, 36% (9%) at 1.5,

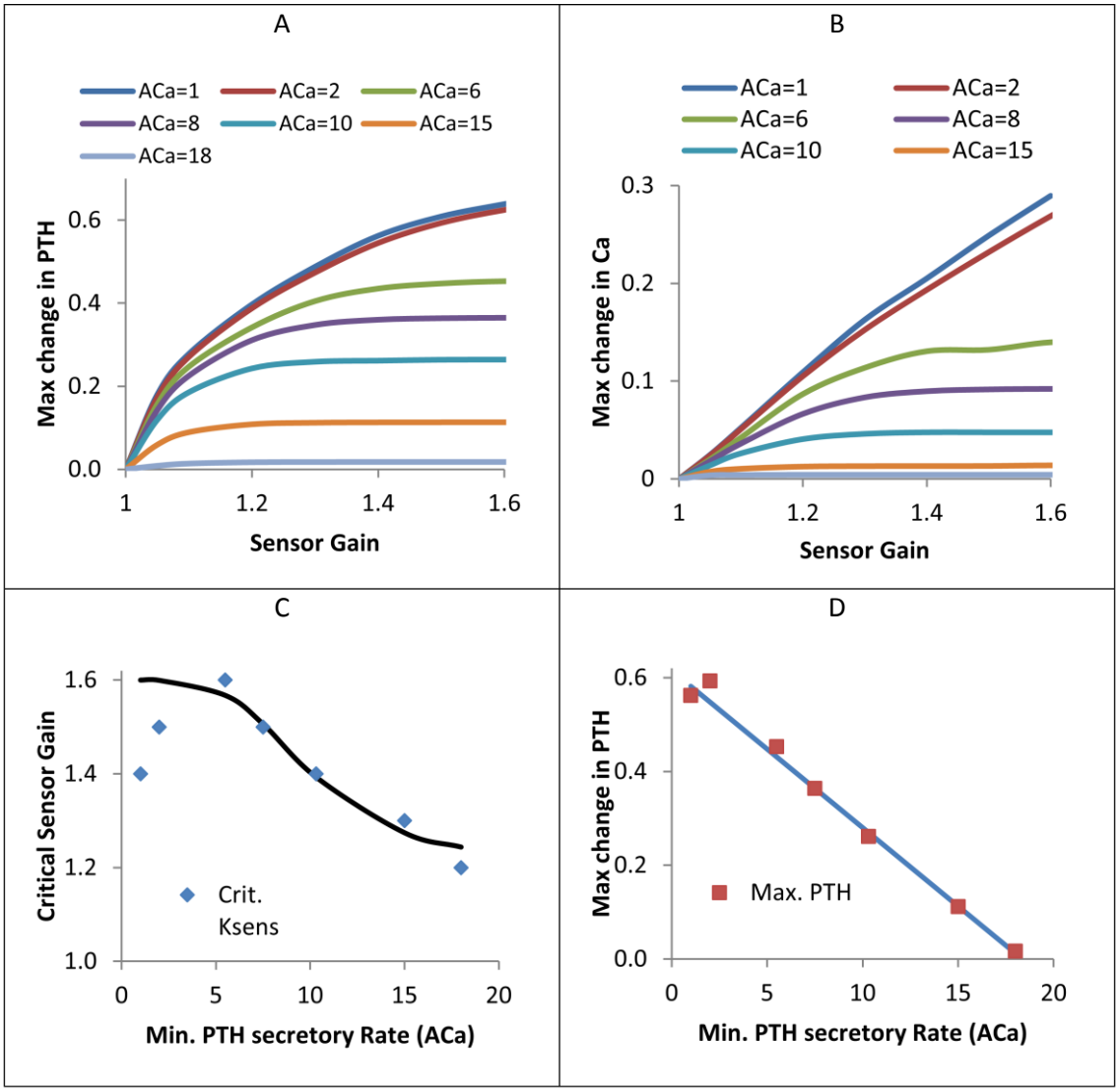

Figure 5.2. Simulation results of sensor gain changes in healthy model (ACa =1) and various stages of PHPT (ACa >1):
(A) Maximum change in PTH; (B) Maximum change in plasma Ca. Correlation between PHPT severity and (C) critical sensor gain, and (D) Maximum change in PTH

and 11% (1%) at 1.3 for A_{Ca} of 6, 8 and 15, respectively (Figure 5.2A-B). However, for the $A_{Ca} = 2$ (i.e. 'very' early PHPT), hypocalcemia occurs before the maximum PTH change is observed. As such, we define the critical sensor gain ($K_{sens,crit}$) as the value of K_{sens} beyond which any further increase will result in either hypocalcemia or no observable change in PTH levels. From these we infer that the relationship between A_{Ca} and $K_{sens,crit}$ can be represented by the logistic function; and the relationship between A_{Ca} and maximum change in PTH is a linear (Figs. 5.2C-D).

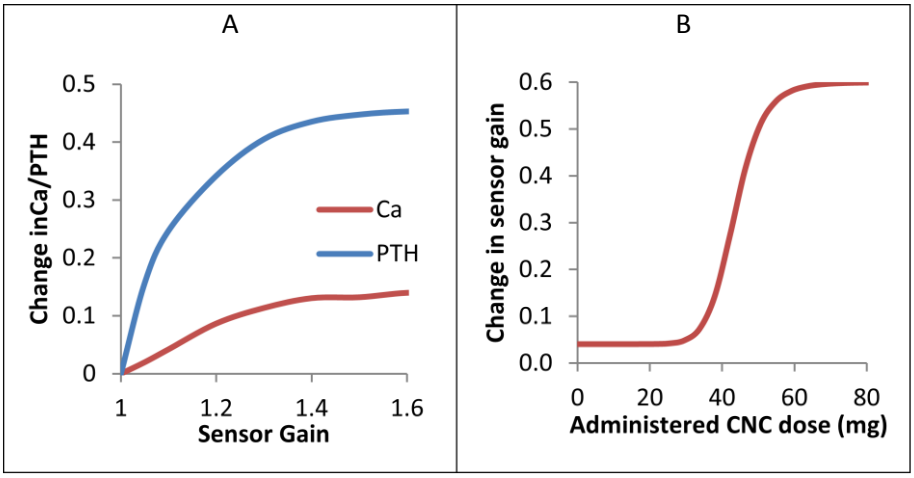

Figure 5.3. Simulation results of :

(A) changes in plasma Ca and PTH in response to changes in sensor gain in the CNC-treated PHPT cohort (18). (B) Correlation between prescribed CNC and expected changes in sensor gain

5.3.2. Cinacalcet Therapy

In order to implement cinacalcet therapy in our model, a relationship between the activation of the CaR and CNC in the plasma is required; however, no such information is available. This relationship is inferred by using information from the maximum observed PTH change, on Day 1, in clinical administration of CNC (18) and our correlation between K_{sens} and PTH change.

From the CaR activation profile of the CNC-treated PHPT model, there was a maximum PTH reduction of 45%, with a corresponding plasma Ca of 14%, occurring at a K_{sens} of 1.6 (Fig. 5.3A). From the literature (18), the maximum observed PTH reductions for 30mg, 40mg and 50mg doses of CNC were, on average, 15%, 37% and 47%, respectively. Using these observations and the profile in Figure 5.3A, we used a logistic function to describe the correlation between the change in K_{sens} and the administered CNC dose (Fig. 5.3B). Minimum stimulation of the CaR ($\Delta K_{sens} = 0.04$) occurs up to approximately 25 mg of administered CNC, between 25mg and 65 mg, K_{sens} changes proportionally with CNC dose. At a dose of 65mg CNC, $\Delta K_{sens} = 0.6$ and no significant change is observed in K_{sens} beyond 65 mg.

The estimated profiles of CNC in the GI tract and plasma for twice daily doses of 50mg CNC are shown in Figure 5.4A. The maximum CNC observed in the plasma increases between the first and second doses and remains constant in subsequent doses. Owing to the frequency of CNC intake, the minimum CNC in the plasma is approximately 40% of the maximum amount. The corresponding effects of plasma CNC on

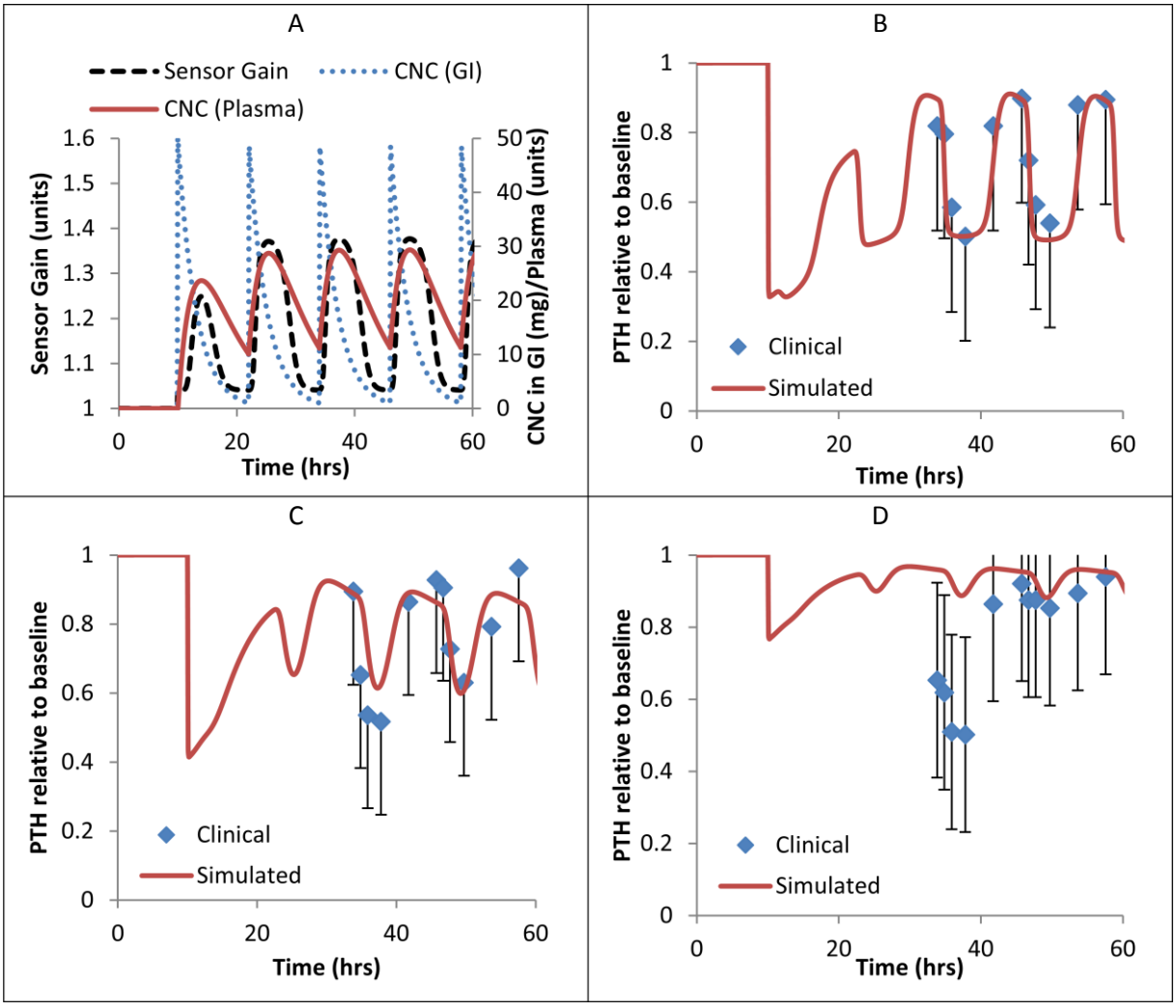

Figure 5.4. Simulation results of CNC therapy:

(A) twice daily dose of 50 mg cinacalcet: CNC release profile in the GI tract and plasma and, Sensor gain response. (B-C) Simulated vs. Clinical PTH response to twice daily dose of (B) 50mg, (C) 40mg, and (C) 30mg cinacalcet in patients diagnosed with PHPT. The bars represent the standard error recorded in the literature 188).

K_{sens} are also presented in Figure 5.4A. Upon first dose, K_{sens} increases to a maximum of 1.25; in subsequent doses, the attained maximum is 1.4, while the minimum observed K_{sens} is 1.04.

In Figures 5.4B-D, the simulated PTH responses to 50mg, 40mg and 30mg doses of CNC are within the PTH ranges measured in the clinical study (18). The simulation results provide a better prediction of the clinically observed mean at 40mg and 50mg than at 30mg. For both 30mg and 40mg, PTH results for the second of the two daily doses more closely match the clinically observed mean than for the first dose. There is a minimum observed PTH level that occurs within one hour of the first administered dose of CNC while all subsequent minima are higher and coincide with the maximum plasma CNC, which occurs

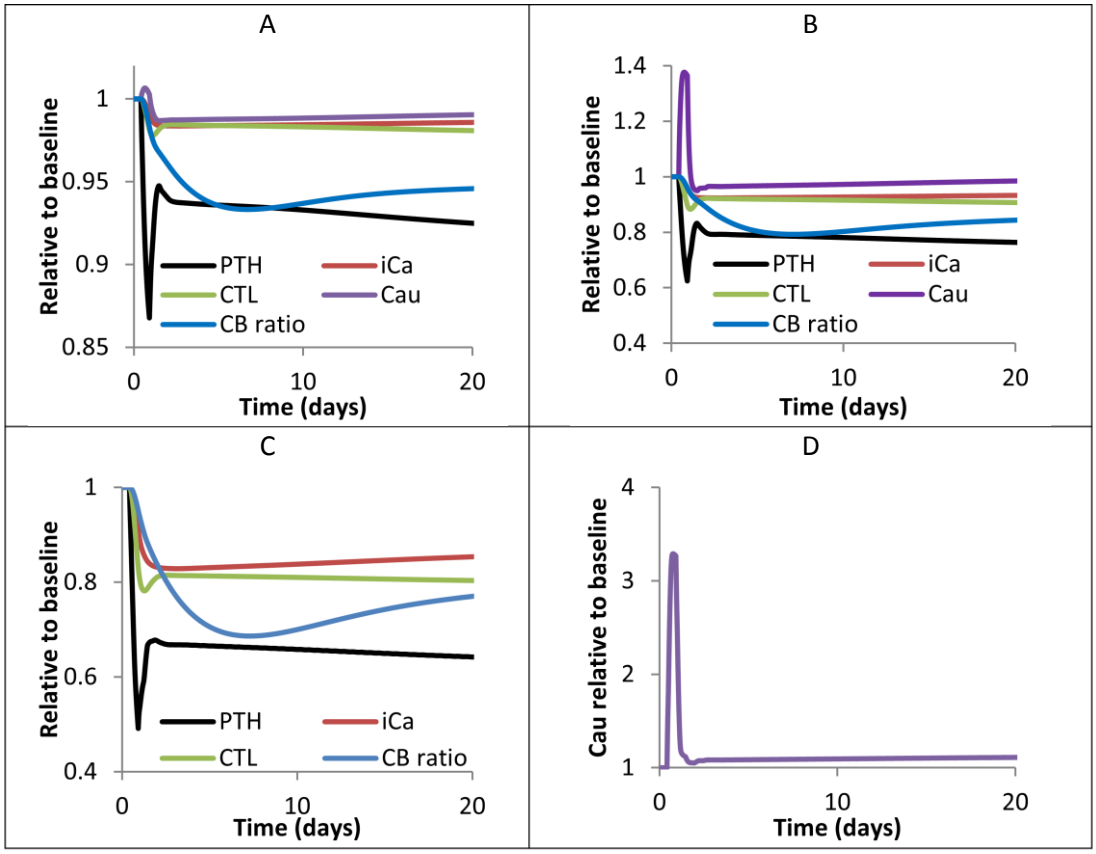

Figure 5.5. 12-hr moving average of calciotropic response to twice daily dose of cinacalcet over 20 days.

(A) 30mg; (B) 40mg; (C) 50mg; (D)Renal Ca excretion profile for twice daily 50mg CNC

2-6 hours post-dose. For example, at 40 mg, the initial minimum PTH reached is approximately 40% of basal levels, while successive doses of 40 mg CNC result in a minimum PTH of 60% of basal levels (Figure 5.4C). During CNC-therapy, PTH does not return to basal levels, but instead varies within a sub-basal range of: 50% - 85% for 50mg, 60% - 85% for 40mg and 87% - 92% for 30mg (Figures 5.4B-D).

The calciotropic response to 20-day CNC therapy is shown in Figure 5.5. As previously noted, PTH levels decrease proportionally with increasing CNC strength. By day 20, PTH is lowered to an average of 92%, 76% and 64% of baseline for 30mg, 40mg and 50mg CNC, respectively, with corresponding CTL levels of 98%, 91% and 80% of baseline. Bone cell proliferation decreases to a minimum during the first 6 days of drug therapy, but increases to a sub-basal endpoint thereafter; both the observed minimum and 20-day endpoint vary with CNC strength. Although there is an initial increase in Ca excretion, proportional to the change in PTH, there is no significant change in urinary excretion by day 20 for both the 30 mg and 40 mg doses (Figures 5.5 A-B). On the other hand, the Ca excretion endpoint for the 50 mg dose is 10% above baseline (Figure 5.5D). The combined effect of the changes in PTH, CTL, CB and urinary Ca is a reduction in Ca levels to 99% (30mg), 93% (40mg) and 86% (50mg) of baseline.

5.4. Discussion

The results of this study indicate that in the early stages of PHPT, both serum Ca and PTH may be reduced to the normal range, however, as PHPT progresses, normocalcemia is more likely, while PTH remains high; and, in severe cases, both hypercalcemia and elevated PTH levels persist. These findings are supported by clinical observations of CNC therapy in PHPT subjects: i) for patients administered a 50mg CNC over a 15-day period, both serum Ca and PTH were reduced to the normal range in patients with a pre-CNC treatment mean PTH baseline of 91 pg/ml (normal range, 10-62 pg/ml) (18); ii) during a 2-year treatment period, serum ionized Ca was normalized in 81% of patients, while 25% had normal PTH with pre-treatment mean PTH of 141± 78 pg/ml (21); and, iii) for 7 patients treated with CNC over a 3-117 week period (median 31 weeks), normocalcemia was observed in 1 patient, while none showed any observable change in serum PTH, with a pre-treatment mean PTH of 744pg/mL (16). Furthermore, in PHPT, PTH secretion increases with gland size, likewise, the PTG minimum secretory capacity increases with the size. Khosla et al. (19), showed that PTH suppression, through induced hypercalcemia, decreases with increasing gland size. As a whole, the simulation results and clinical observations imply that there is a limit to the effect of CaR activation in suppressing PTH levels in PHPT. This limit is dictated by the difference between the basal and minimum secretory rates, and the limit decreases with increasing severity of PHPT.

Studies have shown that CNC shifts the Ca-PTH setpoint leftward (8, 22), lowers the maximal PTH secretory rate in normal bovine PT cells (8) and reduces the minimum and maximum PTH secretory rates in subjects with secondary hyperparathyroidism (SHPT) (22). The impact of CNC on minimum PTH secretion in PHPT is yet to be addressed; however, some studies have reported that CNC therapy in patients with severe PHPT provides no observable change in PTH levels (15, 16). Therefore, in the absence of sufficient data, one can speculate that if, in severe cases of PHPT, CNC provides no PTH suppression then, in general, CNC does not lower minimum PTH secretion in PHPT. This implies that there is a maximum possible PTH suppression in all cases of PHPT, which remains unchanged with CNC therapy. Therefore, the correlations presented in Figures 5.2C and D can serve as a guide to the clinician in indicating the expected benefits, given a patient's minimum PTH secretory rate.

Since the degree of PTH suppression varies with the severity of PHPT, then the relationships between administered CNC dose and (i) K_{sens}, and (ii) PTH suppression vary according to the severity of the disease. Therefore, there is a family of curves (similar to Figure 5.3B) across the spectrum of the disease. The approach presented herein provides a blueprint with which such curves can be determined; these

curves may then be used as a part of the decision support system in determining the optimal dose of CNC for a desired PTH reduction given the extent of PHPT.

In general, the simulation results for short-term CNC therapy are consistent with the clinical observations. With the exception of Ca excretion, all calciotropic responses decrease proportionally with the administered dose of CNC (18). Although a similar increase in urine calcium for the 50-mg dose was observed in both the simulation and clinical results (11% vs. 13%), there was no similarity between the two results for 30-mg (-1%, simulated vs. 51%, clinical) and 40-mg (-1%, simulated vs. 15% clinical). Nevertheless, the authors reported no consistent trend in the effect of CNC on Ca in urine (18). It is important to note that the model does not account for the effect of renal CaRs, which are known to participate in Ca regulation (23), therefore changes to urinary Ca due to CNC activation of renal CaR are neglected. Regarding bone biology, the decrease in bone osteoclast-to-osteoblast (CB) ratio, across all doses of CNC, indicates a change in bone turnover. No information of the impact of CNC on bone biology was provided in the short-term study (18). However, in a year-long study, the same authors reported that no significant changes in BMD were observed, but bone turnover markers increased in the CNC group (24).

There is a noted difference in K_{sens} required to elicit a significant change in PTH levels in both SHPT and PHPT. In preliminary studies of CaR activation in SHPT, we've noted a K_{sens} up to 1.06 corresponding to approximately 85% decrease in PTH levels in SHPT (not presented). Also, Goodman et al., (25) noted that CNC elicited the same percentage change in PTH levels in SHPT patients, regardless of the biochemical severity of the disease, and the percentage change was proportional to the administered dose of CNC. On the other hand, the simulation results show that the greatest change in PHPT is a 49% reduction in PTH levels in early-PHPT, occurring at a K_{sens} of 1.6; and, clinical observations show that CNC therapy in severe cases of PHPT had no effect on PTH levels (16). Collectively, these findings suggest differences in the two pathologies at the level of the CaR. In SHPT, there is reduced CaR expression in hyperplastic PT cells compared with healthy PT cells (26) and the expression decreases with disease progression in SHPT (27). In PHPT, there is reduced CaR expression in hyperplastic and adenomatous PT cells (28) and a loss-of-function mutation of the CaR has been observed in some cases of PHPT (29-32). Despite the lower CaR expression, several studies have shown substantial decreases in PTH levels to induced hypercalcemia in SHPT patients undergoing dialysis (33-35) while no such observations are reported in PHPT. As a whole, the evidence suggests that there is a difference in the mechanism of CaR-mediated PTH production in both PHPT and SHPT.

As with any model, the accuracy of the results is dependent on the dataset from which the parameters are estimated. Therefore, the relationships derived between the critical sensor gain and PTH severity, and maximum PTH change and PTH severity can be improved with a larger dataset of clinically induced hypercalcemia in various stages of PHPT. Furthermore, a larger dataset of CNC therapy in PHPT patients across the spectrum of the pathology can be used to improve the relationship between sensor gain and CNC dose and maximum PTH change and CNC dose. Additionally, for a better prediction of long-term CNC therapy in the different stages of PHPT, more detailed information regarding the effect of disease progression on the different subprocesses of the Ca-regulatory system should be incorporated.

In conclusion, this study shows that through determining the effect of increases in CaR sensitivity in various stages of PHPT, we can determine the relationship between the critical sensitivity of the PT CaR and the maximum possible change in PTH, for each stage of the disease. For any stage of PHPT, this relationship can be used to identify the potential improvement in PTH levels *a priori*. Furthermore, our model can reproduce the calciotropic effects of short-term cinacalcet therapy in PHPT subjects; and, in so doing we developed a useful method to determine the optimum dose of CNC required to elicit the maximum reduction in PTH levels. Our approach provides a blueprint for developing similar correlations across the different stages of PHPT for CNC and other calcimimetics. Ultimately, these correlations can be used as part of the decision support system in prescribing the optimum doses for a desired PTH change using calcimimetic therapy.

5.5. References

1. **Fraser WD** 2009 Hyperparathyroidism. Lancet 374:145-158
2. **Kovacs WJ, Ojeda SR** 2012 Textbook of Endocrine Physiology. 6th ed. Oxford: Oxford University Press
3. **Orr-Walker BJ, Evans MC, Clearwater JM, Horne A, Grey AB, Reid IR** 2000 Effects of Hormone Replacement Therapy on Bone Mineral Density in Postmenopausal Women With Primary Hyperparathyroidism: Four-Year Follow-up and Comparison With Healthy Postmenopausal Women. Archives of Internal Medicine 160:2161-2166
4. **Selby PL, Peacock M** 1986 Ethinyl estradiol and norethindrone in the treatment of primary hyperparathyroidism in postmenopausal women. New England Journal of Medicine 314:1481-1485
5. **Silverberg SJ, Rubin MR, Faiman C, Peacock M, Shoback DM, Smallridge RC, Schwanauer LE, Olson KA, Klassen P, Bilezikian JP** 2007 Cinacalcet hydrochloride reduces the serum calcium concentration in inoperable parathyroid carcinoma. Journal of Clinical Endocrinology and Metabolism 92:3803-3808
6. **Nemeth EF, Steffey ME, Hammerland LG, Hung BCP, Van Wagenen BC, DelMar EG, Balandrin MF** 1998 Calcimimetics with potent and selective activity on the parathyroid calcium receptor. Proceedings of the National Academy of Sciences of the United States of America 95:4040-4045
7. **Hammerland LG, Garrett JE, Hung BCP, Levinthal C, Nemeth EF** 1998 Allosteric activation of the Ca2+ receptor expressed in Xenopus laevis oocytes by NPS 467 or NPS 568. Molecular Pharmacoly 53:1083-1088
8. **Nemeth EF, Heaton WH, Miller M, Fox J, Balandrin MF, Van Wagenen BC, Colloton M, Karbon W, Scherrer J, Shatzen E** 2004 Pharmacodynamics of the type II calcimimetic compound cinacalcet HCl. Journal of Pharmacology and Experimental Therapeutics 308:627-635
9. **Mizobuchi M, Hatamura I, Ogata H, Saji F, Uda S, Shiizaki K, Sakaguchi T, Negi S, Kinugasa E, Koshikawa S** 2004 Calcimimetic compound upregulates decreased calcium-sensing receptor expression level in parathyroid glands of rats with chronic renal insufficiency. Journal of the American Society of Nephrology 15:2579-2587
10. **Colloton M, Shatzen E, Miller G, Stehman-Breen C, Wada M, Lacey D, Martin D** 2005 Cinacalcet HCl attenuates parathyroid hyperplasia in a rat model of secondary hyperparathyroidism. Kidney International 67:467-476
11. **Marcocci C, Chanson P, Shoback D, Bilezikian J, Fernandez-Cruz L, Orgiazzi J, Henzen C, Cheng S, Sterling LR, Lu J, Peacock M** 2009 Cinacalcet reduces serum calcium concentrations in patients with intractable primary hyperparathyroidism. Journal of Clinical Endocrinology and Metabolism 94:2766-2772
12. **Peacock M, Bilezikian JP, Bolognese MA, Borofsky M, Scumpia S, Sterling LR, Cheng SF, Shoback D** 2011 Cinacalcet HCl Reduces Hypercalcemia in Primary Hyperparathyroidism across a Wide Spectrum of Disease Severity. Journal of Clinical Endocrinology and Metabolism 96:E9-E18
13. **Block GA, Martin KJ, de Francisco AL, Turner SA, Avram MM, Suranyi MG, Hercz G, Cunningham J, Abu-Alfa AK, Messa P** 2004 Cinacalcet for secondary hyperparathyroidism in patients receiving hemodialysis. New England Journal of Medicine 350:1516-1525

14. **Lindberg JS, Culleton B, Wong G, Borah MF, Clark RV, Shapiro WB, Roger SD, Husserl FE, Klassen PS, Guo MD, Albizem MB, Coburn JW** 2005 Cinacalcet HCl, an oral calcimimetic agent for the treatment of secondary hyperparathyroidism in hemodialysis and peritoneal dialysis: a randomized, double-blind, multicenter study. Journal of the American Society of Nephrology 16:800-807
15. **James Norman M, Lopez J, Doug Politz M** 2012 Cinacalcet (Sensipar) provides no measurable clinical benefits for patients with primary hyperparathyroidism and may accelerate bone loss with prolonged use. Annals of Surgical Oncology 19:1466-1471
16. **Krajewska J, Paliczka-Cieslik E, Krawczyk A, Szpak-Ulczok S, Michalik B, Hasse-Lazar K, Jurecka-Lubieniecka B** 2009 The results of cinacalcet therapy in patients with severe or refractory hypercalcemia due to primary hyperparathyroidism. Endocrine Abstracts 20:239
17. **Montecino MA, Lian JB, Stein JL, Stein GS, van Wijnen AJ, Cruzat F** 2010 Biological and molecular effects of vitamin D on bone. In: Vitamin D: Springer; 189-209
18. **Shoback DM, Bilezikian JP, Turner SA, McCary LC, Guo MD, Peacock M** 2003 The calcimimetic cinacalcet normalizes serum calcium in subjects with primary hyperparathyroidism. Journal of Clinical Endocrinology and Metabolism 88:5644-5649
19. **Khosla S, Ebeling PR, Firek AF, Burritt MM, Kao PC, Heath H, 3rd** 1993 Calcium infusion suggests a "set-point" abnormality of parathyroid gland function in familial benign hypercalcemia and more complex disturbances in primary hyperparathyroidism. Journal of Clinical Endocrinology and Metabolism 76:715-720
20. **Amgen Inc.** 2004 Sensipar® (cinacalcet) tablets. In: Amgen Inc.
21. **Sajid-Crockett S, Singer FR, Hershman JM** 2008 Cinacalcet for the treatment of primary hyperparathyroidism. Metabolism: clinical and experimental 57:517-521
22. **Valle C, Rodriguez M, Santamaría R, Almaden Y, Rodriguez ME, Canadillas S, Martin-Malo A, Aljama P** 2008 Cinacalcet reduces the set point of the PTH-calcium curve. Journal of the American Society of Nephrology 19:2430-2436
23. **Rodriguez M, Nemeth E, Martin D** 2005 The calcium-sensing receptor: a key factor in the pathogenesis of secondary hyperparathyroidism. American Journal of Physiology-Renal Physiology 288:F253-F264
24. **Peacock M, Bilezikian JP, Klassen PS, Guo MD, Turner SA, Shoback D** 2005 Cinacalcet hydrochloride maintains long-term normocalcemia in patients with primary hyperparathyroidism. Journal of Clinical Endocrinology and Metabolism 90:135-141
25. **Goodman WG, Hladik GA, Turner SA, Blaisdell PW, Goodkin DA, Liu W, Barri YM, Cohen RM, Coburn JW** 2002 The calcimimetic agent AMG 073 lowers plasma parathyroid hormone levels in hemodialysis patients with secondary hyperparathyroidism. Journal of the American Society of Nephrology 13:1017-1024
26. **Kifor O, Moore F, Wang P, Goldstein M, Vassilev P, Kifor I, Hebert S, Brown E** 1996 Reduced immunostaining for the extracellular Ca2+-sensing receptor in primary and uremic secondary hyperparathyroidism. Journal of Clinical Endocrinology and Metabolism 81:1598-1606
27. **Gogusev J, Duchambon P, Hory B, Giovannini M, Goureau Y, Sarfati E, Drüeke TB** 1997 Depressed expression of calcium receptor in parathyroid gland tissue of patients with hyperparathyroidism. Kidney International 51:328-336

28. **Yano S, Sugimoto T, Tsukamoto T, Chihara K, Kobayashi A, Kitazawa S, Maeda S, Kitazawa R** 2003 Decrease in vitamin D receptor and calcium-sensing receptor in highly proliferative parathyroid adenomas. European Journal of Endocrinology 148:403-411
29. **Frank-Raue K, Leidig-Bruckner G, Haag C, Schulze E, Lorenz A, Schmitz-Winnenthal H, Raue F** 2011 Inactivating calcium-sensing receptor mutations in patients with primary hyperparathyroidism. Clinical Endocrinology 75:50-55
30. **Hannan FM, Nesbit MA, Christie PT, Lissens W, Van der Schueren B, Bex M, Bouillon R, Thakker RV** 2010 A homozygous inactivating calcium-sensing receptor mutation, Pro339Thr, is associated with isolated primary hyperparathyroidism: correlation between location of mutations and severity of hypercalcaemia. Clinical Endocrinology 73:715-722
31. **Warner J, Epstein M, Sweet A, Singh D, Burgess J, Stranks S, Hill P, Perry-Keene D, Learoyd D, Robinson B** 2004 Genetic testing in familial isolated hyperparathyroidism: unexpected results and their implications. Journal of Medical Genetics 41:155-160
32. **Carling T, Szabo E, Bai M, Ridefelt P, Westin G, Gustavsson P, Trivedi S, Hellman P, Brown EM, Dahl N, Rastad J** 2000 Familial Hypercalcemia and Hypercalciuria Caused by a Novel Mutation in the Cytoplasmic Tail of the Calcium Receptor. Journal of Clinical Endocrinology and Metabolism 85:2042-2047
33. **Ramirez JA, Goodman WG, Gornbein J, Menezes C, Moulton L, Segre GV, Salusky IB** 1993 Direct in vivo comparison of calcium-regulated parathyroid hormone secretion in normal volunteers and patients with secondary hyperparathyroidism. Journal of Clinical Endocrinology and Metabolism 76:1489-1494
34. **Pahl M, Jara A, Bover J, Rodriguez M, Felsenfeld AJ** 1996 The set point of calcium and the reduction of parathyroid hormone in hemodialysis patients. Kidney International 49:226-231
35. **Rodriguez M, Caravaca F, Fernandez E, Borrego MJ, Lorenzo V, Cubero J, Martin-Malo A, Betriu A, Jimenez A, Torres A** 1999 Parathyroid function as a determinant of the response to calcitriol treatment in the hemodialysis patient. Kidney International 56:306-317

6. Identifying potential therapeutic targets in hyperparathyroidism

This chapter is, in some sense, a continuation of the previous chapter. However, the objective here is to show how the process systems engineering methods can be applied to the models of Ca regulation in identifying potential sites for therapeutic intervention in related pathologies and customizing therapies for individual patients. In comparison to the previous chapters, the focus more on the mathematical aspects of the research.

6.1. Introduction

Hyperparathyroidism (HPT) develops due to increased parathyroid activity emanating from within the PTG or from an external abnormal change affecting Ca regulation thus inducing increased PTG activity. Primary HPT (PHPT) develops from an unprovoked adenomatous or hyperplastic growth of the PTG and is characterized by high PTH levels, hypercalcemia and low bone mineral density (1). Secondary HPT (SHPT) is a late-stage complication of chronic kidney disease (CKD) and is characterized by high PTH levels, hypocalcemia and increased bone loss (1). The current medical treatments for HPT include: hormone replacement therapy and bisphosphonates, both of which reduce plasma Ca and bone resorption, (2, 3) and calcimimetics, which suppresses PTH production (4).

Calcimimetics are a class of drugs that potentiate the effects of ionized Ca in parathyroid cells (5) through positive allosteric modulation of the Ca-sensing receptor (CaR) (6). The compounds enhance signal transduction in the receptor, thus increasing receptor sensitivity to plasma Ca, through binding to the CaR, while not triggering any functional activity in the CaR (6, 7). In clinical studies, cinacalcet (CNC), a second-generation calcimimetic, has been shown: to upregulate CaR expression and decrease PTH levels in uremic rats (8); and, to inhibit PT cellular proliferation and prevent PTG weight and/or volume increases in partially nephrectomized rats (9). In humans, CNC has been proven to provide long-term reductions in serum PTH, Ca and phosphate levels across the entire spectrum of PHPT severity and in SHPT (10-13).

The developments in the fields of control theory and digital computing have facilitated greater research in the area of physiological control systems (14) to the extent that medical devices have been developed for administering optimal therapeutic treatment in a variety of diseases (15). Calcium (Ca) regulation is one of the more important control systems in the body (16), yet, only limited work has been performed in the mathematical modeling of Ca regulation in humans (17-19). The models of Ca regulation presented in the literature were either empirical models or a single monolithic system of differential equations, neither of which lends itself easily to quantitative analysis. Jaros et al., (17) first purported an empirical control

system model of Ca regulation; however, since then, more detailed mechanistic information of several Ca-regulatory subprocesses have been elucidated. As a result, in Chapter 2, we developed a model of plasma Ca regulation using an engineering control system (ECS) framework to represent the biological process of Ca regulation in both the healthy and diseased states. We now seek to apply process systems engineering methods to both PHPT and SHPT with an aim of: identifying potential target sites for therapeutic intervention, validating our results with existing therapies; and providing a means for determining optimum treatment given the extent of the pathology and the desired patient outcome.

6.2. Modeling & Computational Strategy

6.2.1. State-space patient models

In this chapter, two different versions of the model of Ca/phosphate regulation are employed. The first, used in the simulations associated with PHPT and outlined in detail in Chapter 2, provides a comprehensive description of the mechanisms involved in Ca regulation, but only a minimal representation of phosphate control. The second model, used in the simulations associated with SHPT, incorporates a more detailed description of phosphate regulation and is described in Chapter 3. A first principles approach is used in describing the processes of: phosphate sensing, fibroblast growth factor-23 (FGF-23) production, intestinal phosphate absorption, and renal phosphate reabsorption. Finally, the mathematical description for PTH production in the controller is updated to include the effects of plasma phosphate and FGF-23 on PTH synthesis.

Although SHPT occurs due to abnormal activity of the controller (PTG), the condition is a late-stage complication of chronic kidney disease (CKD), an actuator defect. A brief description of the modifications to the second model in representing CKD and SHPT are described.

In CKD, the fractional decline in renal function is represented by an independent, dimensionless term RF, which varies between 0.1 and 1, indicating complete failure or normal renal function, respectively. In determining urine Ca and phosphate, RF pre-multiplies the GFR and the hormone-dependent portions of Ca and phosphate reabsorption. As CTL production declines disproportionately with renal failure, a CTL-production degradation factor ($r_{CTL,deg}$) is introduced, which is a function of the RF. As CKD worsens, the increase in phosphate retention leads to precipitation of calcium-phosphate salts, therefore, two additional terms, λ_{PO4d} and λ_{Cad} are added to the plasma calcium and phosphate balance equations such that a fraction of the excess plasma phosphate, and by extension Ca, is consumed in CaHPO4 formation. Finally, PTG hyperplasia is modeled as previously described in Chapter 2. All equations and parameter values used in the model are listed in the Appendix.

6.2.2. Identification of target site and model behavior over the parameter space

In identifying the potential target sites for therapeutic intervention, we used the expression for the normalized sensitivity analysis (Eq. 6.1) (20) to identify the parameters to which PTH and Ca are most sensitive. The system variables (PTH and Ca) are denoted by y, and the model parameters by p.

$$NSC_{ij}(t) = \frac{p_j}{y_i}\frac{\partial y_i(t,\boldsymbol{p})}{\partial p_j}\Big|_p, i = 1,2; j = 1, \dots, \text{n} \qquad 6.1$$

All model parameters are explored in the analysis as follows:

Step 1. Initialize parameters with the reference values.
Step 2. Run simulation until steady-state is achieved.
Step 3. Input 2-hr Ca disturbance to induce hypercalcemia, as described in the literature (21), and continue simulation until steady-state is achieved
Step 4. Calculate NSC
Step 5. Change parameter p_j, Repeat Steps 2-4
Step 6. Reinitialize p_j with reference value. Repeat Step 5.

The more important parameters are reported along with their physiological significance. Additionally, from the results of the sensitivity analysis, we identify the behavior of the model variables over the parameter space.

6.2.3. Implementation of existing cinacalcet (CNC) therapy

Ingested CNC is dissolved in the GI tract and transferred to the plasma where it is transported to the site of action—*the sensor*—which induces a change in PTH secretion. The sequence of actions can be represented by the expressions g_1, g_2, g_3 in Eqn. 6.2: where the subscripts p, and gi represent the plasma and gastrointestinal (GI) tract, respectively.

$$\begin{aligned} \Delta PTH &= g_1(\Delta K_{Ca,sens}) \\ \Delta K_{Ca,sens} &= g_2(CNC_{(p)}) \\ CNC_{(p)} &= g_3(CNC_{(gi)}) \end{aligned} \qquad 6.2$$

From identifying the PTH response over the range of sensor gain, the function g_1 is determined. Plasma CNC concentration profile, g_3, is approximated by the series reaction expression given in Eqn. 6.3. The parameters are defined as follows: the subscript $gi, 0$ refers to the ingested amount at $t = 0$; the rates of transfer from the GI tract to the plasma, $k_{CNC_{gi}}$, and CNC removal from the plasma, k_{CNC_p}, are estimated

such that the maximum CNC in plasma occurs at 4 hours post dose, in PHPT (22); for SHPT, $k_{CNC_{gi}}$ and k_{CNC_p} are estimated using pharmacokinetic data from the literature (23). Finally, clinical studies of CNC administration in PHPT and SHPT subjects provide data for the change in PTH for each dose of oral CNC administered (24, 25); therefore, g_2 can be determined. All expressions and parameter estimates are described in Tables 6A.3-4.

$$CNC_{(p)} = \frac{k_{CNC_{gi}} CNC_{gi,0}}{k_{CNC_p} - k_{CNC_{gi}}} \left(e^{-k_{CNC_{gi}} t} - e^{-k_{CNC_p} t} \right) \quad 6.3$$

6.2.4. Model predictive control

A nonlinear model predictive controller is constructed for plasma PTH control in the SHPT model based on PTH levels and daily CNC intake. The optimization problem solved by the MPC is given by:

$$\min_{\mathbf{\Delta u}(\mathrm{k})} \left(\mathbf{\Delta u}(\mathrm{k})^{\mathrm{T}} \mathbf{H} \mathbf{\Delta u}(\mathrm{k}) + \mathbf{c}^{\mathbf{T}} \mathbf{\Delta u}(\mathrm{k}) \right)$$

$$\text{Subject to: } \mathbf{Az} \leq \mathbf{b} \quad 6.4$$

Where **H** and **A** are matrices of tuning parameters and hard constraints, respectively; the vectors **z** and **b** are linear functions of the output prediction vector and past inputs. The aim of the quadratic program is to minimize the error in setpoint tracking and the manipulated input movement, over the sequence of future input moves, $\mathbf{\Delta u}(\mathrm{k})$ (26).

In this application, the ultimate goal is to reduce the PTH to the desired setpoint in SHPT. This is achieved by determining the CNC dose needed (manipulated variable) through minimizing the error between the model PTH output and the setpoint. The modeling strategy used is based on the CNC administration protocol. CNC is available in 30, 60 and 90 mg tablets, and for SHPT, should be titrated no more frequently than ever 2-4 weeks through sequential doses of 30mg increments, once daily, up to a maximum of 180mg (22). Therefore, the considerations for the MPC strategy are as follows: i) a mixed-integer quadratic program (MIQP) solver (27) is used such that 1 unit represents 30 mg of CNC; ii) incremental changes in CNC dose constraints— $\mathbf{\Delta u}(\mathrm{k}) \in \mathbb{Z} = \{-1,0,1\}$; and, iii) CNC dose constraints— $u \in \mathbb{Z} = \{0,1,\ldots,6\}$.

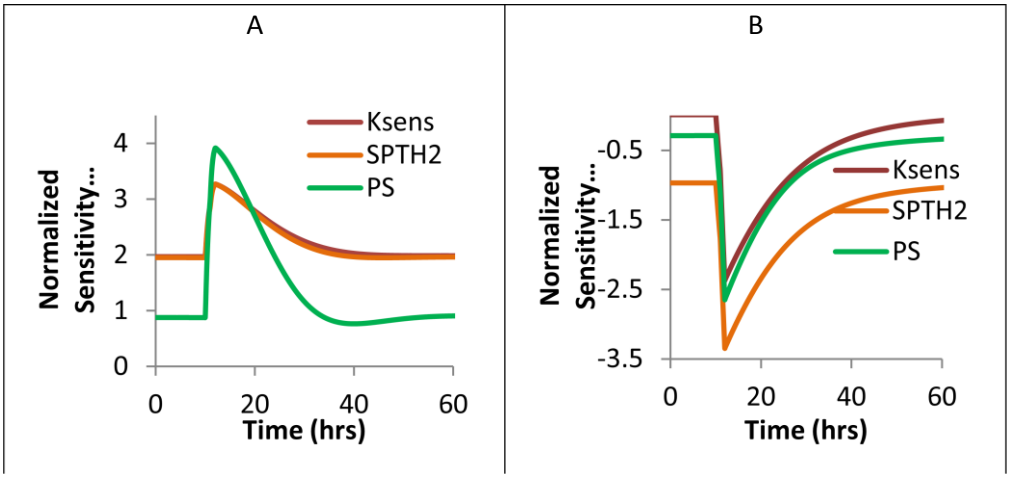

Figure 6.1. Model parameter sensitivities for selected parameters with the greatest influence on:

(A) PTH with the corresponding (B) Ca results.

6.3. Results & Discussion

6.3.1. Sensitivity Analysis in PHPT

Figure 6.1A shows the normalized sensitivity coefficients over time for the three parameters to which PTH is most sensitive along with the NSC profile with respect to Ca (Fig. 6.1B). Additionally, the parameters with a NSC > 0.75 are listed in Table 6.1. The most sensitive parameters are associated with processes that directly impact PTH secretion or Ca transfer to/from plasma (Table 6.1). The steady-state concentration of PTH is most strongly affected by $K_{Ca,sens}$ (sensor gain—CaR sensitivity), and $S_{PTH,2}$ (the concentration of PTH that determines the amount of PTH-induced Ca reabsorption); however, of the two, $S_{PTH,2}$ has a greater impact on Ca at steady-state. On the other hand, during induced

Table 6.5. Maximum Normalized Sensitivity Coefficient at steady-state for Select Parameters

Parameter	Sub-process	NSC (PTH)	NSC (Ca)
$K_{Ca,sens}$	Ca - sensing	1.97	0.01
$S_{PTH,2}$	Ca excretion	1.95	-0.20
GFR		1.12	-0.25
kB	Bone Resorption	1.09	-0.22
$m_{PTH,1}$	CTL production	1.03	-0.16
DA		0.88	-0.17
k_4	Bone Resorption	0.87	-0.17
PS		0.77	-0.25

hypercalcemia, PS—the ratio of PTH binding/unbinding in the bone— has a greater effect on both Ca and PTH.

These results underscore the importance of these parameters in Ca regulation. Since PTH is the regulatory response of the controller, any change in the signal transmitted from the sensor will result in a corresponding response in the controller. Therefore, changes in $K_{Ca,sens}$ —a measure of the CaR sensitivity — result in a compensatory change in PTH. The kidneys play a key role in plasma Ca regulation, retaining about 98%–99% of the filtered Ca (28). A portion of the Ca retained is PTH-dependent and $S_{PTH,2}$ indicates the amount of PTH required for half-maximal reabsorption of Ca. Therefore, changes to $S_{PTH,2}$ have a direct impact on Ca transfer to the plasma thus plasma Ca levels and, via the sensor, PTH secretion. Interestingly, PS has a more indirect role on Ca than the previous two parameters; altering the rate of PTH binding and unbinding in the bone determines the amount of bone cell proliferation, which ultimately impacts on net Ca transfer between the bone and plasma (29). At steady-state, plasma Ca and PTH are mildly affected, however, during induced hypercalcemia, the change in PS greatly impacts net bone formation thus plasma Ca levels and ultimately PTH.

6.3.2. Exploration of the parameter space

With the exception of $K_{Ca,sens}$, all the parameters listed in Table 6.1 indirectly modify PTH secretion through altering plasma Ca levels which is detected by the sensor. The sensor gain, however, alters PTH levels through directly stimulating the PTH secretory mechanism. As such, we seek to explore the effect of changing CaR sensitivity on model behavior.

In Chapter 4, we identified the key parameters that change with PHPT severity and the range of over which each parameter varies; also, the minimum secretory rate parameter A_{Ca} can be used as a quantitative identifier of the stage of disease (Chapter 4). Therefore we use this information to simulate how changes in $K_{Ca,sens}$ affect Ca-regulatory behavior in different stages of PHPT. Figures 6.2A-B show the simulation results of changes in $K_{Ca,sens}$ in early-stage and mid-stage PHPT, respectively. Increases in $K_{Ca,sens}$ cause a corresponding decrease in PTH which induces changes in CTL, CB ratio (an indicator of net bone resorption) and Cau (renal Ca excretion) , leading to lower plasma Ca. The magnitude of change across all the calciotropic variables decreases from early to mid-stage PHPT (Figs 6.2A-B).

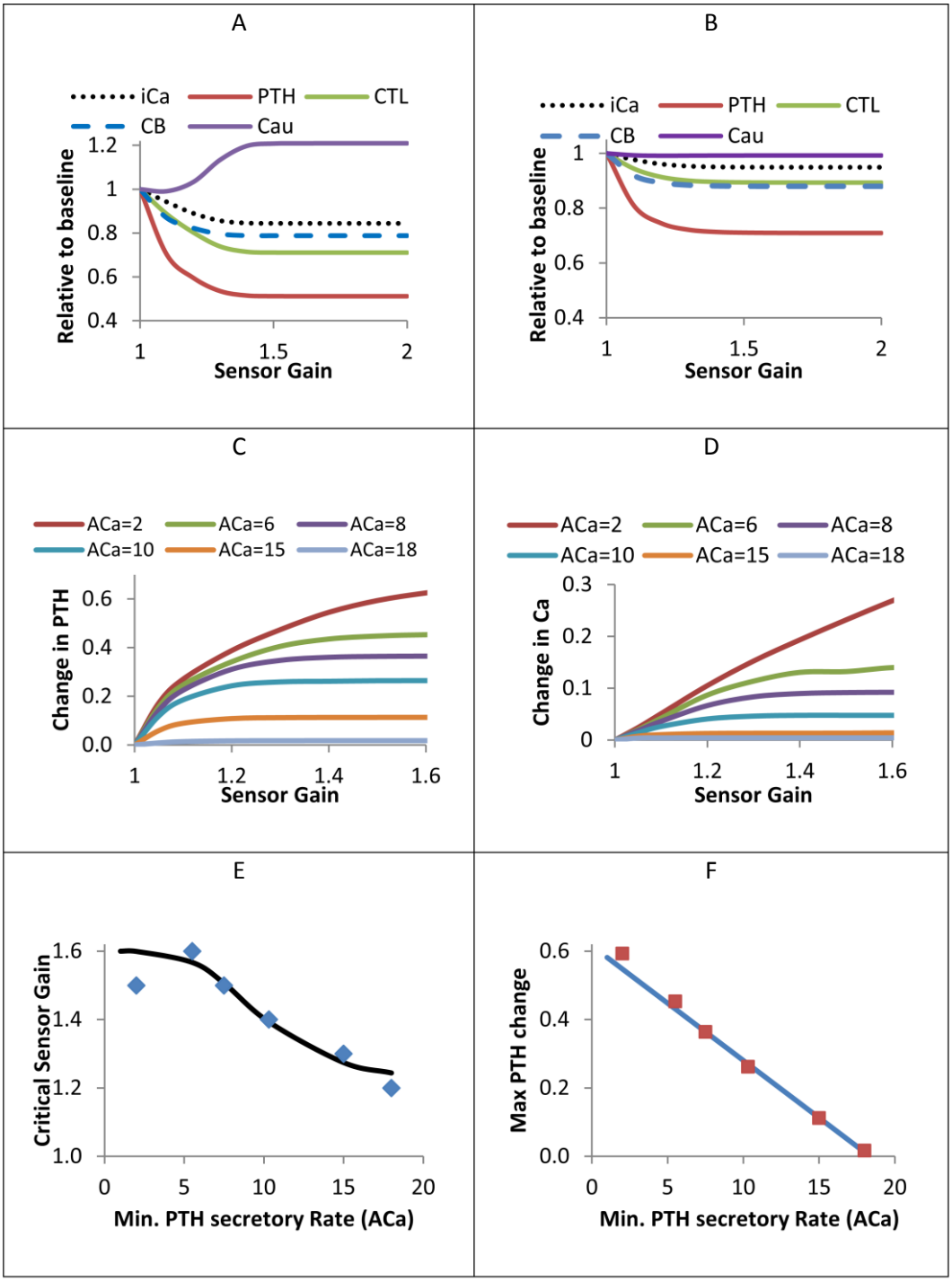

Figure 6.2. Simulated calciotropic response (ionized Ca, PTH, CTL, urinary Ca (Cau) and CB ratio) to changes in sensor gain in PHPT

(A) Early-stage (ACa = 6) and, (B) Mid-stage (ACa = 10).
Simulation results of sensor gain changes in various stages of PHPT: (C) Maximum change in PTH; (D) Maximum change in plasma Ca.
Correlations between PHPT severity, (measured by the minimum secretory rate, ACa) and: (E) critical sensor gain; (F) Maximum change in PTH.

Note that there is a corresponding change in renal Ca excretion (Cau) in early-stage PHPT (Fig. 6.2A)

while there is no significant change in mid-stage PHPT (Fig. 6.2B). Renal Ca reabsorption is partially PTH-dependent, increasing with PTH levels up a particular threshold (30) beyond which, maximum hormone-dependent reabsorption occurs. PTH levels increase with PHPT progression, however in the early-stages PTH levels are high, but close to the healthy range, and more importantly, below this threshold. As PTH levels decrease, due to changes in the $K_{Ca,sens}$, the Ca reabsorbed, via the PTH-dependent portion, also decreases leading to an overall increase in Ca excretion. Conversely, in later stages of PHPT, PTH levels are much higher than the threshold PTH in the kidneys. As a result, CaR-induced decreases in PTH levels do not reduce PTH below this threshold, thus there is no change in hormone-dependent reabsorption and Ca excretion.

There is a corresponding decrease in change in PTH levels (and Ca) across the spectrum of PHPT severity (Fig. 6.2 C-D) and, for each stage of the disease there is a maximum observable change in the PTH. As observed in clinical studies, this maximum change is dictated by the gland size (21), which determines the minimum PTH secretory rate, A_{Ca} (Chapter 4). Furthermore, this maximum change in PTH first appears at a particular sensor gain, which is defined as the critical sensor gain ($K_{Ca,sens,crit}$)— the value of $K_{Ca,sens}$ beyond which any further increase results in no observable change in PTH levels. A plot of the $K_{Ca,sens,crit}$ vs A_{Ca} reveals a correlation that can be represented by the logistic function (Fig. 6.2E); also, the change in PTH is inversely proportional to the extent of the disease (A_{Ca}) (Fig. 6.2F). In the very early stages of PHPT ($A_{Ca} < 5$) the correlation overestimates the $K_{Ca,sens,crit}$ (Fig. 6.2E) because hypocalcemia occurs before the maximum change in PTH is observed. The utility in these findings is that they can be used to infer the best possible outcome—in terms of PTH reduction—for any given case of PHPT. Any therapy designed to enhance CaR sensitivity, without causing a functional change in the receptor, will result in identical responses as shown in Fig. 6.2C. The therapy will need to stimulate the CaR to a maximum sensitivity as shown in Fig. 6.2E and provide a maximum reduction in PTH as depicted in Fig. 6.2F. With this in mind, we apply our findings to calcimimetics used in PHPT.

6.3.3. Cinacalcet Therapy in PHPT

Since $K_{Ca,sens}$ is the equivalent of the sensitivity of the CaR, then the impact of calcimimetics on increased CaR sensitivity is represented by the analysis above. As such, we apply the results to a case study of CNC therapy in PHPT subjects. A cohort of 16 patients with PHPT having similar plasma PTH and Ca were divided into three groups given 30mg, 40mg or 50mg CNC; each group was administered twice daily doses of CNC for a 15-day period. Plasma biochemistries were monitored hourly on day 1 and day 15 starting at the time of first dose (24).

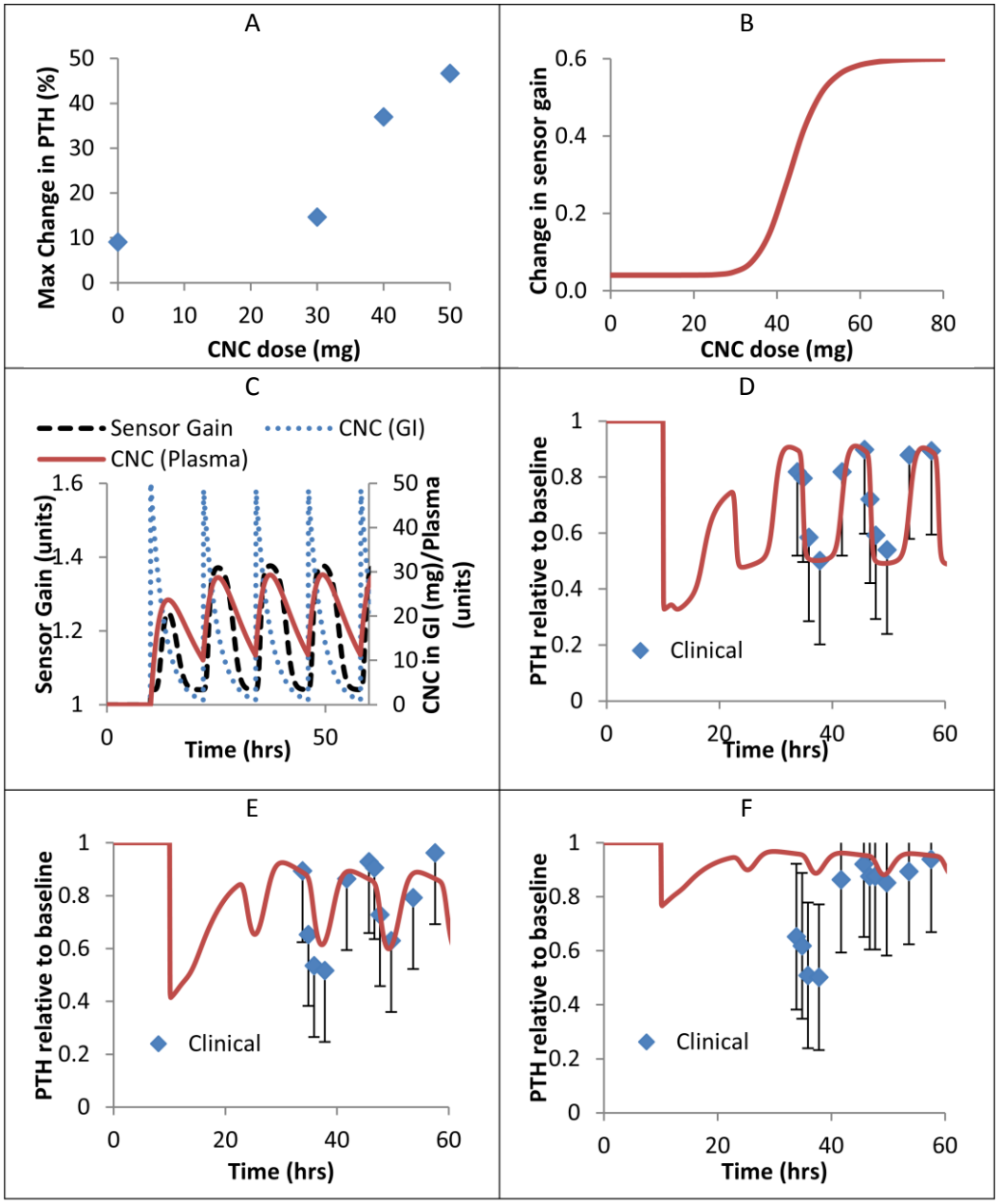

Figure 6.3. Simulation results of response to CNC administration.

(A) Clinical data of maximum change in PTH vs administered CNC dose. (B) Correlation between prescribed CNC dose and change in sensor gain. (C) Simulation results of CNC profile in the GI tract and plasma and corresponding sensor gain response from twice daily dose of 50 mg cinacalcet. (D-F) Simulated vs. Clinical PTH response to twice daily dose of (B) 50mg, (C) 40mg, and (D) 30mg cinacalcet in patients diagnosed with PHPT. The bars represent the standard error recorded in the literature (24).

Using the baseline plasma biochemistry and the maximum observed change in PTH, on Day 1, we estimated the parameters to represent the severity of PHPT and predict the group behavior. Likewise, we used the data of the maximum recorded PTH at each dose strength on Day 1 (Fig. 6.3A) to determine the

Table 6.6. Comparison of reductions in calciotropic responses between Days 1 and Day 15

	30mg		40mg		50 mg	
	Clinical	Simulated	Clinical	Simulated	Clinical	Simulated
Ca	11%	1%	18.7%	7%	18.5%	14%
PTH*	-	8%	-	24%	-	36%
CTL	-	2%	-	9%	-	20%
CB	-	5%	-	15%	-	22%
Urinary Ca	-51%	1%	-15%	1%	-15%	-11%

- Individual group PTH results on Day 15 were not reported, instead a mean predose PTH reduction of 20.3% was reported for the combined CNC-treated cohort. The average PTH simulated reduction for the cohort is 22.7% .

corresponding $K_{Ca,sens,crit}$, therefore, the change in sensor gain; which resulted in a correlation for this stage of the disease (Fig. 6.3B). Fig. 6.3C shows the CNC release profiles in the GI tract and plasma and the corresponding sensor gain for twice daily dose of 50mg CNC and Figs. D-F show the predicted and clinical PTH response profile to twice daily CNC dose on Day 15 (24). The simulation results provide a better prediction of the clinically observed mean at 40mg and 50mg than at 30mg. For both 30mg and 40mg, PTH results for the second of the two daily doses more closely match the clinically observed mean than for the first dose. In general, the model is a good predictor of PTH response to CNC therapy.

Table 6.2 outlines the reductions in calciotropic response between Day 1 baseline and Day 15; the simulation results are the final 12-hr average of the relevant variable on Day 15. In general, the simulation results show a proportional improvement in the calciotropic response with increase in CNC dose. Although individual group PTH values are not reported for Day 15, the clinical average PTH reduction for the CNC-treated cohort (20.3%) is similar to that of the 12-hour average of the simulated PTH reduction on day 15 (22.7%). The model generally underestimates the calcium response, but provides a better prediction for the 50 mg dose rather than the 30 and 40 mg doses. The predictions for Ca excretion vary greatly from the clinical observations, however, the authors reported no consistent trend in urine Ca (24). Nonetheless, a general increase in urinary Ca can be expected because the decrease in PTH may lower the PTH-dependent Ca reabsorption, thus increasing Ca excretion. It is important to note that the model does not account for the effect of renal CaRs, which are known to participate in Ca regulation (31), therefore changes to urinary Ca due to CNC activation of renal CaR are neglected. No clinical observations were made on markers of bone biology and CTL levels, but our simulations show a reductions in CTL and CB ratio proportional to the dose of CNC. This is expected because PTH stimulates CTL synthesis and bone cell proliferation; therefore CNC-induced changes in PTH will cause an associated decrease in CTL levels and CB ratio.

6.3.4. Validation of SHPT model

Before we can identify the potential therapeutic target sites in SHPT, we show that the model is robust enough to predict the various stages of CKD leading to SHPT. Clinical data of four groups of patients with CKD who are not undergoing dialysis nor taking phosphate binders (32) is used in validating our model. The comparison between simulation results and clinical observations are presented in Figure 6.4. In general, our model predicts the profile of all four plasma biochemistries very well. At very low renal function (RF <0.3), the model overestimates plasma phosphate (Figure 6.4D), this may occur due to unaccounted changes in phosphate regulation. Owing to insufficient data, the effect of FGF-23 on renal phosphate reabsorption is lumped with PTH, therefore, any change in FGF effect on the renal tubules during CKD is unaccounted for. Additionally, the fraction of phosphate consumed during phosphate salt precipitation may be underestimated by the model; however, given the limited data available on phosphate salt formation, any changes would be purely speculative and would affect Ca concentration, given the stoichiometry involved.

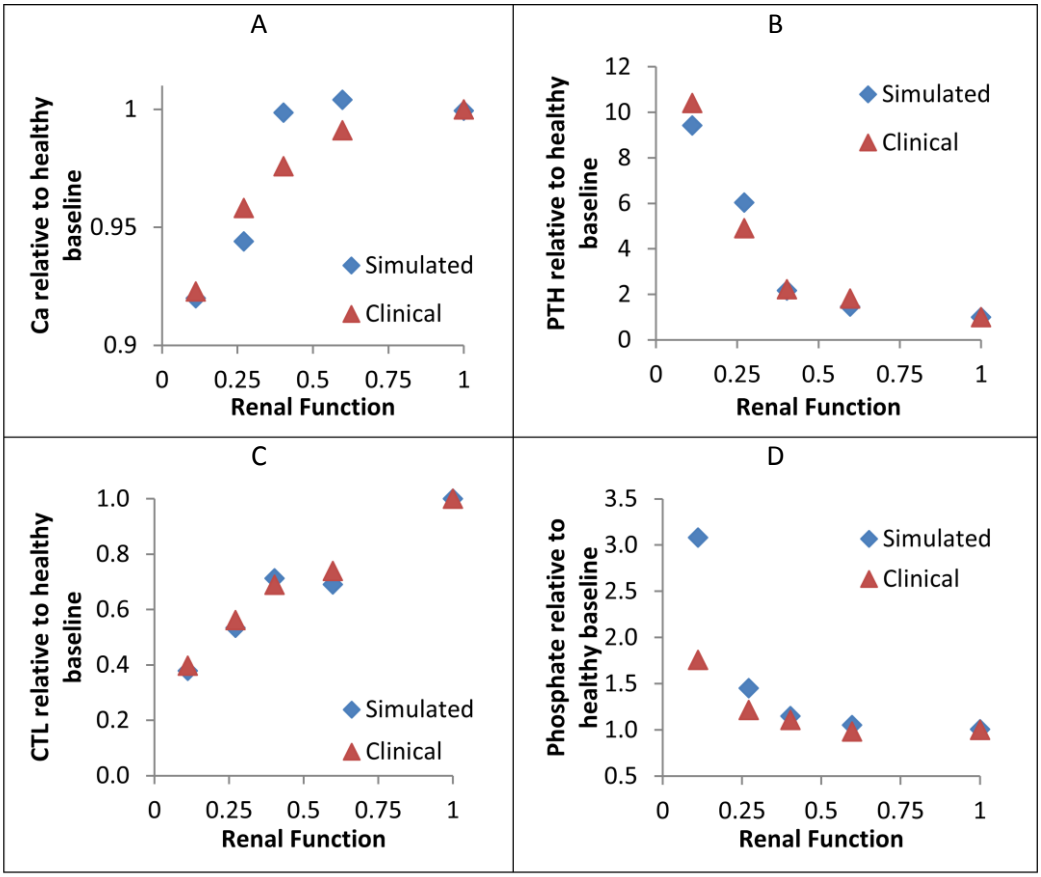

Figure 6.4. Comparison of Simulated results and clinical observations of plasma biochemistry changes among patients with varied severity of kidney disease (as determined by a decline in renal function/GFR) (32).
All biochemistries are presented relative to the healthy basal levels: (A) Ionized Calcium; (B) PTH; (C) Phosphate; (D) Calcitriol.

6.3.5. Responses in SHPT to changes in sensor gain

Similar parameter sensitivity analysis was done on the model of SHPT to determine the parameters to which PTH is most sensitive. We found that, similarly to PHPT, PTH is very sensitive to changes in $K_{Ca,sens}$ in SHPT. Therefore, an exploration of model response over the range of $K_{Ca,sens}$ is carried out. Unlike in PHPT, changes in PTH occur over a shorter range in SHPT (Fig. 6.5A), maximum PTH reduction is observed at $\Delta K_{Ca,sens} = 0.06$ compared to $\Delta K_{Ca,sens} = 0.6$ in PHPT. The magnitude of reduction observed in SHPT (85%) is much greater than in PHPT (60% at the onset of PHPT–Fig. 6.2C, $A_{Ca} = 2$).

Interestingly, unlike PHPT, the magnitude of PTH change in SHPT is independent of the degree of the disease (results not shown). Similar clinical observations were made in CNC treatment of SHPT patients where CNC caused the same percentage change in PTH levels regardless of the biochemical severity of

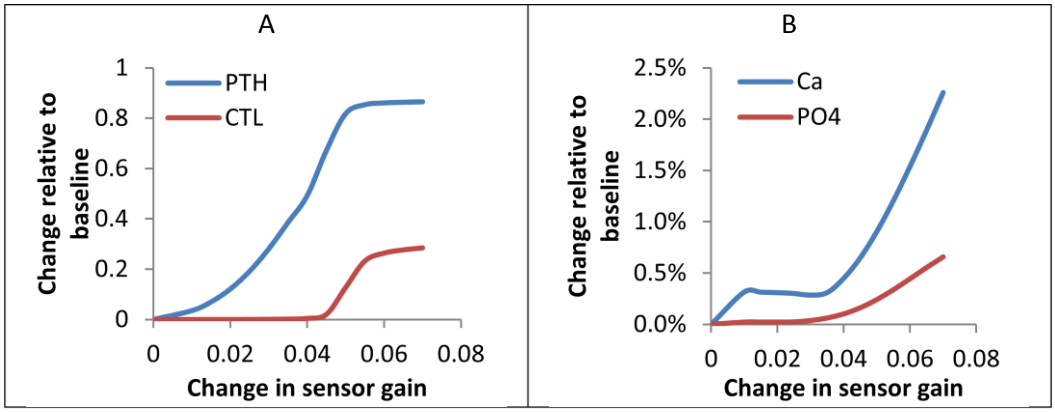

Figure 6.5. Simulation results of sensor gain changes in SHPT:

(A) Changes in PTH and CTL; (B) Changes in plasma ionized Ca and phosphate.

the disease (25). In both SHPT and PHPT, there is reduced CaR expression in hyperplastic PT cells (33, 34); however, a loss-of-function mutation of the CaR has been observed in some cases of PHPT (35-38). Despite the lower CaR expression, several studies have shown substantial decreases in PTH levels to induced hypercalcemia in SHPT patients undergoing dialysis (39-41) while no such observations are reported in PHPT. As a whole, the evidence suggests that there is a difference in the mechanism of CaR-mediated PTH production in both PHPT and SHPT.

6.3.6. Cinacalcet therapy in SHPT

From published pharmacokinetic data of CNC administration in SHPT patients and changes in plasma PTH (23), parameters for the expressions in Eqn. 6.2 and 6.3 are determined and the correlation for change in sensor gain and administered CNC is given in Fig 6.6A.

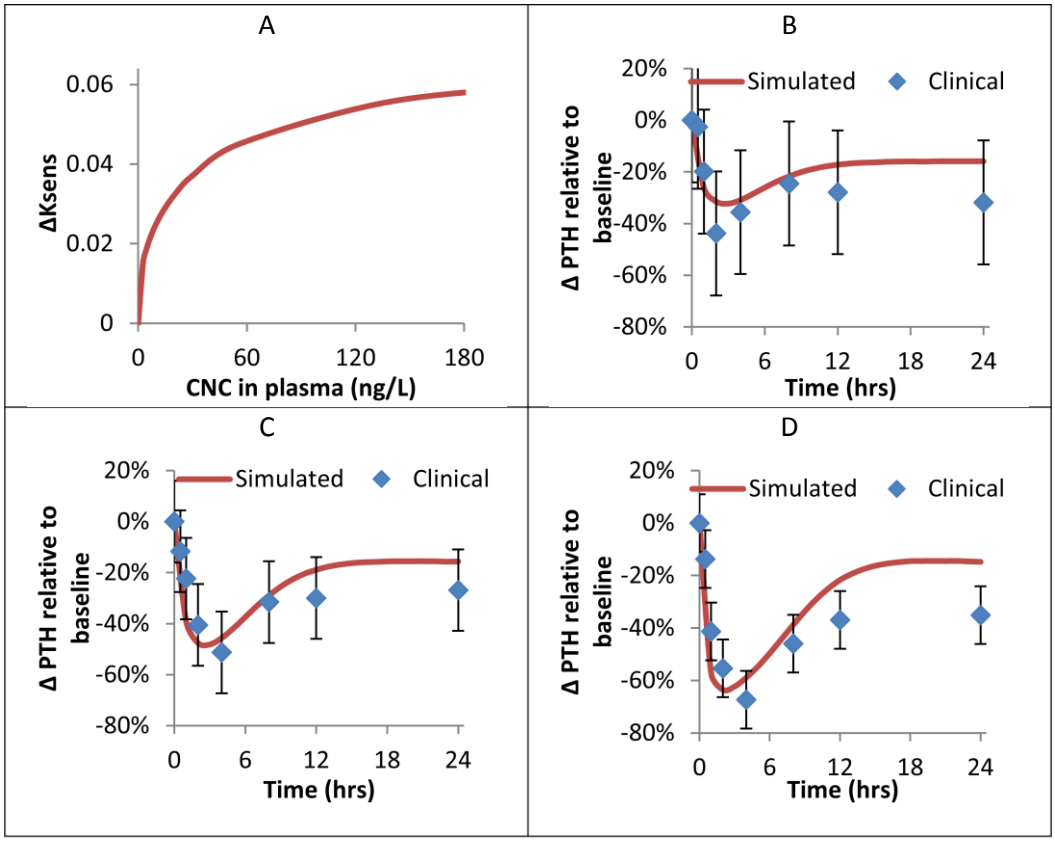

Figure 6.6. Simulation results of CNC therapy in SHPT.

(A) Correlation between administered CNC and maximum change in sensor gain, estimated from (23). Simulation results vs. Clinical observations of PTH response to clinical administration of (B) 25 mg; (C) 50 mg; (D) 100mg CNC SHPT patients (25).

In validating the model, clinical data of CNC administration in 3 groups of SHPT patients on hemodialysis, administered once daily dose of 25mg, 50mg or 100mg CNC was used (25). The baseline biochemistry data for the cohort was used to estimate the parameters to represent the stage of the disease. The comparisons of the simulated results and clinical observations are shown in Fig. 6.6B-D. In general, the model provides good prediction of the clinically observed PTH response; however, at higher CNC doses (100mg), the model overestimates the change in PTH beyond 12-hrs postdose. The deviations may be due to the differences between the clinical groups/data used for parameter estimation and results validation, or the expression used for g_3 may not be representative. Although important in the treatment of CKD/SHPT (1), the results for plasma Ca and phosphate levels are not addressed since the changes are negligible at maximum CaR sensitivity Fig 6.5B.

6.3.7. Model Predictive Control (MPC) in CNC Therapy

Having successfully validated the model of CNC administration in SHPT, we seek to highlight the utility of MPC in customizing CNC dosage given various desired outcomes. The results for three different scenarios are presented.

From Fig. 6.7A, the maximum change in PTH is not directly proportional to the dose of CNC, therefore an impulse profile for each dose is determined. Also, the effect of 120mg, 150mg and 180mg doses are marginally different; as a result, the profile of 150mg is used to estimate the response profile of all three doses. Therefore, four impulse response profiles are generated (30mg, 60mg, 90mg, 150mg); accordingly, a dynamic matrix and all dependent matrices are computed for each of the four doses. In implementing the QDMC strategy, at each step of the on-line computation, the gradient vector, $\boldsymbol{c}$, is computed using the dynamic matrix associated with the previous CNC dose; likewise, the corresponding matrix, **H**, for the previous CNC dose is used.

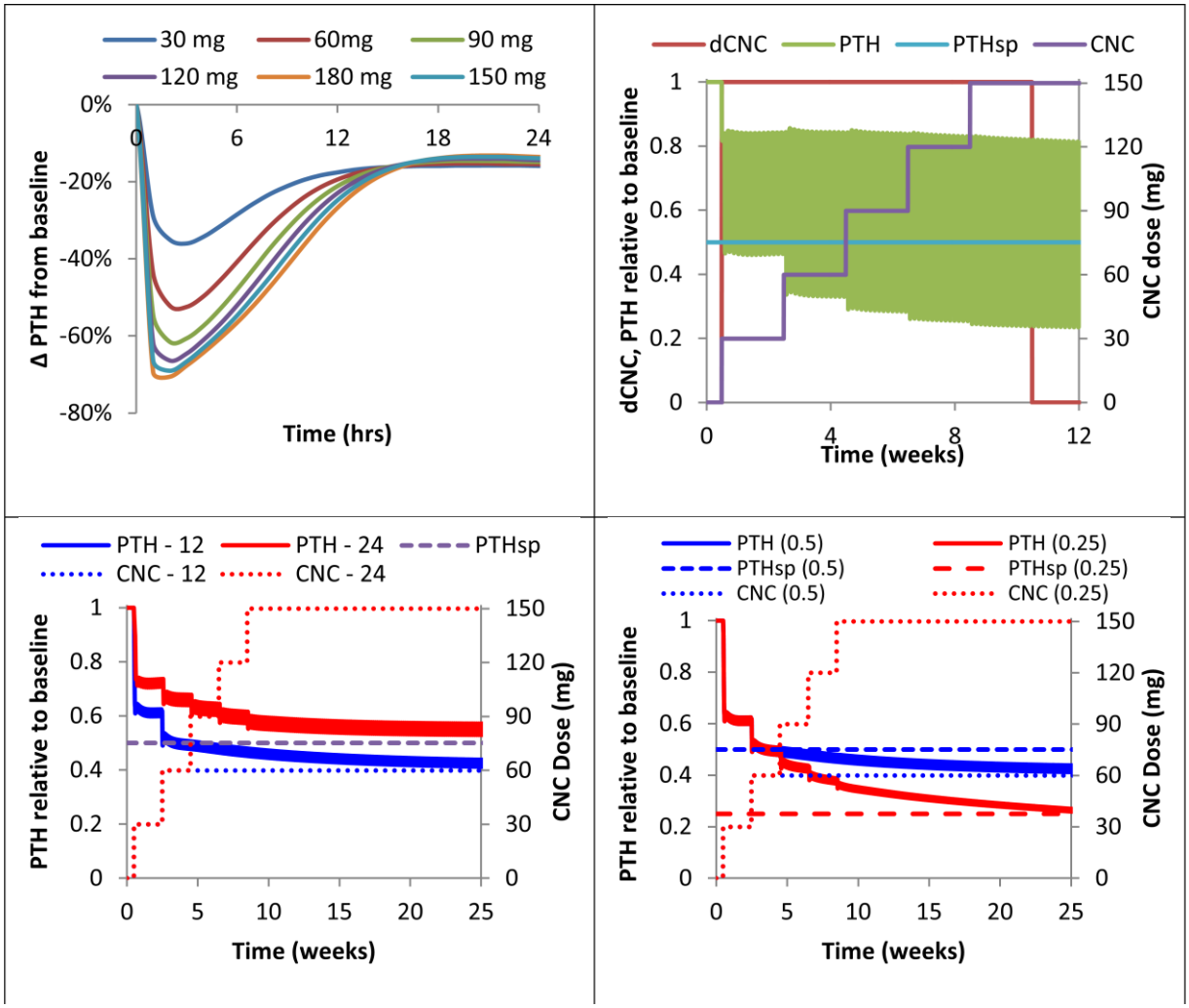

Figure 6.7. Simulation results of MPC use in CNC therapy in SHPT subjects.

(A) 24-hr PTH profile for CNC doses of 30mg -180mg. (B–D) Simulation results of Model Predictive Control use in determining optimum dosage profile for SHPT under different conditions: (B) PTH response to CNC therapy over a 12-week period targeting a PTH setpoint of 0.5. dCNC is the incremental change in CNC at each input period and CNC is the actual dose of CNC administered. (C) PTH response to MPC of CNC administration for a target PTH setpoint of 0.5 and a dosage frequency of every 12- or 24-hours. (D) PTH response to MPC of CNC administration for a target PTH setpoint of 0.5 or 0.25 and a dosage frequency of every 12-hours.

6.3.7.1. Scenario 1: Determine the dosage profile for a PTH setpoint of 50% of baseline

A maintenance dose of 150mg is required for a 50% reduction in PTH levels (Fig. 6.7B), the titration phase is 8 weeks. Note that the PTH levels reach a minimum within 3-hours postdose and settle at a maximum level of approximately 85% of baseline within 16-hours postdose (Fig. 6.7A), therefore PTH levels fluctuate around the setpoint, as seen in Fig. 6.7B. For ease of comparison, the 12-hr average PTH is used in subsequent results.

6.3.7.2. Scenario 2: For a PTH setpoint of 50% of baseline, compare the dosage profiles of CNC administered once or twice daily

The maintenance dose of CNC decreases with an increase in daily frequency. For a frequency of twice daily, a CNC dose of 60 mg is required, with a 2 week titration phase compared to 150 mg once daily and an 8 week titration phase. Additionally, after 25 weeks at twice daily CNC, the average PTH is approximately 40% of baseline compared to 55% at once daily.

6.3.7.3. Scenario 3: At a frequency of twice daily, compare the dosage profiles for PTH setpoints of 50% and 25% of baseline

At a setpoint of 25%, the maintenance dose is 150mg with an 8 week titration phase compared to 60 mg at 50%.

6.4. Conclusions

The results presented in this work show that process systems engineering concepts can be applied successfully to models of Ca-related pathologies. Applying parameter sensitivity analysis (PSA) to the model of PHPT, we found that the processes of: calcium-sensing in the PTG; hormone-dependent Ca reabsorption in the kidneys; and PTH binding/unbinding in the bone offer the greatest potential benefit in altering both PTH and Ca levels. However, of the three processes, only Ca-sensing directly affects PTH production and secretion; the other processes affect PTH through changes in plasma Ca concentration.

Having identified the parameter(s) of interest, determining the model behavior over the parameter space allows for determining the extent of the benefit of the parameter. In PHPT, the maximum reduction in PTH decreases with increasing PHPT severity; likewise, there is a critical sensor gain at which this maximum is observed and the critical sensor gain decreases with PHPT severity. From this analysis, we developed two key correlations: i) between the critical sensor gain and PHPT severity (indicated by minimum PTH secretory rate); and, ii) between the maximum PTH reduction and PHPT severity. The two correlations describe the change in CaR sensitivity required to achieve a maximum reduction in PTH at any given stage of PHPT.

Exploring the parameter space also provides insight into the differential behavior of the same sub-process in different pathologies. The change in sensor gain required to elicit a substantial change in PTH levels in PHPT is one order of magnitude greater than the change in sensor gain needed in SHPT. Additionally, the reduction in PTH is independent of disease severity in SHPT and is greater than the change in PHPT. This

highlights a fundamental difference in the way CaR affects PTH production and secretion in both PHPT and SHPT.

One application of the correlations derived through parameter space exploration is the prediction of cinacalcet behavior in PHPT and SHPT. The models provide a good prediction of clinical CNC therapy in both pathologies. Additionally, a further correlation was developed that allows for determining the CNC prescription based on the desired change in PTH; however, this correlation is particular to the stage of PHPT modeled. Nevertheless, the approach used herein provides a blueprint with which a family of such curves can be developed for varying stages of PHPT. Ultimately, these correlations between sensor gain and CNC dose across the spectrum of PHPT severity can be used to deduce the optimum CNC dose given a particular stage of the pathology.

Chronic Kidney Disease is a complex pathology with varying complications, including SHPT; effective treatment requires controlling several key variables (plasma biochemistries) within a target range. Model Predictive Control offers a unique opportunity to customize CNC therapy for SHPT patients. The preliminary work presented herein, with varying PTH setpoints and CNC dose frequency shows that satisfactory predictions of SHPT behavior is possible and CNC dosage regimen can be customized to achieve different patient outcomes under different administration protocols.

In summary, this work shows that process systems engineering methods can be used to identify potential therapeutic target sites in Ca-related pathologies. Parameter space exploration helps to determine the extent to which these sites affect the different plasma biochemistries in the pathology and by extension, the maximum benefit they provide. The findings can be applied to existing therapies in order to validate the approach as well as to improve the patient care through dosage customization.

6.5. Reference

1. **Fraser WD** 2009 Hyperparathyroidism. Lancet 374:145-158
2. **Orr-Walker BJ, Evans MC, Clearwater JM, Horne A, Grey AB, Reid IR** 2000 Effects of Hormone Replacement Therapy on Bone Mineral Density in Postmenopausal Women With Primary Hyperparathyroidism: Four-Year Follow-up and Comparison With Healthy Postmenopausal Women. Archives of Internal Medicine 160:2161-2166
3. **Selby PL, Peacock M** 1986 Ethinyl estradiol and norethindrone in the treatment of primary hyperparathyroidism in postmenopausal women. New England Journal of Medicine 314:1481-1485
4. **Silverberg SJ, Rubin MR, Faiman C, Peacock M, Shoback DM, Smallridge RC, Schwanauer LE, Olson KA, Klassen P, Bilezikian JP** 2007 Cinacalcet hydrochloride reduces the serum calcium concentration in inoperable parathyroid carcinoma. Journal of Clinical Endocrinology and Metabolism 92:3803-3808
5. **Nemeth EF, Steffey ME, Hammerland LG, Hung BCP, Van Wagenen BC, DelMar EG, Balandrin MF** 1998 Calcimimetics with potent and selective activity on the parathyroid calcium receptor. Proceedings of the National Academy of Sciences of the United States of America 95:4040-4045
6. **Hammerland LG, Garrett JE, Hung BCP, Levinthal C, Nemeth EF** 1998 Allosteric activation of the Ca2+ receptor expressed in Xenopus laevis oocytes by NPS 467 or NPS 568. Molecular Pharmacology 53:1083-1088
7. **Nemeth EF, Heaton WH, Miller M, Fox J, Balandrin MF, Van Wagenen BC, Colloton M, Karbon W, Scherrer J, Shatzen E** 2004 Pharmacodynamics of the type II calcimimetic compound cinacalcet HCl. Journal of Pharmacology and Experimental Therapeutics 308:627-635
8. **Mizobuchi M, Hatamura I, Ogata H, Saji F, Uda S, Shiizaki K, Sakaguchi T, Negi S, Kinugasa E, Koshikawa S** 2004 Calcimimetic compound upregulates decreased calcium-sensing receptor expression level in parathyroid glands of rats with chronic renal insufficiency. Journal of the American Society of Nephrology 15:2579-2587
9. **Colloton M, Shatzen E, Miller G, Stehman-Breen C, Wada M, Lacey D, Martin D** 2005 Cinacalcet HCl attenuates parathyroid hyperplasia in a rat model of secondary hyperparathyroidism. Kidney International 67:467-476
10. **Marcocci C, Chanson P, Shoback D, Bilezikian J, Fernandez-Cruz L, Orgiazzi J, Henzen C, Cheng S, Sterling LR, Lu J, Peacock M** 2009 Cinacalcet reduces serum calcium concentrations

in patients with intractable primary hyperparathyroidism. Journal of Clinical Endocrinology and Metabolism 94:2766-2772

11. **Peacock M, Bilezikian JP, Bolognese MA, Borofsky M, Scumpia S, Sterling LR, Cheng SF, Shoback D** 2011 Cinacalcet HCl Reduces Hypercalcemia in Primary Hyperparathyroidism across a Wide Spectrum of Disease Severity. Journal of Clinical Endocrinology and Metabolism 96:E9-E18
12. **Block GA, Martin KJ, de Francisco AL, Turner SA, Avram MM, Suranyi MG, Hercz G, Cunningham J, Abu-Alfa AK, Messa P** 2004 Cinacalcet for secondary hyperparathyroidism in patients receiving hemodialysis. New England Journal of Medicine 350:1516-1525
13. **Lindberg JS, Culleton B, Wong G, Borah MF, Clark RV, Shapiro WB, Roger SD, Husserl FE, Klassen PS, Guo MD, Albizem MB, Coburn JW** 2005 Cinacalcet HCl, an oral calcimimetic agent for the treatment of secondary hyperparathyroidism in hemodialysis and peritoneal dialysis: a randomized, double-blind, multicenter study. Journal of the American Society of Nephrology : JASN 16:800-807
14. **Khoo MCK, IEEE Engineering in Medicine and Biology Society., Institute of Electrical and Electronics Engineers.** 2000 Physiological Control Systems : Analysis, Simulation, and Estimation. New York: IEEE Press
15. **Doyle FJI, Bequette BW, Middleton R, Ogunnaike B, Paden B, Parker RS, Vidyasagar M** 2011 Control in Biological Systems. In: Samad T, Annaswamy A eds. The Impact of Control Technology: IEEE Control Systems Society
16. **Mundy GR, Guise TA** 1999 Hormonal control of calcium homeostasis. Clinical Chemistry 45:1347-1352
17. **Járos GG, Coleman TG, Guyton AC** 1979 Model of short-term regulation of calcium-ion concentration. Simulation32:193-204
18. **Raposo JF, Sobrinho LG, Ferreira HG** 2002 A minimal mathematical model of calcium homeostasis. Journal of Clinical Endocrinology and Metabolism 87:4330-4340
19. **Peterson MC, Riggs MM** 2010 A physiologically based mathematical model of integrated calcium homeostasis and bone remodeling. Bone 46:49-63
20. **Chung SW, Miles FL, Sikes RA, Cooper CR, Farach-Carson MC, Ogunnaike BA** 2009 Quantitative modeling and analysis of the transforming growth factor beta signaling pathway. Biophysical journal 96:1733-1750
21. **Khosla S, Ebeling PR, Firek AF, Burritt MM, Kao PC, Heath H, 3rd** 1993 Calcium infusion suggests a "set-point" abnormality of parathyroid gland function in familial benign hypercalcemia

and more complex disturbances in primary hyperparathyroidism. Journal of Clinical Endocrinology and Metabolism 76:715-720

22. **United States Pharmacopeial C** 2007 USP DI. Vol. III, Vol. III. USP DI Vol III, Vol III
23. **Harris RZ, Padhi D, Marbury TC, Noveck RJ, Salfi M, Sullivan JT** 2004 Pharmacokinetics, pharmacodynamics, and safety of cinacalcet hydrochloride in hemodialysis patients at doses up to 200 mg once daily. American journal of kidney diseases 44:1070-1076
24. **Shoback DM, Bilezikian JP, Turner SA, McCary LC, Guo MD, Peacock M** 2003 The calcimimetic cinacalcet normalizes serum calcium in subjects with primary hyperparathyroidism. Journal of Clinical Endocrinology and Metabolism 88:5644-5649
25. **Goodman WG, Hladik GA, Turner SA, Blaisdell PW, Goodkin DA, Liu W, Barri YM, Cohen RM, Coburn JW** 2002 The calcimimetic agent AMG 073 lowers plasma parathyroid hormone levels in hemodialysis patients with secondary hyperparathyroidism. Journal of the American Society of Nephrology 13:1017-1024
26. **Maciejowski JM** 2002 Predictive Control: With Constraints: Prentice Hall
27. **Currie J, Wilson DI** 2012 OPTI: Lowering the Barrier Between Open Source Optimizers and the Industrial MATLAB User. In: Sahinidis N, Pinto J eds. Foundations of Computer-Aided Process Operations. Savannah, Georgia, USA
28. **Kovacs WJ, Ojeda SR** 2012 Textbook of Endocrine Physiology. 6th ed. Oxford: Oxford University Press
29. **Lemaire V, Tobin FL, Greller LD, Cho CR, Suva LJ** 2004 Modeling the interactions between osteoblast and osteoclast activities in bone remodeling. Journal of theoretical biology 229:293-309
30. **Parfitt AM** 1993 Calcium homeostasis. Heidelberg, Allemagne: Springer
31. **Rodriguez M, Nemeth E, Martin D** 2005 The calcium-sensing receptor: a key factor in the pathogenesis of secondary hyperparathyroidism. American Journal of Physiology-Renal Physiology 288:F253-F264
32. **Rix M, Andreassen H, Eskildsen P, Langdahl B, Olgaard K** 1999 Bone mineral density and biochemical markers of bone turnover in patients with predialysis chronic renal failure. Kidney International 56:1084-1093
33. **Kifor O, Moore F, Wang P, Goldstein M, Vassilev P, Kifor I, Hebert S, Brown E** 1996 Reduced immunostaining for the extracellular Ca2+-sensing receptor in primary and uremic secondary hyperparathyroidism. Journal of Clinical Endocrinology and Metabolism 81:1598-1606

34. **Yano S, Sugimoto T, Tsukamoto T, Chihara K, Kobayashi A, Kitazawa S, Maeda S, Kitazawa R** 2003 Decrease in vitamin D receptor and calcium-sensing receptor in highly proliferative parathyroid adenomas. European Journal of Endocrinology 148:403-411

35. **Frank-Raue K, Leidig-Bruckner G, Haag C, Schulze E, Lorenz A, Schmitz-Winnenthal H, Raue F** 2011 Inactivating calcium-sensing receptor mutations in patients with primary hyperparathyroidism. Clinical Endocrinology 75:50-55

36. **Hannan FM, Nesbit MA, Christie PT, Lissens W, Van der Schueren B, Bex M, Bouillon R, Thakker RV** 2010 A homozygous inactivating calcium-sensing receptor mutation, Pro339Thr, is associated with isolated primary hyperparathyroidism: correlation between location of mutations and severity of hypercalcaemia. Clinical Endocrinology 73:715-722

37. **Warner J, Epstein M, Sweet A, Singh D, Burgess J, Stranks S, Hill P, Perry-Keene D, Learoyd D, Robinson B** 2004 Genetic testing in familial isolated hyperparathyroidism: unexpected results and their implications. Journal of Medical Genetics 41:155-160

38. **Carling T, Szabo E, Bai M, Ridefelt P, Westin G, Gustavsson P, Trivedi S, Hellman P, Brown EM, Dahl N, Rastad J** 2000 Familial Hypercalcemia and Hypercalciuria Caused by a Novel Mutation in the Cytoplasmic Tail of the Calcium Receptor. Journal of Clinical Endocrinology and Metabolism 85:2042-2047

39. **Ramirez JA, Goodman WG, Gornbein J, Menezes C, Moulton L, Segre GV, Salusky IB** 1993 Direct in vivo comparison of calcium-regulated parathyroid hormone secretion in normal volunteers and patients with secondary hyperparathyroidism. Journal of Clinical Endocrinology and Metabolism 76:1489-1494

40. **Pahl M, Jara A, Bover J, Rodriguez M, Felsenfeld AJ** 1996 The set point of calcium and the reduction of parathyroid hormone in hemodialysis patients. Kidney International 49:226-231

41. **Rodriguez M, Caravaca F, Fernandez E, Borrego MJ, Lorenzo V, Cubero J, Martin-Malo A, Betriu A, Jimenez A, Torres A** 1999 Parathyroid function as a determinant of the response to calcitriol treatment in the hemodialysis patient. Kidney International 56:306-317

Table 6A.7. Model Equations – Ca/Phosphate Control (Healthy)

$$H_i(x) = (A_{ix} - B_{ix})/\left[1 + \left({}^{x}/_{S_{ix}}\right)^{m_{ix}}\right] + B_{ix} \quad (1)$$

Process – Plasma

$$dCa_{(p)}/dt = Ca_{(i)} + Ca_{(b)} - Ca_{(u)} \pm Ca_{(d)} \quad (2)$$

$$dPO_{4(p)}/dt = PO_{4(i)} + PO_{4(b)} - PO_{4(u)} \pm PO_{4(d)} \quad (3)$$

Sensor – Ca-sensing receptor (CaR) on PTG

$$Ca_{(s)} = K_{Ca,sens} Ca_{(p)} \quad (4)$$

Controller – PTG (PTH production)

$$dPTH/dt = PTG\left[H\left(Ca_{(s)}\right) + H_1\left(PO_{4(p)}\right) + H(FGF) - 1\right] - k_{PTH} PTH \quad (5)$$

$$\frac{dPTG}{dt} = \frac{\lambda_{PTG}}{PTG_0}\begin{Bmatrix}(PTG_{max} - PTG)[\varphi_{PTG} T^{-}_{PTG} + (1 - \varphi_{PTG})] \\ -PTG[\varphi_{PTG} T^{+}_{PTG} + (1 - \varphi_{PTG})]\end{Bmatrix} \quad (6)$$

$$T^{\pm}_{PTG} = 1 \pm tanh[\lambda_{CTL}(CTL - CTL_0)] \quad (7)$$

Actuator – Intestines (Ca/PO4 absorption)

$$Ca_{(i)} = \frac{Ca_{meal}}{V}(H_1(CTL) + \lambda_{Cai}) \quad (8)$$

$$PO_{4(i)} = \frac{PO_{4,meal}}{V}\left[H_2(CTL) + \lambda_{PO4,i}\right] \quad (9)$$

Actuator – Kidneys (CTL Production, Ca/PO4 excretion)

$$dCTL/dt = [H_1(PTH) + H(PTHrP)]H_2\left(PO_{4(p)}\right) - k_{CTL} CTL \quad (10)$$

$$Ca_{(u)} = \frac{GFR}{V}\begin{Bmatrix} Ca_{(p)}[0.1 - 0.09H_2(PTH)], & Ca_{(p)} \le Ca_{thr} \\ \left(\alpha_{Cau} Ca_{(p)} + \beta_{Cau}\right), & Ca_{(p)} > Ca_{thr} \end{Bmatrix} \quad (11)$$

$$PO_{4(u)} = \frac{GFR}{V}\begin{Bmatrix} PO_{4(p)}[H(PTH + FGF)], & PO_{4(p)} \le PO_{4,thr} \\ \left(\alpha_{PO4u} PO_{4(p)} + \beta_{PO4u}\right), & PO_{4(p)} > PO_{4,thr} \end{Bmatrix} \quad (12)$$

Actuator - Bone (Resorption/Formation)

$$Ca_{(b)} = \sigma_{Cab}\begin{Bmatrix}(1 - \lambda_{Cab}) + \lambda_{Cab}\left[H(OC)\left({}^{RANKL}/_{OC}\right)^{\gamma_{Cab}}\right] \\ -\frac{Ca_{(p)}}{Ca_{(p)0}}\left[(1 - \lambda_{Cab}) + \lambda_{Cab}\left(\frac{OB}{OB_0}\right)\right]\end{Bmatrix} \quad (13)$$

$$\pi_P = \lambda_b\left(\frac{PTH + PTHrP}{PTH_0}\right)\Big/\left[\lambda_b\left(\frac{PTH + PTHrP}{PTH + PTHrP - PTH_0}\right) + PS\right] \quad (14)$$

Phosphate detection by osteocytes

$$PO_{4(s)} = K_{PO4,sens} PO_{4(p)} \quad (15)$$

$$PO_{4(b)} = \lambda_{PO4b} Ca_{(b)} \quad (16)$$

Osteocytes (FGF-23 production)

$$dFGF/dt = \left[H_3\left(PO_{4(s)}\right) + H_3(CTL) - 1\right] - k_{FGF} FGF \quad (17)$$

Table 6A.8. Model Equations – Pathologies as Component defects

PHPT – Controller Defect

$$H\left(Ca_{(s)}\right) = \frac{A_{Ca}\chi_{ACa} - B_{Ca}\chi_{BCa}}{\left[1 + \left(Ca_{(s)}/S_{Ca}\right)^{m(Ca_{(s)})}\right]} + B_{Ca}\chi_{BCa}$$

$$m\left(Ca_{(s)}\right) = \chi_{mCa}\left\{\frac{m_{Ca}A - m_{Ca}B}{\left[1 + \left(Ca_{(s)}/m_{Ca}S\right)^{m_{Ca}m}\right]} + m_{Ca}B\right\}$$

$$\chi_{mCa} < 1$$

$$S_{Ca} = Ca_{(s)}\left\{\frac{A_{Ca}\chi_{ACa} - k_{PTH}PTH_{PHPT,0}}{k_{PTH}PTH_{PHPT,0} - B_{Ca}\chi_{BCa}}\right\}^{-1/m(Ca_{(s)})}$$

PHPT – PTH resistance in CTL production

$$H_1(PTH) = \frac{A_{1,PTH} - B_{1,PTH}\chi_{B1PTH}}{\left[1 + \left(PTH/S_{1,PTH}\right)^{m_{1,PTH}}\right]} + B_{1,PTH}\chi_{B1PTH}$$

Cinacalcet Therapy in PHPT – CaR targeting

$$Ca_{(s)} = [H_1(CNC_2) + 1]K_{Ca,sens}Ca_{(p)}$$

CNC as ingested: $dCNC_1/dt = -k_{CNC1,PHPT}CNC_1$

CNC detected by CaR: $dCNC_2/dt = k_{CNC1,PHPT}CNC_1 - k_{CNC2,PHPT}CNC_2$

Chronic Kidney Disease – Actuator Defect

Renal Failure: $RF = RF_{tf} + \left(1 - RF_{tf}\right)e^{-(k_{RF}t)}$

CTL Degradation

$$dCTL/dt = r_{CTL,deg}\left\{[H_1(PTH) + H(PTHrP)]H_2\left(PO_{4(p)}\right)\right\} - k_{CTL}CTL$$

$$r_{CTL,deg} = \left\{[1 - H(RF)]e^{-(k_{RF}t)} + H(RF)\right\}$$

Reduced Ca/PO4 excretion

$$Ca_{(u)} = \frac{GFR}{V}RF\begin{Bmatrix} Ca_{(p)}[0.1 - 0.09H_2(PTH)RF], & Ca_{(p)} \le Ca_{thr} \\ \left(\alpha_{Cau}Ca_{(p)} + \beta_{Cau}\right), & Ca_{(p)} > Ca_{thr} \end{Bmatrix}$$

$$PO_{4(u)} = \frac{GFR}{V}RF\begin{Bmatrix} PO_{4(p)}[H(PTH + FGF)RF], & PO_{4(p)} \le PO_{4,thr} \\ \left(\alpha_{PO4u}PO_{4(p)} + \beta_{PO4u}\right), & PO_{4(p)} > PO_{4,thr} \end{Bmatrix}$$

CaHPO4 Formation

$$Ca_{(d)} = \begin{cases} 0, & Ca_{(p)} \times PO_{4(p)} \le Ca \times PO_{4_{thr}} \\ \left(PO_{4(p)} - PO_{4(p),0}\right)\lambda_{Cad}, & Ca_{(p)} \times PO_{4(p)} > Ca \times PO_{4_{thr}} \end{cases}$$

$$PO_{4(d)} = \begin{cases} 0, & Ca_{(p)} \times PO_{4(p)} \le Ca \times PO_{4_{thr}} \\ \left(PO_{4(p)} - PO_{4(p),0}\right)\lambda_{PO4d}, & Ca_{(p)} \times PO_{4(p)} > Ca \times PO_{4_{thr}} \end{cases}$$

Cinacalcet Therapy in SHPT – CaR targeting

$$Ca_{(s)} = [f(CNC_2) + 1]K_{Ca,sens}Ca_{(p)}$$

$$f(CNC_2) = S_{CNC2,SHPT}\left[\frac{A_{dK} - B_{dK}}{H_2(CNC_2) - B_{dK}} - 1\right]^{1/m_{dK}}$$

	CNC as ingested: $dCNC_1/dt = -k_{CNC1,SHPT}CNC_1$ **CNC detected by CaR:** $dCNC_2/dt = k_{CNC1,SHPT}CNC_1 - k_{CNC2,SHPT}CNC_2$

Table 6A.9. Parameter Estimates

Parameter	Value	Units	Parameter	Value	Units
$Ca_{(p)0}$	1.715E+01	mmol	$A_{Ca(s)}$	4.641E+02	pmol.hr^{-1}
CTL_0	1.260E+03	pmol	$B_{Ca(s)}$	6.276E+03	pmol.hr^{-1}
OB_0	7.282E-04	pM cells	$m_{Ca(s)}A$	-3.000E+01	Unitless
$PO_{4(ic)0}$	4.516E+04	mmol	$m_{Ca(s)}B$	-2.500E+02	Unitless
$PO_{4(p)0}$	1.680E+01	mmol	$m_{Ca(s)}m$	-1.500E+02	Unitless
PTG_0	5.000E-01	Unitless	$m_{Ca(s)}S_1$	1.800E+01	mmol
PTH_0	5.526E+01	pmol	$m_{Ca(s)}S_2$	1.500E+01	mmol
$\mathrm{Ca_{meal}}$	9.158E-01	mmol.hr^{-1}	$A_{1,CTL}$	4.150E-01	Unitless
$\mathrm{Ca_{thr}}$	3.108E+01	mmol	$B_{1,CTL}$	0.000E+00	Unitless
GFR	6.000E+00	L.hr^{-1}	$m_{1,CTL}$	-8.416E+00	Unitless
$\mathrm{k_{CTL}}$	8.660E-02	hr^{-1}	$S_{1,CTL}$	1.306E+03	pmol
$\mathrm{k_{PTH}}$	3.199E+01	hr^{-1}	$A_{1,PTH}$	3.228E+00	hr^{-1}
$\mathrm{k_{PTHrP}}$	6.932E+00	hr^{-1}	$B_{1,PTH}$	1.000E+00	hr^{-1}
$\mathrm{K_{Ca,sens}}$	1.000E+00	Unitless	$m_{1,PTH}$	-2.000E+01	Unitless
$\mathrm{PO_{4,meal}}$	5.695E-01	mmol.hr^{-1}	$S_{1,PTH}$	9.823E+01	pmol
PS	1.500E+02	Unitless	$A_{2,PTH}$	1.045E+00	Unitless
$\mathrm{PTG_{max}}$	1.000E+00	Unitless	$B_{2,PTH}$	0.000E+00	Unitless
V	1.400E+01	L	$m_{2,PTH}$	-6.520E+00	Unitless
α_{Cau}	3.146E-01	Unitless	$S_{2,PTH}$	5.186E+01	pmol
α_{PO4u}	5.545E-02	Unitless	$A_{1,\mathrm{PO4}}$	1.034E+00	Unitless
β_{Cau}	-5.710E+00	mmol	$\mathrm{B_{1,PO4}}$	4.182E-01	Unitless
γ_{Cab}	6.038E-01	Unitless	$\mathrm{m_{1,PO4}}$	1.242E+01	Unitless
λ_{b}	2.907E+00	Unitless	$\mathrm{S_{1,PO4}}$	1.860E+01	mmol
λ_{Cab}	1.500E-01	Unitless	$\mathrm{A_{OC}}$	1.271E+00	Unitless
λ_{Cai}	1.500E-01	Unitless	$\mathrm{B_{OC}}$	9.951E-01	Unitless
λ_{CTL}	2.143E-03	pmol^{-1}	$\mathrm{m_{OC}}$	-1.188E+00	Unitless
λ_{PO4b}	4.640E-01	Unitless	$\mathrm{S_{OC}}$	9.615E-01	pM cells/pM cells
λ_{PO4i}	7.000E-01	Unitless	$\mathrm{A_{PTHrP}}$	-4.630E-01	hr^{-1}
λ_{PTG}	7.500E-02	hr^{-1}	B_{PTHrP}	5.280E-01	hr^{-1}
π_{P}	-	Unitless	$\mathrm{S_{PTHrP}}$	1.534E+00	pM
σ_{Cab}	7.973E-01	hr^{-1}	$\mathrm{m_{PTHrP}}$	5.888E+00	Unitless
φ_{PTG}	8.500E-01	Unitless	$\mathrm{R_{PTHrP}}$	1.04E+01 to 3.0E+01	pMhr^{-1}

Simulation of pathologies

In simulating the different pathologies, the following forcing function is used. The actual parameters and their healthy and disease state values are listed in Table 3.

$$p_{path} = p_{diseased} + \left(p_{healthy} - p_{diseased}\right)e^{-k_{path}t}$$

[e.g. $K_{sens,FBH} = K_{sens,FBH,diseased} + \left(K_{sens,healthy} - K_{sens,FBH,diseased}\right)e^{-k_{FBH}t}$]

Table 6A.10. Parameter estimates for pathologies

	Parameter	**Value at healthy state**	**Value at diseased state**
FBH	k_{FBH}	2.315E-02	-
	$K_{sens,FBH}$	1.000E+00	8.800E-01
	$A_{Ca(s),FBH}$	6.033E+02	7.526E+02
	$B_{Ca(s),FBH}$	9.414E+03	1.774E+04
	$m_{Ca}A_{FBH}$	-4.500E+01	-4.342E+01
ADH	k_{ADH}	2.315E-02	-
	$K_{sens,ADH}$	1.000E+00	1.12E+00
	$A_{Ca(s),ADH}$	6.033E+02	5.958E+02
	$B_{Ca(s),ADH}$	9.414E+03	7.021E+03
PHPT	k_{PHPT}	2.777E-02	-
	$A_{Ca(s),PHPT}$	4.022E+02	4.022E+03
	$B_{Ca(s),PHPT}$	1.255E+04	3.766E+04
	$m_{Ca}A_{PHPT}$	-2.305E+01	-1.544E+01
	$m_{Ca}B_{PHPT}$	-2.500E+02	-1.674E+02
	$m_{Ca}S_{1,PHPT}$	1.800E+01	2.122E+01
	$m_{Ca}S_{2,PHPT}$	1.500E+01	1.769E+01
HoPT	k_{HoPT}	2.777E-02	-
	$A_{Ca(s),PHPT}$	4.022E+02	2.370E+02
	$B_{Ca(s),PHPT}$	1.255E+04	4.927E+03
	$m_{Ca}A_{PHPT}$	-2.305E+01	-
	$m_{Ca}B_{PHPT}$	-2.500E+02	-
	$m_{Ca}S_{1,PHPT}$	1.800E+01	1.080E+01
	$m_{Ca}S_{2,PHPT}$	1.500E+01	9.000E+00
HHM	k_{HHM}	1.390E-02	-
	R_{PTHrP}	1.040E+01	4.160E+01
	$A_{Ca(s),PHPT}$	4.022E+02	-
	$B_{Ca(s),PHPT}$	1.255E+04	-

	$m_{Ca}A_{PHPT}$	-2.305E+01	-
	$m_{Ca}B_{PHPT}$	-2.500E+02	-
Vitamin D Deficiency	$dCTL/dt = \chi_{VDD}[H_1(PTH) + H(PTHrP)]H(PO_4) - k_{CTL}CTL$		
	k_{VDD}	4.630E-01	-
	χ_{VDD}	1.00E+00	0.00E+00
CTL missense	$T_{PTG}^{\pm} = 1 \pm tanh[\lambda_{CTL}(\chi_{CTLmiss}CTL - CTL_0)]$		
	$k_{CTLmiss}$	6.994E-01	-
	$\chi_{CTLmiss}$	1.00E+00	0.05E+00

7. Conclusions and Future work

7.1. Conclusion

This research offers an alternate approach to modeling and investigating physiological control systems. In our work, the physiological subprocesses of Ca regulation are mapped onto their corresponding engineering control system (ECS) block components. Thus, the subprocesses of Ca control are grouped based on their function in the control system as opposed to being grouped based on the organ in which the subprocesses occur. In so doing, the approach facilitates a fundamental understanding of the complex physiological process of Ca regulation. The impacts of the individual subprocesses (or individual component blocks) on Ca regulation are explored through partial or complete removal of the different blocks or through varying the parameters in the underlying equations in each block. The Ca regulatory response to each scenario (partial or total block removal or variation of parameter estimates) ,when compared to clinical observations of Ca-related diseases, indicate how the pathologies can be represented by the model. As such, the framework allows for the ease of exploration of Ca-related pathologies through representing the diseases as component block defects or external factors causing a system disturbance.

One of the interesting things about the model is that it provides insight into the transient behavior of some of the model variables. For instance, in model predictions of healthy subjects calciotropic response post-Ca infusions (Fig. 3.5C) there are fluctuations in the FGF-23 levels induced by the opposing effects of diverging increases and decreases in PO_4 and CTL levels on FGF-23 secretory rate. Fluctuations are also observed in the CTL levels when simulating HHM due to dissimilar effects of decreasing PTH concentration and increasing PTHrP levels on CTL secretory rate (Fig. 2.6A). Another example is the PTH undershoot (Fig. 2.4C), or overshoot (Fig. 2.4E) when retuning to steady-state after induced hypo- or hypercalcemia, respectively. This is caused by the expression used to model Ca-dependent PTH secretion. These observations could be viewed as artifacts of the model, and owing to insufficient clinical data, we cannot currently validate these model predictions. However, we are confident that these predictions are representative of the physiological response as in the case of Ca infusion in the model of healthy subjects, the overall model has been validated using clinical observations during Ca infusion; and in the cases of HHM, the steady-state responses are consistent with clinical presentations of the pathology.

Another benefit of this approach is that it allows for the isolation of pathologies that are associated with a particular function of the organ of interest rather the entire organ. As an example, in previous models, Ca

detection in the PTG by the Ca-sensing receptors is not separated from PTH production and secretion; however, in our work, the two subprocesses are treated separately (Ca-detection—sensor; PTH production/secretion—controller). As such, genetic mutations of the CaR are easily represented as defects of the sensor while, based on previous models, the pathologies can only be represented as a defect of the PTG.

Our approach opens another gateway in further exploring the known and unknown mechanisms involved in the different subprocesses of Ca regulation. Each parameter or set of parameters, in the model, is related to a physiological entity, thus exploring the range over which the parameter(s) affect the Ca regulatory system gives insight into the behavior of the associated physiological entity in Ca regulation in both health and disease. In the case of models of pathologies, exploring the parameter(s) range(s) provides an indication of: the extents to which the pathology may progress as well as the extents to which the site could possibly be perturbed when considering potential therapies.

Representing Ca regulation as an ECS allows for the ease of addition of component blocks, as such, interacting control systems and/or external factors can easily be incorporated into our model of Ca control (e.g. estrogen control system, due to its effect on PTH and CTL levels; or, intracellular Ca control system, which may affect plasma Ca levels). By the same token, our model of Ca regulation can be included in any broader model of physiological control systems. For example, plasma Ca is necessary for blood coagulation and muscle contraction, therefore a model for the regulation of blood coagulation, or muscle contraction, will include plasma Ca and therefore, allows for the addition of the overall system of Ca control.

The model of Ca regulation offers the ease of supplementing or replacing defective blocks in the Ca regulatory system with external control systems, whether via drugs or a combination of biomedical devices and drugs developed to replace the defective components. For example, in some cases of thyroidectomy, parathyroidectomy, or radial neck surgery the parathyroid glands (the sensor and controller in the Ca regulatory system) may be partially or completely removed leading to long term hypoparathyroidism. At present, the only therapy is managing the symptoms through administration of Ca supplements and Vitamin D metabolites. Using the model of Ca regulation, we can explore the behavior of PTH in maintaining normocalcemia and develop a biomedical device—external sensor and controller—to replace the activity of the PTG.

Notwithstanding the opportunities presented by our model, the scope of application may be limited due to some of the challenges faced and underlying assumptions made in developing the model. The major challenge faced in developing the model is the lack of sufficient data for estimating some of the model

parameters and validating some component blocks. Since all the clinical data used in this research is taken from the literature, parameter estimates are only as good as the quality of the available data. For processes that are heavily researched (e.g. Ca-dependent PTH production) we are confident in the parameter estimates. However, in many cases only limited data is available to estimate the relevant parameters; this is often due to either too few data points being reported or, in many cases, the researchers may only be interested in the interactions of few biochemical variables that elicit a given response while our model requires information of additional variables. As an example, PTH production is affected by Ca, CTL, PO_4 and FGF-23, however, in clinical studies of the impact of plasma Ca infusion (or chelation) on PTH, Ca and PTH levels are reported throughout the period of observation, while for plasma CTL and PO_4, if reported, only the baseline values are given. For, FGF-23 it has only been recently discovered (compared to CTL and PTH) hence, there is only limited research data available on FGF-23 in Ca regulation; and, there is a major discrepancy, and no correlation, between the two measuring techniques that are currently used in measuring FGF-23 levels.

In our model, we neglect the effects of subject demographics (age, sex, and ethnicity) on Ca regulation. It is known that PTH levels vary across age, sex, and ethnicity, however no such information is available for the other calciotropic hormones. Additionally, the available datasets used in estimating the relevant parameters vary across the different subject demographics such that it is infeasible to consider the group's (or patient's) age, sex, or ethnicity when validating or predicting calciotropic behavior.

For simplicity, we assumed that plasma biochemical concentration is uniformly distributed throughout the body; therefore the concentrations of Ca, PTH, CTL, PO_4 and FGF-23 in all regions of the plasma are constant. However, this assumption is not correct as there may be localized excess or scarcity of hormones or ions in the plasma surrounding certain tissues based on cell-to-plasma hormone/ion flux owing to ongoing intracellular Ca- or PO_4-dependent activity. Likewise hormone concentrations will vary between the site of production and the target site due to the time taken to travel around the circulatory system and across the different membranes. In order to take this non-uniformity into account

Consistent with receptor theory and physiological dose-response characteristics, the rates of secretion, production, or cell proliferation, and all hormone/ion dependencies, are described by the logistic function that only considers, as input, the concentration of the stimulating variable. However, in some instances where the responses are fast, i.e. within minutes, the rate of change of the stimulating variable may also be a factor in the response and should possibly be incorporated as an input to the logistic function. For instance, in Fig. 4.2 A-C, our model provides a satisfactory prediction of PTH response to induced hypercalcemia with varying calcium infusion rates; however, the model does not fully capture the

transient PTH response caused by the changing rates of calcium infusion. Although this phenomenon is rarely experienced in adulthood, it is important in the growth dynamics of children. Therefore, in order to extend the model to pediatrics or in diseases related to the bone where there may be large changes in the bone-plasma Ca flux, PTH dependence on the rate of change of Ca would need to be considered.

While qualitatively accurate in general, quantitatively, the model predictions of pathological conditions do not always match all clinical observations of Ca, PTH, CTL, urinary Ca, and/or CB ratio as precisely. This is likely due to the fact that our model simulations of pathologies are based on individual component defects in the model representing the healthy state (i) without accounting for the possible effects of external hormones/ions on Ca regulation under pathological conditions; and (ii) assuming that the pathologies in question manifest as defects isolated to a single component with no "interactions" from or on other sub-processes.

7.2. Future work

Future research in computational Ca regulation can be distributed in three general areas: i) expanding the equations in the component blocks to include the mechanistic details of the relevant processes; ii) incorporating other physiological control systems into the framework; and, iii) exploring other pathologies and potential therapies. Coupled with each of these areas is the need for clinical research to provide the necessary data for parameter estimates and validation.

7.2.1. Improving the mechanistic details:

The rates of secretion, production or proliferation, and all hormone/ion dependencies, detailed in this research, are determined based on the macroscopic variables (Ca, PTH, CTL, PO_4 and FGF-23). However, the mechanisms involved in hormone production and secretion and cell proliferation involve many other biological factors. With sufficient clinical data, we could model the effect of these factors on hormone production and cell proliferation. Such an improvement could provide a better understanding of the intracellular/molecular actions involved in Ca regulation. Also, a more detailed description of the mechanisms involved in the different subprocesses could indicate what intracellular activities initiate the development of Ca-related pathologies. Some specific examples for detailed mechanisms are listed below.

7.2.1.1. Sensor:

In our model, one parameter, the sensor gain, is used as an indicator of the plasma Ca detection and signal transmission. In reality, intracellular signaling occurs through a complex signaling network within the cytoplasmic region. Therefore, the sensor gain represents all the interactions occurring within the cell. With sufficient clinical data of the intracellular factors involved in signaling, we could incorporate these pathways into the sensor block. Ultimately, this improvement would be useful in offering insight into the differing behavior of the CaR in both PHPT and SHPT. One question left unanswered by the current model is, what accounts for the differences in CaR-mediated PTH reduction in PHPT and SHPT?

7.2.1.2. Controller:

CTL, PO_4, FGF-23 and Ca affect intracellular PTH mRNA transcription and stability and ultimately PTH production and secretion. These mechanisms are not considered in our model; however, with sufficient clinical data of intermediate product, a more detailed description of all these intracellular mechanisms involved in PTH secretion could prove insightful in further investigating how pathologies such as SHPT and PHPT develop and progress.

PT cellular proliferation occurs during PTH production and secretion in hypocalcemia and in several pathologies; a minimal representation of PTG growth is used in the model. At present, the mechanisms involved in PT cellular proliferation have yet to be unravelled; however, once sufficient clinical data becomes available, we can incorporate the mechanisms of PTG growth which could elucidate the mechanisms through which PTG-related pathologies develop and progress.

7.2.1.3. Actuator: Kidneys – CTL Production

The model does not consider the mechanisms involved in CTL synthesis; however, very little is information is available about the pathways involved. Once sufficient clinical data becomes available, we can incorporate this information into our model which will then allow us to investigate the impact of renal failure on CTL production. Additionally, since Vitamin D is a precursor to CTL production, the improvement will allow us to study the impact of Vitamin D deficiency on renal function.

7.2.1.4. Actuator: Kidneys – Ca/PO4 reabsorption

The data used in estimating the parameters for Ca and PO_4 absorption does not account for the PTH– and FGF-23–dependent portions of Ca and PO_4 reabsorption because of insufficient clinical data. However, when clinical data specific to PTH– and FGF-23–mediated renal Ca and PO_4 reabsorption becomes available, we could use this date to reevaluate the parameter estimates thus improving the model predictions for renal Ca and PO_4 excretion. This improvement would allow for further research into how Ca and PO_4 reabsorption changes during renal failure.

7.2.1.5. Actuator: Bone

The hormone/ion transport across the different sections of the bone (bone tissue and bone fluid) and the different boundaries (bone tissue-bone fluid and bone fluid-plasma boundaries) can be described by the diffusivity and the mechanisms of mass transport. With sufficient experimental data, we could estimate the relevant parameters. Such an improvement in the model could be prove useful in investigating the development of osteoporosis and the propensity for bone fractures, as well as, to elucidate the disparity in bone resorption during HHM and PHPT.

7.2.2. Incorporating other physiological control systems:

Calcium in the extracellular fluid is important for many physiological functions including blood clotting and muscle contraction. Our model of Ca regulation could be incorporated into computational models of these physiological processes. Such an improvement may allow for: (i) greater understanding of the

interactions between the two processes and (ii) exploration of additional pathologies. It is important to note, that variations in localized plasma concentrations has to be considered when undertaking this coupling of "separate" models (e.g. the model of Ca regulatory and the model of blood coagulation). For the reason that these processes do not occur throughout the body at the same time, but rather localized at a particular site of action.

Magnesium (Mg) deficiency affects some aspects of Ca regulation, namely, PTH production and renal Ca retention; and is associated with vascular calcification in chronic kidney disease. Mg concentration is regulated through similar processes as Ca control; therefore, incorporating plasma Mg control in our model of Ca regulation could provide additional insight in the progression of some Ca-related pathologies. Likewise, incorporating Mg control in the model will increase the number of pathologies we can investigate.

The half-life of CTL in the plasma is increased due to transcalciferin, which is affected by estrogen levels. Likewise, estrogen blocks PTH-induced osteoclast formation, and is a part of therapeutic intervention in osteoporosis. Therefore, estrogen regulation could be incorporated in the overall model which would be useful for further exploring the development and progression of PHPT and ultimately, osteoporosis.

7.2.3. Exploring pathologies and potential therapies

In this research, the correlation between CNC dose and PTH reduction is developed for one stage of PHPT. Therefore, more clinical data of CNC therapy in various stages of PHPT is needed to develop the correlations of CNC dose vs. PTH reductions across the spectrum of PHPT.

In terms of parameter space exploration, only a small number of parameters were investigated (see Chapters 4-6). As such, further exploration into the parameter space of relevant parameter combinations, along with performing uncertainty analysis on these parameters would provide further insight into Ca regulation in health and disease.

Although consistent with clinical observations, the model for SHPT does not accurately predict the observed PO_4 and Ca response to CNC therapy. Therefore, further clinical exploration of the effect of CNC on Ca-PO_4 regulation in SHPT is needed and the results used to improve the model of SHPT.

We proposed a method to customize CNC therapy for individual patients with SHPT given the stage of the disease and a target PTH level. We could validate this method using the following clinical data: i) patient plasma biochemistry (Ca, PTH, PO_4, and CTL) before and during CNC therapy; ii) CNC dosage regimen during both titration and maintenance periods. Additionally, with an improved model of SHPT,

we can include additional biochemical constraints based on the Kidney Disease Outcome Quality Indicators (KDOQI) guidelines to further improve CNC dose regimen.

Several drugs are used in the treatment of CKD, phosphate binders, CTL substitutes, cinacalcet and Ca supplements. We could identify the pharmacodynamic effect of the different drugs on the Ca-PO_4 regulatory system and in so doing, develop a protocol to identify the optimal dose of the combination of drugs given various biochemical targets and constraints. Again, we could compare these model prediction to clinical observations of patients administered any, or a combination, of these drugs.

PTG behavior varies with age, gender and race; however, in determining the relationship between the PTG size and minimum PTH secretory rate in PHPT, these factors were neglected due to insufficient data. Therefore, more clinical data of PTH response to induced hypercalcemia in PHPT and PTG mass post parathyroidectomy could be used to first determine if these demographics are important enough to be considered, and if so, determine the parameter estimates for PTG size prediction for different patient groups.